

NACA TN No. 1795

8242

0144933



# NATIONAL ADVISORY COMMITTEE FOR AERONAUTICS

TECHNICAL NOTE

No. 1795

APPLICATION OF RADIAL-EQUILIBRIUM CONDITION TO AXIAL-FLOW  
COMPRESSOR AND TURBINE DESIGN

By Chung-Hua Wu and Lincoln Wolfenstein

Lewis Flight Propulsion Laboratory  
Cleveland, Ohio



Washington  
January 1949

AFMPC  
TECHNICAL NOTE  
1795



## NATIONAL ADVISORY COMMITTEE FOR AERONAUTICS

TECHNICAL NOTE NO. 1795

## APPLICATION OF RADIAL-EQUILIBRIUM CONDITION TO AXIAL-FLOW

## COMPRESSOR AND TURBINE DESIGN

By Chung-Hua Wu and Lincoln Wolfenstein

## SUMMARY

Basic general equations governing the three-dimensional compressible flow of gas through a compressor or a turbine are given in terms of velocity components, total enthalpy, and entropy. These equations are used to determine the radial motion of gas through an axial-flow compressor or a turbine and the corresponding effect on the radial variations of the state of gas between successive blade rows in the case of steady, axially symmetrical flow. The aspect ratio of the blade row is found to be an important factor in the calculation when the effect of radial motion is included. The usual method, which neglects the effect of radial motion, is shown to be good only for the limiting case of zero blade-row aspect ratio, that is for the case where the axial length of the blade row is much larger than the radial length of the blade row. A sinusoidal radial-flow path is found to give the effect of radial motion on the radial variation of gas state between blade rows as small as likely without any discontinuity in the curvature of the streamline and is suggested for use in design calculations.

The equations are applied to investigate the maximum compatible number of the radial variations of the gas properties between successive blade rows that a designer is free to specify. The various ways of taking up these degrees of freedom and the different types of design obtained are discussed. A general procedure is given to calculate the characteristics of a compressor or turbine of any given type of design, taking into account the effect of radial motion of gas. Numerical calculations made for two types of compressor and one type of turbine show that even in the case of non-tapered passage, there is appreciable radial motion and that the corresponding effects are of significant magnitude and should be taken into account in design.

## INTRODUCTION

The design of a compressor or a turbine hereinafter called a turbomachine may be divided into two phases. The first phase concerns the type of design to be used or the determination of the most desirable variations of velocity and thermodynamic properties of the gas in planes normal to the axis of the machine between successive blade rows. The second phase concerns the design of blades that will give the desired variations of velocity and other properties of gas in these planes. In the first phase, the condition of radial equilibrium, that is, the radial component of the equation of motion, must be used. The flow of gas in a turbomachine is curvilinear; it is curved not only by the whirling motion of gas, but also by the radial motion of the gas. The equation of motion then specifies the radial pressure gradient required to provide the centripetal force to maintain the curved flow.

In figure 1(a), a curved stream surface over four stages of a multistage turbomachine is shown and in figures 1(b) and 1(c) are shown its intersections with planes normal to and containing the axis of the machine, respectively. The radial pressure gradient due to the whirling motion of gas is always positive, whereas that due to the radial motion of gas may be either positive or negative depending on whether the curvature caused by the motion is either inward or outward from the axis of the machine at the point of consideration. If the gas lying on a normal plane between two blade rows, such as station 1 in figure 2(a), is considered, the equation of motion gives (neglecting small terms)

$$\frac{1}{\rho} \frac{\partial p}{\partial r} = \frac{V_{\theta}^2}{r} - V_z \frac{\partial V_r}{\partial z} = V_{\theta}^2 \frac{1}{r} - V_z^2 \frac{d^2 r}{dz^2}$$

where  $p$  and  $\rho$  are the pressure and the density of the gas particle, respectively,  $r$  and  $z$  are the radial distance from and the distance along the axis of the gas particle, respectively, and  $V_r$ ,  $V_{\theta}$ , and  $V_z$  are the radial, tangential, and axial components of the velocity of the gas particle, respectively. From this equation it is seen that the effect of the two motions on the radial pressure gradient is quite similar. The effects of the two motions are both proportional to the product of the square of the velocity and the curvature ( $1/r$  and  $d^2 r/dz^2$ , respectively) involved. Even when the radial motion involved is small, if the axial velocity is high and the blade-row aspect ratio is large, the second term in the equation is of comparable magnitude to the first and should be included in the calculation. In the

1035

past, however, the radial motion and its effect were usually neglected (references 1 to 3). (Such methods of calculation will hereinafter be referred to as the "simplified-radial-equilibrium approximation.") In reference 1, a general form of the Euler equation is presented but is not used later on in the through-flow analysis because the simplified-radial-equilibrium consideration may be expected to hold sufficiently far downstream of a single row of blades where the radial velocity of the gas becomes small. For this reason, this approximation is adequate to predict most of the experimental results available on the radial variation of the gas state far downstream of a single row of blades (references 1 and 3). No satisfactory data or theory exist for the general case of a blade row within a closely spaced series of blade rows, as in a multistage compressor or turbine where the effect of radial motion may be quite significant. In the present paper, the effect of the radial motion of gas is considered in applying the radial-equilibrium condition to turbomachine design.

In the ANALYSIS, the general equations governing the flow of gas in axial-flow turbomachines are developed primarily for the case of steady axially symmetrical flow, which corresponds to the limiting case of an infinite number of blades. The blades are replaced in the calculation by an appropriate force field. A method of solution involving the use of the basic equations in finite-difference form is discussed. Expressions are developed for the use of a large number of successive axial stations and for the use of three stations for a stage in which an appropriate radial-flow path is assumed.

The equations are applied to investigate the maximum number of radial variations of the velocities and other properties of the gas that a designer is free to specify in any particular design. The various ways of using these degrees of freedom and the different types of design obtained are discussed.

In the last part of this report, a general procedure of calculation for any type of design is given. It is used to calculate two types of compressor and one type of turbine with the purpose of investigating the effect of radial motion on design calculations.

This investigation, conducted at the NACA Cleveland laboratory, was completed in April 1948.

## SYMBOLS

The following symbols are used in this report:

A	aspect ratio of blade row, $\left(\frac{r_t - r_h}{L}\right)$
a	velocity of sound
$C_L$	lift coefficient
$c_p$	specific heat of gas at constant pressure
$c_v$	specific heat of gas at constant volume
$\frac{D}{Dt}$	differentiation with respect to time following motion of gas
$\bar{F}$	force acting on gas particles by blades per unit mass of gas
$F_r$	radial component of $\bar{F}$
$F_\theta$	tangential component of $\bar{F}$
$F_z$	axial component of $\bar{F}$
f	form of radial-flow path
G	mass flow per unit flow area perpendicular to axis of turbomachine
g	form of radial-displacement distribution
H	total enthalpy per unit mass of gas, $\left(h + \frac{v^2}{2}\right)$
h	enthalpy per unit mass of gas, $\left(u + \frac{p}{\rho}\right)$
K	constant
L	axial length of blade row (fig. 2)
M	Mach number of gas
m	mass of gas

n	polytropic exponent of actual expansion or compression process of gas
p	static pressure
Q	external heat transferred to gas particle along its path of motion per unit mass per unit time
R	gas constant
r	radius measured from axis of turbomachine
$r_0$	mean radius of radial-flow path (fig. 2(a))
$r' = \frac{r}{r_t - r_h}$	
s	entropy per unit mass of gas
s.r.e.	simplified-radial-equilibrium approximation
T	absolute stream temperature of gas
t	time
U	magnitude of $\bar{U}$
$\bar{U}$	vector velocity of rotor blades at radius r
u	internal energy per unit mass of gas with 0° absolute as base temperature
V	magnitude of $\bar{V}$
$\bar{V}$	absolute vector velocity of gas
$V_r$	radial component of $\bar{V}$
$V_\theta$	tangential component of $\bar{V}$
$V_z$	axial component of $\bar{V}$
W	magnitude of $\bar{W}$
$\bar{W}$	vector velocity of gas relative to rotor blade

$W_{\theta}$	tangential component of $\bar{W}$
$y$	maximum radial displacement over blade height
$z$	distance along axis of turbomachine
$\alpha$	angle between relative velocity of gas entering rotor and axis of turbomachine
$\beta$	angle between absolute velocity of gas entering stator and axis of turbomachine
$\gamma$	ratio of specific heats, $(c_p/c_v)$
$\Delta$	radial displacement across rotor, $(r_2 - r_1)$
$\delta$	dimensionless turning, $\left(\frac{\xi_2 - \xi_1}{r_1 U_{1,t}}\right)$
$\eta$	small-stage or polytropic efficiency
$\theta$	angular distance measured from some fixed radial line
$\mu$	viscosity of gas
$\nu$	kinematic viscosity of gas, $(\mu/\rho)$
$\xi$	angular momentum about $z$ axis per unit mass of gas, $(rV_{\theta})$
$\rho$	mass density
$\sigma$	blade solidity
$\phi$	dissipation of energy due to viscosity per unit volume of gas per unit time
$\varphi$	function
$\omega$	angular velocity of rotor

## Subscripts:

1	in front of rotor
2	behind rotor and in front of stator

3	behind stator and in front of next rotor
4	behind next rotor
c	satisfying continuity equation
e	satisfying radial-equilibrium and total-enthalpy equations
h	at hub
i	any station
j	station short distance downstream of station i
k	any station in front of rotor
L	limiting value
l	any station in front of stator
m	used with r to indicate mean radius
n	used with r to indicate radius where maximum radial displacement occurs
s	simplified-radial-equilibrium approximation
t	at tip

## ANALYSIS

### Basic Equations

The state of gas in three-dimensional motion is completely specified by its absolute vector velocity  $\bar{V}$ , or its three components  $V_r$ ,  $V_\theta$ , and  $V_z$  referred to cylindrical coordinates  $r$ ,  $\theta$ , and  $z$ , respectively, and two thermodynamic properties. These last two properties are usually chosen as the static pressure  $p$  and the static density  $\rho$ , but herein it is more convenient to use the total enthalpy per unit mass  $H$  and entropy per unit mass  $s$ , which are defined by

$$H = h + \frac{V^2}{2} \quad (1)$$



and

$$T ds = du + p dp^{-1} \quad (2)$$

For the range of temperature and pressure encountered in compressors and turbines;  $p$ ,  $\rho$ , and  $T$  are accurately related by the following equation of state

$$p = \rho RT \quad (3)$$

The Navier-Stokes equation of motion for a real fluid is given, in vector form, by

$$\frac{D\bar{v}}{Dt} = \bar{F} - \frac{1}{\rho} \nabla p + \frac{\mu}{\rho} \left[ \nabla^2 \bar{v} + \frac{1}{3} \nabla(\nabla \cdot \bar{v}) \right] \quad (4)$$

The energy equation for a real fluid is given by (references 4 and 5)

$$\frac{Du}{Dt} + p \frac{Dp^{-1}}{Dt} = Q + \frac{\phi}{\rho} \quad (5)$$

The continuity equation can be written as

$$\frac{\partial \rho}{\partial t} + \nabla \cdot (\rho \bar{v}) = 0 \quad (6)$$

or

$$\nabla \cdot \bar{v} + \frac{D}{Dt} \log_e \rho = 0 \quad (6a)$$

When the preceding equations are combined, the following four general equations are obtained (for derivation, see appendix A):

$$\nabla H = \bar{F} + T \nabla s + \bar{v} \times (\nabla \times \bar{v}) - \frac{\partial \bar{v}}{\partial t} + \nu \left[ \nabla^2 \bar{v} + \frac{1}{3} \nabla(\nabla \cdot \bar{v}) \right] \quad (7)$$

$$\frac{DH}{Dt} = Q + \frac{\phi}{\rho} + \frac{1}{\rho} \frac{\partial p}{\partial t} + \bar{v} \cdot \left\{ \bar{F} + \nu \left[ \nabla^2 \bar{v} + \frac{1}{3} \nabla(\nabla \cdot \bar{v}) \right] \right\} \quad (8)$$

$$\frac{Ds}{Dt} = \frac{Q}{T} + R \frac{\phi}{p} \quad (9)$$

$$\nabla \cdot \bar{v} + \frac{1}{\gamma-1} \frac{D}{Dt} \log_e T - \frac{D}{Dt} \left( \frac{s}{R} \right) = 0 \quad (10)$$

Equation (7) gives the gradient of total enthalpy in terms of blade force, viscous forces, velocity, and other properties of the gas. This vector equation gives three scalar equations in three dimensions. Equation (8) gives the rate of change of total enthalpy of gas along a streamline in terms of rate of heat addition, rate of work done by blade and viscous forces, and so forth. Equation (9) gives the rate of change of entropy along a streamline in terms of rate of external heat addition and of dissipation of energy due to viscosity. Equation (10) gives the continuity relation in terms of velocity, temperature, and entropy of gas. It should be noted that of the six scalar equations given by equations (7) to (10) only five are independent, because they are derived from equations (4) to (6), among which equation (4) yields three scalar equations, giving a total of five independent equations. (The energy relation is used in the derivation of both equations (8) and (9).)

#### Steady Axially Symmetric Flow

Axial symmetry, that is symmetry about the axis of rotation, can be assumed to exist sufficiently far downstream of any blade row and is true everywhere for the limiting case of an infinite number of blades. This assumption is usually made to simplify the analysis. The blades are then replaced by a volume distribution of forces, the magnitude of which is obtained by maintaining constant the product of the number of blades and the resultant force at any point on the blade as the number of blades is increased. (The resultant force is the difference between the forces on the two sides of the blade.) That is, the resultant force acting on the gas by a blade element at any radius is considered to be evenly distributed over the stream sheet between two blades at that radius. Reference 1 shows that for incompressible and frictionless flow the value thus obtained gives an average value with respect to the coordinate  $\theta$ . Because the number of blades is usually large, this assumption is considered reasonable for steady operation of turbomachines, and particularly for this investigation. Thus all partial derivatives of gas properties with respect to time and angular position  $\theta$  will be taken as equal to zero. The state of gas is considered as a function of  $r$  and  $z$  only, that is, the problem is reduced to a two-dimensional treatment. With this simplification and by

transforming  $\nabla^2 \bar{v}$  into  $[\nabla(\nabla \cdot \bar{v}) - \nabla \times (\nabla \times \bar{v})]$ , there are obtained the radial, tangential, and axial components of equation (7):

$$\begin{aligned} \frac{\partial H}{\partial r} = & F_r + T \frac{\partial s}{\partial r} + \frac{v_\theta}{r} \frac{\partial(rv_\theta)}{\partial r} + v_z \frac{\partial v_z}{\partial r} - v_z \frac{\partial v_r}{\partial z} \\ & + v \left[ \frac{4}{3r} \frac{\partial^2(rv_r)}{\partial r^2} - \frac{4}{3r^2} \frac{\partial(rv_r)}{\partial r} + \frac{1}{3} \frac{\partial^2 v_z}{\partial r \partial z} + \frac{\partial^2 v_r}{\partial z^2} \right] \end{aligned} \quad (7a)$$

$$0 = F_\theta - \frac{v_r}{r} \frac{\partial(rv_\theta)}{\partial r} - v_z \frac{\partial v_\theta}{\partial z} + v \left[ \frac{1}{r} \frac{\partial^2(rv_\theta)}{\partial r^2} - \frac{1}{r^2} \frac{\partial(rv_\theta)}{\partial r} + \frac{\partial^2 v_\theta}{\partial z^2} \right] \quad (7b)$$

and

$$\begin{aligned} \frac{\partial H}{\partial z} = & F_z + T \frac{\partial s}{\partial z} + v_r \frac{\partial v_r}{\partial z} - v_r \frac{\partial v_z}{\partial r} + v_\theta \frac{\partial v_\theta}{\partial z} \\ & + v \left[ \frac{4}{3r} \frac{\partial^2(rv_r)}{\partial r \partial z} + \frac{4}{3} \frac{\partial^2 v_z}{\partial z^2} - \frac{\partial^2 v_r}{\partial r \partial z} + \frac{\partial^2 v_z}{\partial r^2} \right] \end{aligned} \quad (7c)$$

In the radial equilibrium equation (7a), the relative importance of the various terms depends mainly on the type of design. The radial force exerted by the blade depends on the twist and the taper of the blade in the radial direction. The radial variation of entropy depends on the radial variations of external heat subtraction and of dissipation of energy due to viscous effect. In ordinary compressors and turbines, the amount of heat transfer is small per unit mass of gas flow, and its effect on the radial variation of entropy is negligible. But in turbines with blade cooling, the heat transfer may be quite large and it may give a significant radial variation of entropy, which must be taken into consideration. The increase of entropy due to dissipation of energy by

1035

viscosity is small and may be assumed to be the same at all radii over the main portion of gas outside the boundary layers at the rotor drum and the inner wall of the outer casing. The third term on the right-hand side of the equation is equal to zero for free-vortex type of design, in which  $rV_\theta$  is set constant at all radii, and has a nonzero value in other types of design. Similarly, the fourth term may have a nonzero value if constant axial velocity at all radii is not specified in design.

The fifth term represents the effect of radial motion on the radial-equilibrium condition. In the gap between two blade rows it is proportional to the product of the square of axial velocity and the curvature of the flow path in the axial plane and is very similar to the effect of whirling motion represented by  $V_\theta^2/r$ . If the curvature caused by radial motion is positive, the effect is to decrease the radial gradient of total enthalpy or pressure caused by the whirling motion of the gas. If the curvature is negative, the effect is to intensify this radial gradient. For design with large blade height, short axial blade length, high whirl, and high axial velocities, it will be shown that the effect of radial motion is large and should be considered in the calculations.

The last four terms in the bracket are usually of the same order of magnitude as the preceding velocity derivatives and because they are multiplied by  $v$ , which is much smaller than other multipliers ( $V_z$  or  $V_\theta$ ), the whole product is much smaller than the other terms in the equation and may be neglected. The same argument applies to similar terms in equations (7b) and (7c). Hence equations (7a), (7b), and (7c) may be simplified to

$$\frac{\partial H}{\partial r} = F_r + T \frac{\partial s}{\partial r} + \frac{V_\theta}{r} \frac{\partial(rV_\theta)}{\partial r} + V_z \frac{\partial V_z}{\partial r} - V_z \frac{\partial V_r}{\partial z} \quad (7d)$$

$$0 = F_\theta - \frac{V_r}{r} \frac{\partial(rV_\theta)}{\partial r} - V_z \frac{\partial V_\theta}{\partial z} \quad (7e)$$

and

$$\frac{\partial H}{\partial z} = F_z + T \frac{\partial s}{\partial z} + V_r \frac{\partial V_r}{\partial z} - V_r \frac{\partial V_z}{\partial r} + V_\theta \frac{\partial V_\theta}{\partial z} \quad (7f)$$

Among the terms on the right-hand side of equation (8), other than the first term (the importance of which depends on whether there is blade cooling),  $\bar{V} \cdot \bar{F}$  is the predominating term in passing through the rotor. Whereas in passing through the stator, all the terms on the right-hand side are of the same order of magnitude. However, by the use of the equation of motion, the energy equation for steady flow, and the assumption that the heat generated from the frictional work remains in the stream,  $DH/Dt$  can be expressed for steady axially symmetrical flow in a more useful form in terms

of only  $Q$ ,  $\omega$ , and  $\frac{D(rV_\theta)}{Dt}$  (see appendix A):

$$\frac{DH}{Dt} = Q + \omega \frac{D(rV_\theta)}{Dt} \quad (8a)$$

In equation (9), the two terms are of comparable magnitudes in ordinary compressors or turbines. With blade cooling, the first term is predominate. For the axially symmetrical flow, it reduces to

$$\frac{Ds}{Dt} = \frac{Q}{T} + \frac{v}{T} \left\{ 2 \left( \frac{\partial v_r}{\partial r} \right)^2 + 2 \left( \frac{v_r}{r} \right)^2 + 2 \left( \frac{\partial v_z}{\partial z} \right)^2 + \left( \frac{\partial v_\theta}{\partial z} \right)^2 + \left( \frac{\partial v_r}{\partial z} + \frac{\partial v_z}{\partial r} \right)^2 + \left[ r \frac{\partial \left( \frac{v_\theta}{r} \right)}{\partial r} \right]^2 - \frac{2}{3} \left[ \frac{1}{r} \frac{\partial (rv_r)}{\partial r} + \frac{\partial v_z}{\partial z} \right]^2 \right\} \quad (9a)$$

For axially symmetrical flow, equation (10) reduces to the following

$$\frac{1}{r} \frac{\partial (rv_r)}{\partial r} + \frac{\partial v_z}{\partial z} + \frac{1}{\gamma-1} \left( v_r \frac{\partial}{\partial r} \log_e T + v_z \frac{\partial}{\partial z} \log_e T \right) - v_r \frac{\partial}{\partial r} \left( \frac{s}{R} \right) - v_z \frac{\partial}{\partial z} \left( \frac{s}{R} \right) = 0 \quad (10a)$$

Among the preceding six equations, equations (7d) to (10a), only five are independent, because both equations (8a) and (9a) represent the energy relation. For nonviscous flow, there is an

additional relation in that the blade force is normal to the surface of the blade and consequently is perpendicular to the relative velocity of the gas, that is,

$$\bar{F} \cdot (\bar{V} - \bar{U}) = 0 \quad (11)$$

Then equation (8a) can be obtained by using the motion and energy equations and equation (11). (See appendix A.) Consequently, either equation (8a) or (11) can be considered as representing this additional relation, giving, in all, six independent equations (equations (7d), (7e), (7f), (9a), (10a), and either (8a) or (11)). For such flow, equation (9a) reduces to simply

$$\frac{Ds}{Dt} = \frac{Q}{T} \quad (9b)$$

For viscous flow, equation (11) is no longer true because the force exerted by the blade is now inclined from the direction perpendicular to the relative velocity of the gas by an amount to be determined from the shearing stresses of the gas adjacent to the blade surface. Under the present consideration of axially symmetrical flow it is found desirable to retain equation (8a) as the energy equation and to obtain the entropy change from  $H$ ,  $V$ , and the polytropic exponent  $n$  of the actual compression or expansion process:

$$p \rho^{-n} = \text{constant} \quad (12)$$

Then the rate of change of entropy along the streamline is (see appendix A)

$$\frac{Ds}{Dt} = R \frac{n-\gamma}{(n-1)(\gamma-1)} \left( v_r \frac{\partial}{\partial r} \log_e T + v_z \frac{\partial}{\partial z} \log_e T \right) \quad (13)$$

In equation (13)  $n$  is considered as known. In a given machine,  $n$  may be obtained directly from measured pressure and temperature data. In a new design,  $n$  may be obtained from the assumed polytropic efficiency used in design calculations:

For the compressor

$$\eta = \frac{\frac{\gamma-1}{n-1}}{n} \quad \text{or} \quad n = \frac{1}{1 - \frac{1}{\eta} \frac{\gamma-1}{\gamma}}$$

For the turbine

$$\eta = \frac{\frac{n-1}{n}}{\frac{\gamma-1}{\gamma}} \quad \text{or} \quad n = \frac{1}{1 - \eta \frac{\gamma-1}{\gamma}}$$

Because the change in  $s$  is usually small compared with the changes in  $H$  and  $V$ , the preceding method of determining  $s$  seems to be adequate to account for viscous effect in calculating the pressure and density change along the streamline for the present problem.

#### Method of Solution

If equations (1), (2), and (3) are considered as the relations to express  $p$ ,  $\rho$ , and  $T$  in terms of  $H$  and  $s$ , then equations (7d), (7e), (7f), (8a), (9b), and (10a) are six independent equations in the case of nonviscous flow, and equations (7d), (7e), (7f), (8a), (10a), and (13) are six independent equations in the case of viscous flow both involving eight variables  $V_r$ ,  $V_\theta$ ,  $V_z$ ,  $H$ ,  $s$ ,  $F_r$ ,  $F_\theta$ , and  $F_z$ . In the direct problem, in which the shape of the blade profile, the shape of the inner and outer wall of the gas passage, the rotor speed, the power input, and the entering and exit conditions of the gas are given, it is theoretically possible to determine the variations of these quantities throughout the machine. In the inverse problem, in which the desirable variations of two of the gas properties are prescribed, it is also theoretically possible to determine the variations of the other properties of the gas and the blade force necessary to achieve the prescribed variation of gas conditions. However, it seems that no general analytical solution of these equations is possible in either problem. Two numerical methods of solution are therefore suggested. In the first method, the previous equations are expressed in finite-difference form and applied to successive axial stations that are a short distance apart. In the second method, only three stations are used for each stage in which an appropriate radial-flow path is assumed.

#### Method of finite difference for successive axial stations.

At each station, if  $rV_\theta$  is denoted by  $\xi$ , equations (7d), (7e), and (7f) can be written as

$$\frac{\partial H}{\partial r} = F_r + T \frac{\partial s}{\partial r} + \frac{\xi}{r^2} \frac{\partial \xi}{\partial r} + V_z \left( \frac{\partial V_z}{\partial r} - \frac{\partial V_r}{\partial z} \right) \quad (7g)$$

$$0 = F_\theta - \frac{V_r}{r} \frac{\partial \xi}{\partial r} - \frac{V_z}{r} \frac{\partial \xi}{\partial z} \quad (7h)$$

and

$$\frac{\partial H}{\partial z} = F_z + T \frac{\partial s}{\partial z} + V_r \left( \frac{\partial V_r}{\partial z} - \frac{\partial V_z}{\partial r} \right) + \frac{\xi}{r^2} \frac{\partial \xi}{\partial z} \quad (7i)$$

Between any two successive stations  $i$  and  $j$  that are a short distance apart (fig. 3), the change in total enthalpy is given by equation (8a)

$$H_j(r_j) - H_i(r_i) = \omega \left[ \xi_j(r_j) - \xi_i(r_i) \right] + \int_{t_i}^{t_j} Q \, dt \quad (8b)$$

where  $(r)$  indicates that the gas properties at a particular station are a function of the radial position of the gas particle in that station. (It should be noted that due to radial motion the radial position of a gas particle at any station  $j$  is different from its radial position at the previous station  $i$ .) In passing through the stator,  $\omega = 0$  and there is no change of  $H$  along each streamline except from heat effect.

The entropy change between the two stations is obtained from equation (13) (see appendix A):

$$s_j(r_j) - s_i(r_i) = R \frac{n-\gamma}{(n-1)(\gamma-1)} \log_e \frac{H_j - \frac{V_j^2}{2}}{H_i - \frac{V_i^2}{2}} \quad (13a)$$

Instead of integrating equation (10a), the continuity relation between the two stations is readily obtained by equating the mass flow at the two stations.

$$G_j r_j \, dr_j = G_i r_i \, dr_i \quad (14)$$



By expressing  $G$  in  $H$ ,  $V$ , and  $s$ , equation (14) becomes (see appendix A):

$$V_{z,j} \left( H_j - \frac{V_j^2}{2} \right)^{\frac{1}{\gamma-1}} e^{-\frac{s_j}{R}} r_j dr_j = V_{z,i} \left( H_i - \frac{V_i^2}{2} \right)^{\frac{1}{\gamma-1}} e^{-\frac{s_i}{R}} r_i dr_i \quad (14a)$$

Equations (7g), (7h), (7i), (8b), (13a), and (14a) are now six independent equations relating the gas properties and blade forces at the two stations. In these equations, the heat-transfer term is negligible in ordinary turbomachines and can be estimated in the case of cooled blades; the temperature  $T$  is a known function of  $H$  and  $V$ ; and  $r_j$  is obtained from  $r_i$  and  $V_{r,i}$ . Hence there are only eight unknowns in  $H_j$ ,  $s_j$ ,  $V_{r,j}$ ,  $V_{\theta,j}$ ,  $V_{z,j}$ ,  $F_{r,j}$ ,  $F_{\theta,j}$ , and  $F_{z,j}$  (those at the first station  $i$  are considered as known). For a given blade operating at a given speed, two additional relations are known among the velocity components from the tangent plane to the blade surface at the point  $(r_j, z_j)$  because the flow of gas has to conform to the shape of the blades. For a new design, the desirable variation of two of the eight variables (usually one of the two is  $V_{\theta}$ ) can be specified and the remaining five determined from the preceding equations. It is to be noted, however, that, in practice, the radial blade force is not essentially an independent variable to be specified by the designer, but is mainly determined by the actual construction of the blade to meet the aerodynamic as well as the mechanical-strength requirements at different radii. The designer has to see to it, of course, that the radial force to be obtained from the blade actually constructed is consistent with that used in or obtained from the design calculations. The procedure of calculation for this step-by-step method varies with the type of design, the conditions given, or the two gas properties prescribed. The calculation is quite laborious and seems to be justified only in the process of actual design.

In order to obtain an over-all picture of the radial motion in a turbomachine and its effect on design considerations, the following method of using only three stations for each stage with prescribed radial-flow path may be used.

Method of prescribed radial-flow path. - In a turbomachine, the radial motion of the gas is caused by three factors:

(1) Tapering of the annular passage either at the inner or outer wall gives the flow a radial displacement across the stage, which is, of course, greatest in the immediate neighborhood of the tapered surface.

(2) Even with a nontapered passage, a radial displacement across the stage may be called for because of a variation in the distribution of specific mass flow over the blade height.

(3) Even if there is no radial displacement across the stage (that is, the same particle occupies the same radial position at the first station of each successive stage), there will, in general, be radial displacement of flow within the stage. This radial flow will then be oscillatory in nature, a radial displacement in the rotor being followed by an equal and opposite radial displacement in the stator. This radial flow arises because of the difference between the radial variation of the specific mass flow within the stage and those at the entrance and exit stations of the stage. (This radial displacement can only be avoided by specifying zero or the same radial variation of specific mass flow at all stations of the stage in the design.)

In general, the radial flow of gas therefore consists of a gradual, generally monotone, radial motion due to factors (1) and (2) with an oscillatory motion of period equal to the stage length due to factor (3) superimposed on it. The radial flow caused by these three factors will be similar to that shown in figure 1. The effect of the radial motion on the calculations arises chiefly through the term  $\partial V_r / \partial z$  in the radial-equilibrium equation (7g). This term is expected to be significant mainly because of the oscillatory motion, which may require significant changes in  $V_r$  within a single row of blades. The case of oscillatory motion within a stage with no over-all radial displacement across the stage will therefore be considered first. That is, the gas passage is nontapered and the radial distribution of gas properties at the entrance and exit stations of the stage is the same.

Because there is no blade force acting on the gas and there is little time available for the gas to mix, the gas flowing through the gap between two blades is under a constant pressure gradient and consequently tends to move with the same curvature it acquires while leaving the first blade. For straight passages, the maximum and minimum points of the radial-flow path are likely to be

somewhere near the middle of the gap. (The intersecting curve of a stream surface with an axial plane is herein referred to as "the radial-flow path." Because of axial symmetry, the radial-flow path is the same in any axial plane.) The stations between blade rows are most conveniently chosen at these points. The stations in front of the rotor, between the rotor and the stator, and behind the stator are denoted by subscripts 1, 2, and 3, respectively. (See fig. 2(a).) If  $r_0$  and  $L$  represent the mean radial distance of the flow path and the axial length of the blade row, respectively, then the radial distance of the gas particle at position  $z$  is given by

$$r - r_0 = - \frac{r_2 - r_1}{2} f\left(\frac{z}{L}\right) \quad (15)$$

at stations 1, 2, and 3

$$\left. \begin{aligned} \frac{z}{L} &= 0, 1, 2 \\ f(0) &= f(2) = 1, f(1) = -1 \\ f'(0) &= f'(1) = f'(2) = 0 \end{aligned} \right\} \quad (16)$$

where  $f$  is a function giving the form of the radial-flow path and the prime indicates differentiation with respect to  $z/L$ . It follows that

$$V_r = V_z \frac{dr}{dz} = - \frac{r_2 - r_1}{2} \frac{1}{L} V_z f'\left(\frac{z}{L}\right) \quad (17)$$

at station 1,  $z = 0$ ,

$$V_{r,1} = 0$$

and

$$\left(\frac{\partial V_r}{\partial z}\right)_1 = - \frac{r_2 - r_1}{2} V_{z,1} \frac{1}{L} f''(0) \quad (18)$$

inasmuch as  $\partial V_z / \partial z$  is practically zero in passing through the gap. Similarly, at station 2,  $z = L$ ,

$$v_{r,2} = 0$$

and

$$\left(\frac{\partial v_r}{\partial z}\right)_2 = -\frac{r_2 - r_1}{2} v_{z,2} \frac{1}{L^2} f''(1) \quad (18a)$$

Because  $f''(z/L)$  determines  $\partial v_r / \partial z$  or the effect of radial motion on the radial-equilibrium condition, it is desirable that it vary continuously; this condition together with those of equation (16) suggests

$$f\left(\frac{z}{L}\right) = \cos \pi \left(\frac{z}{L}\right)$$

Then

$$f''(0) = -\pi^2, \quad f''(1) = \pi^2$$

and equations (15), (18), and (18a) become, respectively,

$$r - r_0 = -\frac{r_2 - r_1}{2} \cos \pi \frac{z}{L} \quad (19)$$

$$\left(\frac{\partial v_r}{\partial z}\right)_1 = \frac{r_2 - r_1}{2} \frac{\pi^2}{L^2} v_{z,1} \quad (20)$$

$$\left(\frac{\partial v_r}{\partial z}\right)_2 = -\frac{r_2 - r_1}{2} \frac{\pi^2}{L^2} v_{z,2} \quad (20a)$$

For the sinusoidal form of  $f(z/L)$ , the maximum absolute value of  $f''(z/L)$  occurs at  $z = 0, L$ , and  $2L$ , and is equal to  $\pi^2$ . Even if  $f''(z/L)$  is assumed constant between  $z = 0$  and  $z = L/2$ , thus minimizing the maximum absolute value of  $f''$  in the interval, the absolute value of  $f''$  equals 8. This assumption, however, necessitates a discontinuity in  $f''$  at  $z = L/2$ . The values of  $\pi^2$  for the absolute values of  $f''(0)$  and  $f''(1)$  can be therefore considered as small as is likely. The smooth variation of  $f''(z/L)$  and the minimization of the absolute value of  $f''(z/L)$

at the stations are reasonable assumptions provided that the radial force exerted by the blade remains relatively small. In such case, the sinusoidal curve is believed to represent the major harmonic of the actual radial-flow path, and the major effect of the radial motion may be obtained through the use of this simple curve.

The radial-equilibrium equation (7g) may be written in terms of  $(r_2 - r_1)$  by use of equation (20)

$$\frac{dH_i}{dr_i} = T_i \frac{ds_i}{dr_i} + \frac{1}{r_i^2} \xi_i \frac{d\xi_i}{dr_i} + V_{z,i} \frac{dV_{z,i}}{dr_i} + (-1)^i \frac{1}{2} (r_2 - r_1) \frac{\pi^2}{L^2} V_{z,i}^2 \quad (21)$$

where

$$i = 1, 2, 3$$

When  $r_i$  is replaced by the dimensionless variable  $r_i' = \left( \frac{r_i}{r_t - r_h} \right)$ , the dependence of this equation on the blade-row aspect ratio  $A$  is seen to be

$$\begin{aligned} \frac{dH_i}{dr_i'} = T_i \frac{ds_i}{dr_i'} + \frac{1}{r_i'^2} \frac{\xi_i}{r_t - r_h} \frac{d}{dr_i'} \left( \frac{\xi_i}{r_t - r_h} \right) \\ + V_{z,i} \frac{dV_{z,i}}{dr_i'} + (-1)^i \frac{1}{2} (r_2' - r_1') \pi^2 A^2 V_{z,i}^2 \quad (21a) \end{aligned}$$

This form of the radial-equilibrium equation is seen to contain a term directly proportional to the radial displacement, to the square of the axial velocity, and to the square of the blade-row aspect ratio. If the blade-row aspect ratio is large or the axial velocity is high, the effect of radial motion may be large even though there is only a small amount of radial displacement across the blade row.

This method is readily extended to the case where there is an over-all radial displacement across the stage due to tapering of the passage or due to variation in the design from stage to stage. In figure 2(b), the radial position of a gas particle originally

at  $r_1$  in station 1 is at  $r_3$  in station 3. For the oscillatory motion required within the stage,  $r_2$  is not generally equal to  $\frac{1}{2}(r_1 + r_3)$ . For the same reason stated in the previous case, it is desirable to have the radial-flow path consisting of a sinusoidal curve superimposed on the line passing through  $(z_1, r_1)$  and  $(z_3, r_3)$ ; that is

$$r = r_1 + \frac{r_3 - r_1}{2} \frac{z}{L} + \frac{1}{2} \left( r_2 - \frac{r_1 + r_3}{2} \right) \left( 1 - \cos \frac{\pi z}{L} \right) \quad (22)$$

Then

$$V_r = \frac{dr}{dz} V_z = V_z \left[ \frac{r_3 - r_1}{2L} + \frac{1}{2} \left( r_2 - \frac{r_1 + r_3}{2} \right) \frac{\pi}{L} \sin \frac{\pi z}{L} \right] \quad (23)$$

and

$$-\left( \frac{\partial V_r}{\partial z} \right)_i = (-1)^i \frac{1}{2} \left( r_2 - \frac{r_1 + r_3}{2} \right) \frac{\pi^2}{L^2} V_{z,i}$$

inasmuch as  $\partial V_z / \partial z$  is practically zero in passing through the gap. With this value of  $\partial V_r / \partial z$ , the radial-equilibrium equation (7g) becomes

$$\frac{dH_1}{dr_1} = T_1 \frac{ds_1}{dr_1} + \frac{f_1}{r_1} \frac{df_1}{dr_1} + V_{z,i} \frac{dV_{z,i}}{dr_1} + (-1)^i \frac{1}{2} \left( r_2 - \frac{r_1 + r_3}{2} \right) \frac{\pi^2}{L^2} V_{z,i}^2 \quad (24)$$

where

$$i = 1, 2, 3$$

This equation is similar to equation (21). (If  $r_3 = r_1$ , it reduces to equation (21).) A similar equation in dimensionless  $r_1'$  can also be obtained for this case by dividing  $r_1$  by  $(r_t - r_h)_i$ .

At any point  $(z, r)$  within the blade region, the magnitude of  $F_r$  consistent with this sinusoidal radial-flow path is obtained from equations (7g) and (23):

$$F_r = \frac{\partial H}{\partial r} - T \frac{\partial S}{\partial r} - \frac{\xi}{r^2} \frac{\partial \xi}{\partial r} - v_z \frac{\partial v_z}{\partial r} + \frac{r_3 - r_1}{2L} v_z \frac{\partial v_z}{\partial z} + \frac{1}{2} \left( r_2 - \frac{r_1 + r_3}{2} \right) \frac{\pi}{L} v_z \left( v_z \frac{\pi}{L} \cos \frac{\pi z}{L} + \sin \frac{\pi z}{L} \frac{\partial v_z}{\partial z} \right) \quad (25)$$

### Degrees of Freedom in Design

Before starting to design a turbomachine it is necessary to decide how the velocity and other properties of the gas should vary radially at successive axial stations to give the best type of design for the particular application. It is therefore necessary for the designer to know beforehand the maximum compatible number of such variations that can be specified.

In the discussion entitled "Method of finite difference for successive axial stations" it is seen that theoretically radial variation of two gas properties can be specified by the designer at each axial station within the blade region with the blade forces determined accordingly. In the free space between blade rows, the properties of gas remain constant along the streamline and no arbitrary change can be specified. In current design practice, the usual procedure is to specify the desirable gas conditions only at stations between blade rows (as well as before the first and after the last blade row) and then either to select some standard blade sections or to design them on the basis of prescribed velocity distribution to achieve the desired change of gas state across the blade row. In either way, one degree of freedom at the second such station is taken up in going from the first station to the second station. The designer is therefore free to specify only one condition at each station throughout the machine, with the exception of one station, usually the entrance station to the first stage.

Ways of specifying degrees of freedom. - In this discussion the following two fundamental equations will be used:

In the stations between blade rows, if the radial variation of entropy is negligible, the radial-equilibrium equation (7g) reduces to

$$\frac{dH_1}{dr_1} = \frac{\xi_1}{r_1^2} \frac{d\xi_1}{dr_1} + v_{z,1} \frac{dv_{z,1}}{dr_1} - v_{z,1} \left( \frac{\partial v_r}{\partial z} \right)_1 \quad (26)$$

Equation (8b) is applied to three successive stations of a stage for the case where there is negligible heat transfer and is differentiated with respect to  $r_1$

$$\frac{dH_1}{dr_1} + \omega \left( \frac{d\xi_2}{dr_2} \frac{dr_2}{dr_1} - \frac{d\xi_1}{dr_1} \right) = \frac{dH_2}{dr_2} \frac{dr_2}{dr_1} = \frac{dH_3}{dr_3} \frac{dr_3}{dr_1} \quad (27)$$

The following ways of taking up the degrees of freedom at these stations between successive blade rows are discussed.

(1) Constant work per unit mass of gas flow over the blade height. This condition is usually specified in the design of a turbomachine. It relates  $\xi$  after the rotor to its value before the rotor in the following manner

$$\xi_2(r_2) = \xi_1(r_1) + r_{1,t} \delta_t U_{1,t} \quad (28)$$

or

$$\frac{d\xi_2}{dr_2} \frac{dr_2}{dr_1} = \frac{d\xi_1}{dr_1} \quad (28a)$$

where  $r_{1,t} \delta_t U_{1,t}$  is equal to  $(\xi_2 - \xi_1)$  at the blade tip and is also equal to  $(\xi_2 - \xi_1)$  at other radii.

Constant work over the blade height gives constant total-enthalpy change over the blade height. If the velocity at the exit of a stage is equal to that at the entrance, this condition also gives constant static-enthalpy change over the blade height.

Under the condition of constant work, equation (27) reduces to

$$\frac{dH_1}{dr_1} = \frac{dH_2}{dr_2} \frac{dr_2}{dr_1} = \frac{dH_3}{dr_3} \frac{dr_3}{dr_1} \quad (27a)$$

(2) Constant total enthalpy over the blade height:

$$\frac{\partial H}{\partial r} = 0 \quad (29)$$



This condition holds for the first stage of a compressor and will hold for all succeeding stages if constant work per unit mass over the blade height is employed. If a nonzero value of  $dH_1/dr_1$  is desired, an initial preparatory stage must be specially designed to obtain this value. In the last stage, however, it is usually desirable that  $\partial H/\partial r$  be nearly zero.

(3) Free-vortex-type distribution of tangential velocity:

$$\frac{\partial \xi}{\partial r} = 0 \quad (30)$$

or

$$\xi_1 = r_1 V_{\theta,1} = K_1 \quad (30a)$$

This condition is commonly used in turbines and compressors. For incompressible flow, in addition to this condition, constant total enthalpy and constant axial velocity over the blade height can be specified. But for compressible flow, radial motion exists and only one of the two additional conditions can be obtained in conjunction with equation (30). (See NUMERICAL EXAMPLE AND DISCUSSION.)

(4) Symmetrical velocity diagram. If  $V_{z,1} = V_{z,2}$  and  $r_1 = r_2 = r$ , the symmetrical velocity diagram gives

$$V_{\theta,1} + V_{\theta,2} = \omega r \quad (31)$$

or

$$\xi_1 + \xi_2 = \omega r^2 \quad (31a)$$

Differentiating with respect to  $r$  yields:

$$\frac{d\xi_1}{dr} + \frac{d\xi_2}{dr} = 2\omega r \quad (31b)$$

If  $r_1 \neq r_2$  or  $V_{z,1} \neq V_{z,2}$ , the symmetrical velocity diagrams may be defined by

$$\xi_1(r_1) + \xi_2(r_2) = \omega r_1^2 \quad (32)$$

Then

$$\frac{d\xi_1}{dr_1} + \frac{d\xi_2}{dr_1} = 2\omega r_1 \quad (32a)$$

If  $V_{\theta,3} = V_{\theta,1}$ , and  $V_{z,3} = V_{z,2} = V_{z,1}$ , the symmetrical velocity diagram gives very similar flows through the rotor and the stator, experiencing the same turning. The change in static pressure or enthalpy is the same in passing through the rotor or the stator and the stage is therefore often referred to as the "50-percent reaction stage." Reference 6 shows that the blade-profile loss is a minimum with the symmetrical velocity diagram if the drag-lift ratio is constant.

(5) Constant axial velocity over the blade height:

$$\frac{\partial v_z}{\partial r} = 0 \quad (33)$$

At very low speed of gas flow with no change in density, the specific mass flow is also constant over the blade height; therefore, there is no radial flow across the blade row and equation (26) reduces to

$$\frac{\partial H}{\partial r} - \frac{1}{r^2} \xi \frac{\partial \xi}{\partial r} = 0 \quad (34)$$

And in case

$$\frac{\partial H}{\partial r} = 0$$

then

$$\frac{\partial \xi}{\partial r} = 0$$

The equivalence of equations (33) and (34) breaks down, however, for current aircraft applications, in which cases the speed of gas flow is high.

If equation (34) is substituted into the radial-equilibrium equation (26), there is obtained

$$\frac{\partial v_z}{\partial r} - \frac{\partial v_r}{\partial z} = 0 \quad (34a)$$

The left-hand side of equation (34a) is the tangential component of fluid rotation  $\nabla \times \bar{V}$ ; thus equation (34) is a condition for potential flow in the free space between blade rows.

If it is desired to correct for the effect of the boundary layers at the inner and outer walls of the gas passage, instead of equation (33) an appropriate axial-velocity variation close to the actual one may be prescribed in design:

$$\frac{\partial v_z}{\partial r} = \varphi(r) \quad (33a)$$

(6) Constant specific mass flow over the blade height. In order to avoid radial movement across the blade row in compressible flow, it has been suggested (for example, in reference 7) that constant axial velocity be replaced by constant specific mass flow

$$\frac{dG_1}{dr} = \frac{dG_2}{dr} = \frac{dG_3}{dr} = 0 \quad (35)$$

Radial displacement can also be prevented by the use of two conditions instead of three

$$\frac{dG_1}{dr} = \frac{dG_2}{dr} = \frac{dG_3}{dr} \quad (36)$$

For designs using either of these two conditions, the simplified-radial-equilibrium calculation is more correct. Designs employing no radial flow have the advantage that the calculation does not involve any radial displacement across the blade row and that the two-dimensional-cascade data can be directly applied. The equations for tangential- and axial-velocity distributions derived from these equations (equations (35) and (36)), however, are difficult to solve and the conditions are incompatible with tapered passage in a multistage turbomachine.

(7) Constant Mach number relative to blade. For a fixed ratio of exit to entrance velocity relative to the blade, the temperature or pressure change of gas across the blade row at any radius is proportional to the square of the entrance Mach number of gas

relative to the blade at that radius. It might therefore be desirable to reach the Mach-number limitation at all radii. That is, for the rotor,

$$M_L^2 = \frac{W_1^2}{a_1^2} = \frac{V_{z,1}^2 + (\omega r_1 - V_{\theta,1})^2}{(\gamma-1) \left( H_1 - \frac{V_{z,1}^2 + V_{\theta,1}^2}{2} \right)} \quad (37)$$

where  $M_L$  is the limiting inlet Mach number for the blade. Differentiating with respect to  $r_1$  gives

$$(\gamma-1) M_L^2 \frac{dH_1}{dr_1} = \left( 1 + \frac{\gamma-1}{2} M_L^2 \right) \frac{d}{dr_1} (V_{z,1}^2 + V_{\theta,1}^2) + 2\omega \left[ \omega r_1 - \frac{d(r_1 V_{\theta,1})}{dr_1} \right] \quad (37a)$$

For stator

$$M_L^2 = \frac{V_2^2}{a_2^2} = \frac{V_{z,2}^2 + V_{\theta,2}^2}{(\gamma-1) \left( H_2 - \frac{V_{z,2}^2 + V_{\theta,2}^2}{2} \right)} \quad (38)$$

Differentiating yields

$$(\gamma-1) M_L^2 \frac{dH_2}{dr_2} = \left( 1 + \frac{\gamma-1}{2} M_L^2 \right) \frac{d}{dr_2} (V_{z,2}^2 + V_{\theta,2}^2) \quad (38a)$$

Equations (37a) and (38a) may be combined with equation (26) to eliminate H.

(8) Constant turning. If the maximum work for a given size is desirable, the limiting turning value may be reached at all radii, which will give, of course, a radial gradient in total enthalpy after the first blade row. This gradient may not be serious in a single- or two-stage unit, but it may not be desirable to use it for all stages of an eight- or nine-stage unit. For compressors, the limiting turning may be expressed by (reference 2)

$$\frac{V_{\theta,2} - V_{\theta,1}}{V_{z,1}} = \varphi(\sigma) \quad (39)$$

or

$$V_{\theta,2} = V_{\theta,1} + \varphi(\sigma) V_{z,1} \quad (39a)$$

where  $\sigma$  is the solidity of the blade element at radius  $r$ . Differentiating yields

$$\frac{dV_{\theta,2}}{dr_2} \frac{dr_2}{dr_1} = \frac{dV_{\theta,1}}{dr_1} + V_{z,1} \frac{d\varphi(\sigma)}{dr_1} + \varphi(\sigma) \frac{dV_{z,1}}{dr_1} \quad (39b)$$

(9) In multistage machines, similar variation in either tangential velocity, axial velocity, or specific mass flow may be specified at the similar stations of each stage

$$\frac{d\xi_1}{dr_1} = \frac{d\xi_3}{dr_3} \frac{dr_3}{dr_1} \quad (40)$$

$$\frac{dV_{z,1}}{dr_1} = \frac{dV_{z,3}}{dr_3} \frac{dr_3}{dr_1} \quad (41)$$

or

$$\frac{dG_1}{dr_1} = \frac{dG_3}{dr_3} \frac{dr_3}{dr_1} \quad (42)$$

Stages of multistage machines designed for similar variations of gas properties from stage to stage are termed "typical stages."

Types of design. - A large number of different types of design may be obtained by different combinations of those conditions specified in equations (26) to (42). These designs may be conveniently divided into two groups. In the first group, the condition of constant work at all radii is specified in the design. That is, equation (28) is specified, which gives:

1035

$$\left. \begin{aligned} & \frac{d\xi_1}{dr_1} = \frac{d\xi_2}{dr_1} \\ \text{and} & \\ & \frac{dH_1}{dr_1} = \frac{dH_2}{dr_1} = \frac{dH_3}{dr_1} \end{aligned} \right\} \quad (43)$$

In cases where the symmetrical velocity diagram is also specified, equations (32a) and (43) give

$$\left. \begin{aligned} & \frac{d\xi_1}{dr_1} = \frac{d\xi_2}{dr_1} = \omega r_1 \\ \text{and} & \\ & \frac{dH_1}{dr_1} = \frac{dH_2}{dr_1} = \frac{dH_3}{dr_3} \end{aligned} \right\} \quad (44)$$

In the second group, the condition of constant work is not specified.

The following tables present a few types of design in each of the two groups. The way in which the degrees of freedom are taken up at each station and the known characteristics of each type are given. In the tables, subscript *i* refers to any station in the machine; *k* refers to any station in front of rotor, that is, stations 1, 3, 5, . . .; and *l* refers to any station in front of stator, that is, stations 2, 4, 6, . . . . A typical stage may be considered as composed of either stations 1, 2, and 3 or stations 2, 3, and 4.

GROUP I

Type	Station	Conditions specified at three stations of any stage	One more condition specified at certain station in machine	Characteristics of any stage
1. Free vortex and constant total enthalpy	1	$\frac{dt_1}{dr_1} = 0$	$\frac{dH_1}{dr_1} = 0$	$\frac{dt_1}{dr_1} = \frac{dt_2}{dr_2} = \frac{dt_3}{dr_3} = 0$ $V_{\theta,1} = k_1/r_1$ $\left(\frac{\partial v_z}{\partial r} - \frac{\partial v_r}{\partial z}\right)_1 = 0$ Small radial gradient in axial velocity for compressible flow Constant axial velocity over blade height for incompressible flow
	2	Constant work		
	3	$\frac{dt_1}{dr_1} = \frac{dt_3}{dr_3}$		
2. Symmetrical velocity diagram and constant total enthalpy	1	{ Symmetrical velocity diagram; constant work $\frac{dt_1}{dr_1} = \frac{dt_3}{dr_3}$	$\frac{dH_1}{dr_1} = 0$	$\frac{dt_1}{dr_1} = \frac{dt_2}{dr_2} = \frac{dt_3}{dr_3} = \omega r_1$ $V_{\theta,1} = \frac{\omega r_1}{2} - \frac{\delta_t U_{1,t} r_{1,t}}{r_1}$ $\frac{dH_1}{dr_1} = \frac{dH_2}{dr_2} = \frac{dH_3}{dr_3} = 0$ $V_{\theta,2} = \left(\frac{\omega r_1}{2} + \frac{\delta_t U_{1,t} r_{1,t}}{r_1}\right) \frac{r_1}{r_2}$ } Combination of wheel-type and vortex-type tangential velocities  Large negative radial gradient of axial velocity at all stations
	2			
	3			
3. Symmetrical velocity diagram and constant axial velocity in front of rotor	1	{ Symmetrical velocity diagram; constant work $\frac{dv_{z,1}}{dr_1} = \frac{dv_{z,3}}{dr_3}$	$\frac{dv_{z,k}}{dr_k} = 0$	$\frac{dt_1}{dr_1} = \frac{dt_2}{dr_2} = \omega r_1$ $V_{\theta,1} = \frac{\omega r_1}{2} - \frac{\delta_t U_{1,t} r_{1,t}}{r_1}$ $\frac{dH_1}{dr_1} = \frac{dH_2}{dr_2} = \frac{dH_3}{dr_3}$ $V_{\theta,2} = \left(\frac{\omega r_1}{2} + \frac{\delta_t U_{1,t} r_{1,t}}{r_1}\right) \frac{r_1}{r_2}$ $\frac{dv_{z,1}}{dr_1} = \frac{dv_{z,3}}{dr_3} = 0$ Total enthalpy increases from hub to tip Behind rotor, axial velocity decreases from hub to tip
	2			
	3			
4. Symmetrical velocity diagram and constant axial velocity in front of stator	2	{ Symmetrical velocity diagram; constant work $\frac{dv_{z,2}}{dr_2} = \frac{dv_{z,4}}{dr_4}$	$\frac{dv_{z,l}}{dr_l} = 0$	$\frac{dt_3}{dr_3} = \frac{dt_4}{dr_4} = \omega r_3$ $V_{\theta,3} = \frac{\omega r_3}{2} - \frac{\delta_t U_{3,t} r_{3,t}}{r_3}$ $\frac{dH_2}{dr_2} = \frac{dH_3}{dr_3} = \frac{dH_4}{dr_4}$ $V_{\theta,4} = \left(\frac{\omega r_3}{2} + \frac{\delta_t U_{3,t} r_{3,t}}{r_3}\right) \frac{r_3}{r_4}$ $\frac{dv_{z,2}}{dr_2} = \frac{dv_{z,4}}{dr_4} = 0$ Total enthalpy increases from hub to tip Behind stator, axial velocity increases from hub to tip
	3			
	4			

GROUP I CONCLUDED

Type	Station	Conditions specified at three stations of any stage	One more condition specified at certain station in machine	Characteristics of any stage
5. Constant axial velocity	1 2 3	$\left\{ \begin{array}{l} \text{Constant work} \\ \frac{dv_{z,1}}{dr_1} = \frac{dv_{z,2}}{dr_1} \\ \\ \frac{dv_{z,1}}{dr_1} = \frac{dv_{z,3}}{dr_1} \end{array} \right.$	$\frac{dv_{z,1}}{dr_1} = 0$	$\frac{dt_1}{dr_1} = \frac{dt_2}{dr_1}$ $\frac{dH_1}{dr_1} = \frac{dH_2}{dr_1} = \frac{dH_3}{dr_1}$ $\frac{dv_{z,1}}{dr_1} = \frac{dv_{z,2}}{dr_2} = \frac{dv_{z,3}}{dr_3} = 0$ <p>In case of incompressible flow, this type requires no radial flow across blade rows. Under simplified-radial-equilibrium consideration this type is equivalent to first type in group.</p>
6. Constant specific mass flow	1 2 3	$\left\{ \begin{array}{l} \text{Constant work} \\ \frac{dG_1}{dr_1} = \frac{dG_2}{dr_1} \\ \\ \frac{dG_1}{dr_1} = \frac{dG_3}{dr_1} \end{array} \right.$	$\frac{dG_1}{dr_1} = 0$	$\frac{dt_1}{dr_1} = \frac{dt_2}{dr_1}$ $\frac{dH_1}{dr_1} = \frac{dH_2}{dr_1} = \frac{dH_3}{dr_1}$ $\frac{dG_1}{dr_1} = \frac{dG_2}{dr_2} = \frac{dG_3}{dr_3} = 0$ <p>No radial flow across rotor and stator blades in case of nontapered passage. Initial stage is necessary if entering gas has different radial gradient in total enthalpy than is required.</p>
7. Same variation in specific mass flow and constant total enthalpy	1 2 3	$\left\{ \begin{array}{l} \text{Constant work} \\ \frac{dG_1}{dr_1} = \frac{dG_2}{dr_2} \\ \\ \frac{dG_1}{dr_1} = \frac{dG_3}{dr_3} \end{array} \right.$	$\frac{dH_1}{dr_1} = 0$	$\frac{dt_1}{dr_1} = \frac{dt_2}{dr_1}$ $\frac{dH_1}{dr_1} = \frac{dH_2}{dr_2} = \frac{dH_3}{dr_3} = 0$ $\frac{dG_1}{dr_1} = \frac{dG_2}{dr_2} = \frac{dG_3}{dr_3}$ <p>No radial flow across rotor and stator blades in case of nontapered passage. Initial guide vane is necessary if entering gas has a different radial gradient of specific mass flow than is required.</p>



## GROUP II

Type	Station	Conditions specified at three stations of any stage	One more condition specified at certain station in machine	Characteristics of any stage
1. No radial displacement across blade rows throughout machine	1	$\frac{dG_1}{dr_1} = 0$	$\frac{\partial H}{\partial r}$ equal to a prescribed value at only one station in the machine	$\frac{dG_1}{dr_1} = \frac{dG_2}{dr_2} = \frac{dG_3}{dr_3} = 0$ plus $\frac{dH}{dr}$ equal to a prescribed value at only one station in the machine
	2	$\frac{dG_2}{dr_2} = 0$		
	3	$\frac{dG_3}{dr_3} = 0$		
2. Constant axial velocity and symmetrical velocity diagram	1	Symmetrical velocity diagram $\frac{dv_{z,1}}{dr_1} = \frac{dv_{z,2}}{dr_1}$ $\frac{dv_{z,1}}{dr_1} = \frac{dv_{z,3}}{dr_1}$	$\frac{dv_{z,1}}{dr_1} = 0$	$\frac{dv_{z,1}}{dr_1} = \frac{dv_{z,2}}{dr_2} = \frac{dv_{z,3}}{dr_3} = 0$ $\frac{dt_1}{dr_1} + \frac{dt_2}{dr_1} = 2\omega r_1$ Under simplified-radial-equilibrium consideration for nontapered passage, tangential velocities and work done are proportional to radius (wheel-type rotation) and square of radius, respectively. (See last part of appendix C.)
	2			
	3			

## GENERAL METHOD OF CALCULATION

## FOR GIVEN TYPE OF DESIGN

In the previous section, examples are given to show how the different types of design are obtained by specifying different conditions compatible with the degrees of freedom available. In the calculation of the variation of the gas state through a turbomachine of any given type of design, the effect of radial motion has to be included, in general, to get a more accurate value. The following procedure of calculation is suggested:

The first step of the calculation is to obtain an approximate solution by assuming that the gas flows on cylindrical and conical surfaces for straight and tapered passages, respectively, and by neglecting the effect of radial motion on the radial-equilibrium equation. This method is the usual simplified-radial-equilibrium calculation and gives an approximate solution for the case of very small blade-row aspect ratio.

The second step is to obtain the solution for the two extreme limiting cases of zero and infinite blade-row aspect ratio. If the difference between the two cases is not large, the solution for the case of a certain finite blade-row aspect ratio may be estimated from the two extremes. If the difference is found to be large, calculation has to be made for the finite aspect ratio.

In the calculation for the case of finite aspect ratio, the method developed using a sinusoidal curve gives exact results if such curve is prescribed in the design and is believed to give good approximate results in cases where it is not prescribed in the design. Even with this simplification, a series of successive approximations is required.

## Simplified-Radial-Equilibrium Calculation

In this approximation, equation (26) becomes

$$\frac{dH_1}{dr_1} = \frac{\xi_1}{r_1^2} \frac{d\xi_1}{dr_1} + V_{z,1} \frac{dV_{z,1}}{dr_1} \quad (26a)$$

In the case of nontapered passage,  $V_r = 0$ ,  $r_1 = r_2 = r_3 = r$ , and equation (26a) is equivalent to

$$\frac{dH_1}{dr_1} = \frac{d\left(\frac{V_1^2}{2}\right)}{dr} + \frac{V_{\theta,1}^2}{r} \quad (26b)$$

When equation (26a) is combined with equation (27)

$$\begin{aligned} \frac{\xi_1}{r_1^2} \frac{d\xi_1}{dr_1} + V_{z,1} \frac{dV_{z,1}}{dr_1} + \omega \left( \frac{d\xi_2}{dr_1} - \frac{d\xi_1}{dr_1} \right) &= \frac{\xi_2}{r_2^2} \frac{d\xi_2}{dr_1} + V_{z,2} \frac{dV_{z,2}}{dr_1} \\ &= \frac{\xi_3}{r_3^2} \frac{d\xi_3}{dr_1} + V_{z,3} \frac{dV_{z,3}}{dr_1} \end{aligned} \quad (27b)$$

For the case of constant work and nontapered passage, equation (27b) reduces to

$$\begin{aligned} V_{z,1} \frac{dV_{z,1}}{dr} &= V_{z,2} \frac{dV_{z,2}}{dr} + \frac{1}{r^2} r_{1,t} \delta_t U_{1,t} \frac{d\xi_1}{dr} \\ &= V_{z,3} \frac{dV_{z,3}}{dr} + \frac{1}{r^2} \left( \xi_3 \frac{d\xi_3}{dr} - \xi_1 \frac{d\xi_1}{dr} \right) \end{aligned} \quad (27c)$$

The radial variation of density and pressure is obtained from equations (26a), (A5), and (A8) (appendix A) for the case  $\frac{\partial s}{\partial r} = 0$ :

$$\frac{p_{t,1}^{\frac{1}{\gamma}}}{\rho_{t,1}} p_1^{-\frac{1}{\gamma}} \frac{dp_1}{dr_1} = \frac{V_{\theta,1}^2}{r_1} - V_{r,1} \frac{dV_{r,1}}{dr_1} \quad (45)$$

$$\gamma \frac{p_{t,1}}{\rho_{t,1}^{\gamma}} \rho_1^{\gamma-2} \frac{d\rho_1}{dr_1} = \frac{V_{\theta,1}^2}{r_1} - V_{r,1} \frac{dV_{r,1}}{dr_1} \quad (46)$$

In these two equations, the last term is very small compared with the next to last term and may be neglected. It becomes zero for the case of nontapered passage and the resulting equations can be more directly derived, as is usually done, by taking the approximation involved as the use of

$$\frac{1}{\rho_1} \frac{dp_1}{dr_1} = \frac{v_{\theta,i}^2}{r_1}$$

for the radial component of equation of motion in place of

$$\frac{1}{\rho_1} \frac{dp_1}{dr_1} = \frac{v_{\theta,i}^2}{r_1} - v_{z,i} \left( \frac{\partial v_r}{\partial z} \right)_1 - v_{r,i} \frac{dv_{r,i}}{dr}$$

For a given type of design and given design values of limiting Mach number and limiting turning, the variations of gas velocity at any inlet station of the stage are known. By inserting the radial variation of tangential velocity into equations (45) and (46), the radial variations of pressure  $p_1(r_1)$  and density  $\rho_1(r_1)$  are determined. By combining the variation of density with the variation of axial velocity, the variation of specific mass flow  $G_1(r_1)$  is obtained. The total mass flow across station 1 is then given by

$$\int_{r_{1,h}}^{r_{1,t}} 2\pi r_1 G_1 dr_1$$

The variation of gas properties at the next station (for example, station 2) must be such that the continuity equation is satisfied

$$\int_{r_{2,h}}^{r_{2,t}} 2\pi r_2 G_2 dr_2 = \int_{r_{1,h}}^{r_{1,t}} 2\pi r_1 G_1 dr_1$$

By assuming the value of a gas velocity, for example,  $v_{z,2}$  at the hub, the velocity and density variations at station 2 can be determined in a similar manner, and total mass flow can be obtained. The correct distribution of  $v_{z,2}$ , and so forth, which gives the correct value of total mass flow, can be obtained in two or three trials.

When the results obtained are substituted into the continuity equation (B5) (appendix B), over a portion of the annulus a certain amount of radial displacement across the blade row quite different from that assumed in the calculation is obtained. The result determined by this simplified-radial-equilibrium consideration is

only close to the case of zero aspect ratio of the blade row, which will be considered in the next section. This calculation can therefore be used only as a first approximation to the zero-aspect-ratio case and also to give a starting value for the calculation of a finite aspect ratio. In appendix C, formulas are given in dimensionless forms for this calculation for two common types of design.

#### Zero-Aspect-Ratio Calculations

The continuity equation in its integral form (equation (B5)) determines only the function  $r_2(r_1)$  and not values of  $\partial v_r / \partial z$ . Two limiting cases will now be discussed for which the evaluation of the term  $\partial v_r / \partial z$  is unnecessary. If the blade row has an axial length sufficiently great relative to the blade height (that is, if the blade-row aspect ratio is sufficiently small), the term  $(\partial v_r / \partial z)_1$  will be negligible in spite of any radial displacement required across the blade row. This extreme situation is designated the zero-aspect-ratio case and differs from the simplified-radial-equilibrium approximation in that the radial displacement across the blade row is properly determined and its effect on the state of gas is included in the calculation. For a constant-area gas passage without taper or with slight taper, this effect is small; consequently, a successive approximation procedure starting with the result of the simplified-radial-equilibrium calculation can be used. This procedure may be outlined as follows:

1. Using the simplified-radial-equilibrium approximation, find  $v_{z,1}$ ,  $v_{z,2}$ ,  $\xi_1$ ,  $\xi_2$ ,  $H_1$ ,  $H_2$ ,  $G_1$ , and  $G_2$  as functions of  $r_1$ .
2. Find  $r_2(r_1)$  by equation (B5), using the value of  $G_2(r_1)$  obtained from step 1.
3. Substitute these values of  $r_2(r_1)$  into equations (26) and (27) with the  $(\partial v_r / \partial z)$  term equal to zero, to get a second solution for  $v_{z,1}$ ,  $v_{z,2}$ ,  $\xi_1$ ,  $\xi_2$ ,  $H_1$ , and  $H_2$  as functions of  $r_1$ .
4. Repeat steps 2 and 3 if necessary, using the value of  $G_2(r_1)$  from step 3.

In step 1 of each process, the same procedure as in the previous calculation has to be followed. That is, the variation of gas

conditions at station 2 is such that it gives the same mass flow as that in station 1. In the case where there is considerable taper at the passage walls, it is better to assume  $r_2$  ( $r_1$ ) according to the taper to start the calculation rather than to use steps 1 and 2.

#### Infinite-Aspect-Ratio Calculation

The other limiting case corresponds to a blade row with axial length negligible as compared with the blade height; this case is designated the infinite-aspect-ratio case. The negligible axial length does not provide space for any appreciable radial displacement, hence for a nontapered passage  $r_2$  may be taken as equal to  $r_1$ , or

$$G_1 = G_2 \quad (47)$$

and for a tapered passage, a relation similar to the one that follows may be used:

$$G_2 = G_1 \frac{r_{1,t}^2 - r_{1,h}^2}{r_{2,t}^2 - r_{1,h}^2} \quad (47a)$$

Because the change in axial length for a very small change in  $V_r$  is also very small,  $(\partial V_r / \partial z)_1$  does not vanish. Although its absolute value does not affect the radial motion because of the negligible blade-row axial length, the relative value of  $\partial V_r / \partial z$  in front of and behind a blade row is needed to determine completely the distribution of gas properties at these stations. If the loading of the blade is relatively symmetrical or is designed to give a sinusoidal radial-flow path, the curvatures of the radial-flow path at the two stations are equal in magnitude and opposite in sense. Then

$$\left( \frac{\partial V_r}{\partial z} \right)_1 = - \left( \frac{\partial V_r}{\partial z} \right)_2 \quad (48)$$

In order to combine this relation with equation (26) in a simple manner, it may be assumed that

$$V_{z,1} \left( \frac{\partial V_r}{\partial z} \right)_1 = - V_{z,2} \left( \frac{\partial V_r}{\partial z} \right)_2 \quad (49)$$

Then combining equation (49) with equation (26) at stations 1 and 2

$$V_{z,1} \frac{dV_{z,1}}{dr} + V_{z,2} \frac{dV_{z,2}}{dr} = \frac{dH_1}{dr} + \frac{dH_2}{dr} - \frac{\xi_1}{r^2} \frac{d\xi_1}{dr} - \frac{\xi_2}{r^2} \frac{d\xi_2}{dr} \quad (49a)$$

For a typical stage of a given design, equation (47) or (47a) together with either equation (48) or equation (49) will completely determine the variation of gas properties at the two stations. If the variation of gas properties is completely given at one station, equation (47) or (47a) alone completely determines the gas state at the other station.

In appendix D, formulas are given in dimensionless forms for two common types of design to calculate the variations of gas properties for the two preceding limiting cases. The results so obtained will give the limits of the variation of the gas properties along the blade height. If the difference is large, it is worthwhile to make the following calculation for a finite blade-row aspect ratio.

#### Finite-Aspect-Ratio Calculation

The results previously obtained for a sinusoidal radial-flow path is used. Inasmuch as there is no general analytical solution of equations (13a), (14a), (24), and (27) that is possible even for simple types of design, the method of successive approximation is used.

The procedure of this calculation is somewhat similar to that used in the case of zero aspect ratio. In the case where a tapered passage or difference in design calls for an  $r_3$  different from  $r_1$ , first estimate the radial positions of gas particles at stations 2 and 3,  $r_2$  and  $r_3$ , respectively, as functions of  $r_1$ . Then calculate the variation of gas properties at stations 1, 2, and 3 by equations (13a), (24), and (27), such that the total mass flow is the same at the three stations. Using this result, find  $r_2(r_1)$  and  $r_3(r_1)$  by the continuity equation (B5) and see if they check the assumed values. By interpolating  $r_2(r_1)$  and  $r_3(r_1)$  obtained after a few trials at different  $r_1$ , the value obtained by the next try will be close to the correct value.

For the general case where  $H_1$ ,  $H_2$ ,  $\xi_1$ , and  $\xi_2$  are determined by design as functions of  $r_1$ , a rough approximate solution gives (see appendix E)

$$r_2 - r_1 = \frac{(r_2 - r_1)_s}{1 + A^2} \quad (50)$$

This value can be used as a starting value for more exact calculation or may be used as the final value for approximate calculation. This approximate value of radial displacement across the rotor is obtained in the following manner:

First take as two separate functions

$\Delta_e (r_1)$  the function  $(r_2 - r_1)$  of  $r_1$  satisfying radial-equilibrium and total-enthalpy-change equations (26) and (27), respectively, for a given distribution of the other variables

$\Delta_c (r_1)$  the function  $(r_2 - r_1)$  of  $r_1$  satisfying continuity equation (14) for a given distribution of other variables

It is assumed in this method that the radial gradients in  $V_z$  and  $\xi$  depend primarily on the magnitude of the radial displacement  $(r_2 - r_1)$  and not on its exact distribution. Accordingly  $\Delta_e (r_1)$  is set equal to

$$\Delta_e (r_1) = y_e g (r_1) \quad (51)$$

where  $y_e$  is the maximum value of  $\Delta_e$  and  $g (r_1)$  is a plausible form for the distribution of  $\Delta_e$  satisfying the boundary conditions:

$$\text{for } \left. \begin{array}{l} g (r_{1,h}) = g (r_{1,t}) = 0 \\ g' (r_{1,n}) = 0, g (r_{1,n}) = 1 \end{array} \right\} \quad (52)$$

If  $\Delta_c$  is calculated for a couple of values of  $\Delta_e$ , it is possible to plot  $y_c$ , the maximum value of  $\Delta_c$ , against  $y_e$ . A fairly good approximate solution might be expected to correspond to the point  $y_c = y_e$ . This process can be further refined by varying  $g(r_1)$  from the function originally assumed in the direction of the calculated function  $\Delta_c/y_c$ .



Distributions of gas properties calculated from  $r_2$  ( $r_1$ ) given by the approximate relation (equation (50)) has been found to agree much better with the value obtained by the previously described method of successive approximation than that calculated under simplified-equilibrium approximations.

#### NUMERICAL EXAMPLE AND DISCUSSION

The method of calculation outlined in the previous sections is applied to the typical stages of a compressor employing symmetrical velocity diagram and constant total enthalpy, and a compressor and a turbine employing free-vortex and constant-total-enthalpy design. The calculation is rendered dimensionless by expressing all velocities in terms of  $U_t$ , total enthalpy in terms of  $U_t^2$ , and  $r$  in terms of  $r_t$ . Because the main purpose of calculation is to determine the magnitude of the oscillatory radial motion and its effect on distribution of gas properties, a nontapered constant-area passage is used. Heat transfer is assumed to be zero in the calculation and the entropy is assumed to be constant at each station. The change of entropy across the blades at all radii is taken equal to that obtained from the polytropic efficiency assumed at the mean radius. It then gives a radial variation of polytropic efficiency decreasing from tip to hub. This variation seems to be in the same direction and of comparable magnitude with those obtained from experimental data. This calculation does not take into account the boundary layers at the rotor drum and the outer casing, and is consequently good only for the main portion of gas flowing between them.

In the comparison of different blade-row aspect ratios in each design, in addition to the same aerodynamic limitations, the same axial velocity at the mean radius is used. The comparison between different cases will be slightly different if another basis of comparison is used.

(1) Symmetrical velocity diagram and constant total enthalpy. - Because the difference between zero- and infinite-aspect-ratio cases is found to be large in this design, calculation is made for a blade-row aspect ratio of 2. The design constants used for all cases are:

Hub-tip ratio . . . . .	0.6
Limiting Mach number relative to rotor blade . . . . .	0.8
Limiting value of $\frac{V_{\theta,2} - V_{\theta,1}}{V_{z,1}}$ . . . . .	0.7
Polytropic efficiency at mean radius . . . . .	0.9
$V_{z,1,m}/U_t$ . . . . .	0.772

(The last value results from the use of  $V_{z,1,h}/U_t = 0.8$  in the simplified-radial-equilibrium calculation, and is used for all cases.) The results of the calculation are shown in figure 4.

Figure 4(a) shows the distribution of specific mass flow in front of and behind the rotor for the different cases considered. It may be seen that in all cases except the infinite-aspect-ratio case, the specific mass flow  $G/G_t$  increases toward the hub faster behind the rotor than in front of the rotor; in other words, passing through the rotor the gas moves toward the axis of the machine. The magnitude of this displacement is obtained from the continuity relation and is shown in figure 4(b). In the simplified-radial-equilibrium calculation, it is assumed that there is no radial motion, but when the distribution of specific mass flow is substituted in the continuity equation (B5), quite large radial displacement across the blade is obtained. This kind of calculation is therefore not a good one. In other calculations, the distributions of gas properties are calculated from assumed radial displacements that are to be checked with the displacements required from the continuity relation with these distributions, and are therefore consistent in themselves. The radial displacement to be used in the approximate calculation for  $A = 2$  is obtained by the approximate formula (equation (50)) and is about 25 percent lower than the correct value.

The variation of axial velocities is presented in figure 4(c), which shows that the axial velocities increase toward the hub in all cases but at different rates. The high value of axial velocity at the hub before the root allows the use of higher turnings throughout the blade height without exceeding the limiting value of  $(V_{\theta,2} - V_{\theta,1})/V_{z,1}$  or  $\sigma_{CL}$  at the hub. It also helps to give a more uniform Mach number relative to the rotor blade over the blade height. As a result, this type of design gives a higher pressure rise and a higher specific mass flow than a free-vortex type of design using the same design limitations. In order to utilize this advantage fully, the variation of axial velocity should be correctly determined.

The calculation of axial velocity based on simplified radial equilibrium gives a result close to the zero-aspect-ratio case, which is also true in the distribution of other properties in this calculation, because in the case of zero aspect ratio, the curvature caused by radial motion is negligible and the difference in gas properties caused by the radial displacement is very small in the case of a nontapered passage.

The variation of tangential velocities is shown in figure 4(d). These velocities in different cases vary in a similar manner and the difference of magnitude between them is mainly due to the different value of  $\delta_t$  determined by the different values of  $V_{z,l,h}/U_t$  in the various cases.

Figure 4(e) shows the variation of air angles entering the rotor and stator blades. The difference between the simplified-radial-equilibrium calculation and the case of aspect ratio of 2 is significant throughout the whole blade height. The simplified-radial-equilibrium calculation gives an error of about  $-3^\circ$  at the tip of the rotor blade and at the hub of the stator blades. This difference results in an error in the angle of attack at the design point by that amount and the range of operation is also reduced.

The variation of Mach number relative to the rotor blades is shown in figure 4(f). The simplified-radial-equilibrium calculation gives a nearly constant value whereas the more correct calculation shows that Mach number actually decreases more than 10 percent toward the tip for the case of blade-row aspect ratio equal to 2. (This variation is only about half of that of a similar free-vortex compressor.)

Figure 4(g) shows the pressure distributions in front of and behind the rotor and the pressure rise across the rotor at different radii. The difference in pressure distributions may explain to a certain extent the difference found between measurement and simplified-radial-equilibrium calculation. The pressure rise across the rotor is fairly uniform in the case of an aspect ratio of 2 and is a desirable feature.

The velocity diagrams at three radii for aspect ratios of 0, 2, and  $\infty$  are shown in figure 4(h). If this stage is used as the first stage of a compressor, the permissible tip rotor speed of this design at standard sea-level conditions is equal to 868 and 826 feet per second for  $A = 0$  and  $A = 2$ , respectively. The

specific mass flow per unit annulus area corrected to standard sea-level conditions is equal to 41.5 and 40.0 pounds per square foot per second for  $A = 0$  and  $A = 2$ , respectively.

(2) Free-vortex and constant-total-enthalpy compressor. - The design constants used are the same as in the previous calculation. In addition,  $V_{\theta,1}$  and  $V_{\theta,2}$  are considered to be equal to  $W_{\theta,2}$  and  $W_{\theta,1}$ , respectively, at the mean radius. In this type of design, the simplified-radial-equilibrium approximation is equivalent to the zero-aspect-ratio case, because axial velocity is also constant over the blade height due to the constant  $H$  and constant  $\xi$  with respect to the radius and the negligible curvature effect caused by radial motion. That is, the same values of  $H_1$ ,  $H_2$ ,  $\xi_1$ ,  $\xi_2$ ,  $V_{z,1}$ , and  $V_{z,2}$  occur in both cases and the entire calculation is the same. (See also equation (E6).)

Because the radial motion involved in this type of design is due only to the compressibility of gas, the difference between the zero- and infinite-aspect-ratio cases is not large; hence the calculation for a finite-aspect-ratio case is not made.

The distribution of specific mass flow in front of and behind the rotor is presented in figure 5(a). Even in the zero-aspect-ratio or simplified-radial-equilibrium case with a constant axial-velocity distribution, there is considerable change in density, which requires an appreciable amount of outward radial motion to obtain the given design conditions behind the rotor. Although the amount of this radial motion is small (fig. 5(b)), its effect on the variation of gas properties is not entirely negligible. Its effect can be seen in the curves of figures 5(c) to 5(g), which are somewhat similar to the symmetrical-velocity-diagram and constant-total-enthalpy design in nature but of smaller magnitudes.

If this stage is used as the first stage of a compressor, the permissible tip rotor speed at standard sea-level conditions is equal to 758 feet per second for  $A = 0$ . This tip speed is about 13 percent lower than that of the corresponding case of the previous design. The specific mass flow corrected to standard sea-level conditions is equal to 38.6 pounds per square foot of annular area per second for  $A = 0$ , which is 7 percent lower than that of the corresponding case of the previous design.

(3) Free-vortex and constant-total-enthalpy turbine. - The design constants used in the calculation are:  $M_L < 1$ ,  $U_t/a_{1,t} = 0.5$ ,  $V_{\theta,1,h}/a_{1,t} = 0.8$ ,  $V_{z,1,m}/a_{1,t} = 0.4$ ,  $V_{\theta,2} = 0$ , and polytropic efficiency at mean radius equal to 0.87. For the simplified-radial-equilibrium approximation or zero aspect ratio,  $V_{z,1}/U_t$  is constant and so is  $V_{z,2}/U_t$ , which is found by the continuity relation to be equal to 0.877. The same velocity at station 2 is used for the case of infinite aspect ratio, thus making the only difference at station 1. The results of the calculation are shown in figure 6.

The distribution of specific mass flow in front of and behind the rotor is shown in figure 6(a). Because of the constant axial exit velocity, the specific mass flow is constant behind the rotor. Except for the case of infinite aspect ratio, there is an inward radial motion of gas in passing through the rotor (fig. 6(b)), the magnitude of which is about two and one-half times that in the previous free-vortex compressor (fig. 5(b)).

The variation of axial velocity in front of the rotor is shown in figure 6(c). An increasing axial velocity toward the hub of about 15 percent would be required for an aspect ratio of 2.

Figure 6(d) shows the radial variation of gas angles entering rotor blades. The difference is only important at the hub. In the actual case of an aspect ratio of 2, the simplified calculation would give an angle of attack  $3^\circ$  to  $4^\circ$  too high at the hub.

The absolute and relative Mach numbers of gas in front of the rotor are shown in figure 6(e). In the actual case of an aspect ratio of 2, the Mach number at the hub is about 3 percent higher than the simplified calculation.

Figure 6(f) shows the pressure distribution in front of the rotor. For an aspect ratio of 2, the pressures at the tip and at the hub are about 2 percent higher and 3 percent lower than the simplified calculation, respectively.

The velocity diagrams at three radii for the zero and infinite aspect ratios are shown in figure 6(g).

## SUMMARY OF ANALYSIS AND CALCULATIONS

In axial-flow turbomachines, radial motion of gas occurs because of the tapering of the passage and the variation of gas conditions across blade rows specified in the design. The direction and the magnitude of this radial flow depend on the type of design, the tapering of the passage, the hub-tip ratio, the blade-row aspect ratio, and the speed of gas flow. Even in the case of free-vortex type of design employing a nontapered passage and requiring no change in velocity distributions from stage to stage, there is an appreciable amount of oscillatory radial motion within the stage.

This radial motion gives an additional term to the ordinary radial-equilibrium equation. In the free space between blade rows, this additional term is very nearly equal to the product of the square of axial velocity and the curvature caused by the radial flow. Depending on whether the curvature is positive or negative, the radial-pressure gradient caused by the whirling motion of gas is decreased or increased, respectively, by this additional term.

The determination of this radial-flow path requires a long process of step-by-step calculation. It is found, however, that a sinusoidal radial-flow path gives an effect on the radial variation of gas condition between blade rows as small as possible without discontinuity in the curvature of the streamline. Inasmuch as it represents the major harmonic of the radial-flow path that may exist in any design in which the radial blade force is effectively small, the calculation based on this simple radial-flow path gives good approximate results. It probably underestimates the effect because of the neglect of higher harmonics.

The analysis made of the maximum compatible number of the degrees of freedom in specifying the radial variations of gas properties in stations between successive blade rows of a turbomachine shows that under the conventional design procedure the designer is free to specify two conditions at any one station and one condition at each of the remaining stations. The various ways to use up these degrees of freedom and the resultant types of design obtained are discussed.

The usual method of calculation, which neglects the radial motion, gives results close only to the case in which the axial length of the blade row is much larger than its radial length, and is not good for the case of a finite blade-row aspect ratio.

The difference between the results obtained by the usual method and the method suggested herein is found to be quite large in a design employing constant total enthalpy and symmetrical velocity diagram. Calculation made for this type of compressor using the same limiting Mach number, same limiting turning, same axial velocity at the mean radius, and for a blade-row aspect ratio of 2 gives the following differences between the usual and the suggested method:

1. The radial variation of axial velocity in front of the rotor is 13 percent for the usual method and 28 percent for the suggested method, and the radial variation of axial velocity behind the rotor is 53 percent for the former and 40 percent for the latter (all expressed in terms of their values at the mean radius).
2. The air angles differ from  $1^\circ$  to  $3^\circ$  at the hub and at the tip.
3. The radial variation of Mach number relative to the rotor blade in the former is 9 percent lower than that in the latter.
4. The radial variation in static-pressure rise across the rotor is 13 percent for the former and only 2 percent for the latter.
5. The mass flow in the former is 4 percent higher than that in the latter.
6. The permissible rotor speed in the former is 5 percent higher than that in the latter.

Lewis Flight Propulsion Laboratory,  
National Advisory Committee for Aeronautics,  
Cleveland, Ohio, October 14, 1948.

## APPENDIX A

## DERIVATION OF EQUATIONS IN ANALYSIS

From equation (3), the definition of  $h$ , and the relations

$$du = c_v dT \quad (A1)$$

and 
$$R = c_p - c_v \quad (A2)$$

$$\gamma = \frac{c_p}{c_v} \quad (A3)$$

there is obtained

$$dh = \frac{\gamma}{\gamma-1} d\left(\frac{p}{\rho}\right) \quad (A4)$$

From equations (1) and (A4)

$$dH = \frac{\gamma}{\gamma-1} d\left(\frac{p}{\rho}\right) + d\left(\frac{v^2}{2}\right) \quad (A5)$$

From equation (2) and the definition of  $h$

$$T ds = dh - \frac{dp}{\rho} \quad (A6)$$

Using equation (A4)

$$T ds = \frac{\gamma}{\gamma-1} d\left(\frac{p}{\rho}\right) - \frac{dp}{\rho} \quad (A7)$$

From equations (2) and (3)



$$\begin{aligned} d\left(\frac{s}{R}\right) &= \frac{1}{\gamma-1} \frac{dp}{p} - \frac{\gamma}{\gamma-1} \frac{d\rho}{\rho} \\ &= \frac{1}{\gamma-1} d\left(\log_e \frac{p}{\rho^\gamma}\right) \end{aligned} \quad (A8)$$

$$= \frac{1}{\gamma-1} d\left(\log_e \frac{p}{\rho}\right) - d(\log_e \rho) \quad (A9)$$

From equations (4) and the following relations

$$\frac{D\bar{V}}{Dt} = \frac{\partial \bar{V}}{\partial t} + (\bar{V} \cdot \nabla) \bar{V}$$

and

$$(\bar{V} \cdot \nabla) \bar{V} = \frac{1}{2} \nabla V^2 - \bar{V} \times (\nabla \times \bar{V})$$

there is obtained

$$\frac{\partial \bar{V}}{\partial t} - \bar{V} \times (\nabla \times \bar{V}) + \frac{1}{2} \nabla V^2 = \bar{F} - \frac{1}{\rho} \nabla p + \frac{\mu}{\rho} \nabla^2 \bar{V} + \frac{\mu}{3\rho} \nabla (\nabla \cdot \bar{V}) \quad (A10)$$

From equations (A5) and (A7)

$$\begin{aligned} \frac{1}{2} \nabla V^2 + \frac{1}{\rho} \nabla p &= \nabla H - \frac{\gamma}{\gamma-1} \nabla \left(\frac{p}{\rho}\right) + \frac{1}{\rho} \nabla p \\ &= \nabla H - T \nabla s \end{aligned}$$

Combination with equation (A10) yields

$$\nabla H = \bar{F} + T \nabla s + \bar{V} \times (\nabla \times \bar{V}) - \frac{\partial \bar{V}}{\partial t} + \frac{\mu}{\rho} \left[ \nabla^2 \bar{V} + \frac{1}{3} \nabla (\nabla \cdot \bar{V}) \right] \quad (7)$$

From equations (1) and (A6)

$$\begin{aligned} \frac{DH}{Dt} &= T \frac{Ds}{Dt} + \frac{1}{\rho} \frac{Dp}{Dt} + \bar{V} \cdot \frac{D\bar{V}}{Dt} \\ &= T \frac{Ds}{Dt} + \frac{1}{\rho} \frac{\partial p}{\partial t} + \bar{V} \cdot \left( \frac{1}{\rho} \nabla p + \frac{D\bar{V}}{Dt} \right) \end{aligned}$$

By combining with equation (4)

$$\frac{DH}{Dt} = T \frac{Ds}{Dt} + \frac{1}{\rho} \frac{\partial p}{\partial t} + \bar{v} \cdot \left\{ \bar{F} + \frac{\mu}{\rho} \left[ \nabla^2 \bar{v} + \frac{1}{3} \nabla (\nabla \cdot \bar{v}) \right] \right\} \quad (A11)$$

When equation (A11) is combined with equations (2) and (5)

$$\frac{DH}{Dt} = Q + \frac{\phi}{\rho} + \frac{1}{\rho} \frac{\partial p}{\partial t} + \bar{v} \cdot \left\{ \bar{F} + \frac{\mu}{\rho} \left[ \nabla^2 \bar{v} + \frac{1}{3} \nabla (\nabla \cdot \bar{v}) \right] \right\} \quad (8)$$

From equations (2) and (5)

$$T \frac{Ds}{Dt} = Q + \frac{\phi}{\rho}$$

or

$$\frac{Ds}{Dt} = \frac{Q}{T} + R \frac{\phi}{p} \quad (9)$$

From equations (6a), (3), and (A9), the following form of continuity relation is obtained:

$$\nabla \cdot \bar{v} + \frac{1}{\gamma-1} \frac{D}{Dt} \log_e T - \frac{D}{Dt} \left( \frac{s}{R} \right) = 0 \quad (10)$$

Equation (8a) is obtained by applying motion and energy equations to a mass system with a fixed control surface as shown by the solid lines in figure 3. Under steady axially symmetrical flow, the mass inflow  $dm_1$  in time  $dt$  is equal to the mass outflow  $dm_j$  in time  $dt$ , the state of gas within the control surface is not changed, and the state of gas at stations  $i$  and  $j$  is constant with respect to  $\theta$ . By equation (A10), the sum of the tangential blade force and the tangential viscous gas forces exerted by the surrounding gas particles on the system is equal to

$$\left\{ \frac{\partial v_\theta}{\partial t} - v_z \left[ \frac{1}{r} \frac{\partial v_z}{\partial \theta} - \frac{r v_\theta}{\partial z} \right] + v_r \left[ \frac{1}{r} \frac{\partial (r v_\theta)}{\partial r} - \frac{1}{r} \frac{\partial v_r}{\partial \theta} \right] + \frac{1}{r} \frac{\partial}{\partial \theta} \left( \frac{v_r^2 + v_\theta^2 + v_z^2}{2} \right) \right\} dm_1$$

$$= \left( \frac{\partial v_\theta}{\partial t} + v_r \frac{\partial v_\theta}{\partial r} + \frac{v_\theta}{r} \frac{\partial v_\theta}{\partial z} + v_z \frac{\partial v_\theta}{\partial z} + \frac{v_r v_\theta}{r} \right) dm_1 = \left( \frac{Dv_\theta}{Dt} + \frac{v_r v_\theta}{r} \right) dm_1 = \frac{1}{r} \frac{D(r v_\theta)}{Dt} dm_1$$

The torque about the z-axis exerted by these tangential forces on the system is therefore simply  $\frac{D(rV_\theta)}{Dt} dm_1$  and the work input to the system by these tangential forces in time  $dt$  is equal to

$$\frac{D(rV_\theta)}{Dt} dm_1 \omega dt = \omega [(rV_\theta)_j - (rV_\theta)_i] dm_1$$

In passing from station  $i$  to station  $j$ , beside receiving this work input, the gas particles are doing work against the axial and radial viscous forces exerted by the surrounding gas particles. However, this negative work is usually small, and if it is assumed that the heat generated from this frictional work is added back to the gas stream then the heat addition cancels the negative work, and the energy equation for steady flow gives

$$(H_j - H_i) dm_1 = \int_{t_i}^{t_j} Q dm_1 dt + \omega [(rV_\theta)_j - (rV_\theta)_i] dm_1$$

or

$$\frac{DH}{Dt} = Q + \omega \frac{D(rV_\theta)}{Dt} \quad (8a)$$

where  $Q$  denotes the rate per unit mass at which the gas stream sheet is receiving heat from external source through blades or other passage walls.

It may be noted that for steady nonviscous flow, equation (8a) can be obtained by using equation (11). For such flow, equation (8) becomes

$$\frac{DH}{Dt} = Q + \bar{F} \cdot \bar{V}$$

From equation (11) it can be seen that  $\bar{F} \cdot \bar{V}$  is equal to  $\bar{F} \cdot \bar{U}$ . However,  $\bar{F} \cdot \bar{U}$  is equal to  $F_\theta U$  or  $F_\theta r \omega$  and  $F_\theta r$  is, by equation (7h), equal to  $\frac{D(rV_\theta)}{Dt}$ . Hence the preceding equation becomes

$$\frac{DH}{Dt} = Q + \omega \frac{D(rV_\theta)}{Dt} \quad (8a)$$

When equation (12) is given, the entropy change can be obtained in the following manner. From equation (A9) and (3)

$$\frac{D}{Dt} \left( \frac{s}{R} \right) = \frac{1}{\gamma-1} \frac{D}{Dt} (\log_e T) - \frac{D}{Dt} (\log_e \rho) \quad (A12)$$

But by equations (12) and (3)

$$\frac{D}{Dt} \log_e \rho = \frac{1}{n-1} \frac{D}{Dt} \log_e T$$

Substitution into equation (A12) gives

$$\begin{aligned} \frac{Ds}{Dt} &= R \left( \frac{1}{\gamma-1} - \frac{1}{n-1} \right) \frac{D}{Dt} \log_e T \\ &= R \frac{n-\gamma}{(n-1)(\gamma-1)} \frac{D}{Dt} \log_e T \end{aligned} \quad (A13)$$

For steady axially symmetrical flow, equation (A13) reduces to

$$\frac{Ds}{Dt} = R \frac{n-\gamma}{(n-1)(\gamma-1)} \left( v_r \frac{\partial}{\partial r} \log_e T + v_z \frac{\partial}{\partial z} \log_e T \right) \quad (13)$$

For successive axial stations  $i$  and  $j$  a short distance apart, equation (A13) gives

$$\begin{aligned} s_j(r_j) - s_i(r_i) &= R \frac{n-\gamma}{(n-1)(\gamma-1)} \left[ \log_e T_j(r_j) - \log_e T_i(r_i) \right] \\ &= R \frac{n-\gamma}{(n-1)(\gamma-1)} \log_e \frac{T_j(r_j)}{T_i(r_i)} \end{aligned} \quad (A14)$$

Inasmuch as the temperature change between the two successive stations is small, the temperature ratio can be considered equal to the enthalpy ratio:

$$\frac{T_j}{T_i} = \frac{h_j}{h_i} = \frac{H_j - \frac{V_j^2}{2}}{H_i - \frac{V_i^2}{2}} \quad (A15)$$

Substitution of equation (A15) into equation (A14) gives

$$s_j (r_j) - s_i (r_i) = R \frac{n-\gamma}{(n-1)(\gamma-1)} \log_e \frac{H_j - \frac{V_j^2}{2}}{H_i - \frac{V_i^2}{2}} \quad (13a)$$

The density ratio between the two stations is obtained from equations (A9) and (3)

$$\frac{\rho_j}{\rho_i} = e^{-\frac{s_j - s_i}{R} \left(\frac{T_j}{T_i}\right)^{\frac{1}{\gamma-1}}} \quad (A16)$$

Combination with equation (A15) yields

$$\frac{\rho_j}{\rho_i} = e^{-\frac{s_j - s_i}{R} \left(\frac{H_j - \frac{V_j^2}{2}}{H_i - \frac{V_i^2}{2}}\right)^{\frac{1}{\gamma-1}}} \quad (A17)$$

Substitution into equation (14) gives

$$V_{z,j} \left(H_j - \frac{V_j^2}{2}\right)^{\frac{1}{\gamma-1}} e^{-\frac{s_j}{R}} r_j dr_j = V_{z,i} \left(H_i - \frac{V_i^2}{2}\right)^{\frac{1}{\gamma-1}} e^{-\frac{s_i}{R}} r_i dr_i \quad (14a)$$

## APPENDIX B

## DETERMINATION OF RADIAL DISPLACEMENT

## FROM CONTINUITY EQUATION

Equation (14) may be written as a linear differential equation for  $r_2^2$  as a function of  $r_1$ , provided  $G_2(r_1)$  is known

$$\frac{d(r_2^2)}{dr_1} = 2 \frac{G_1(r_1)}{G_2(r_1)} r_1$$

$$r_2^2 = - \int_{r_1}^{r_{1,t}} \frac{G_1(r_1)}{G_2(r_1)} 2r_1 dr_1 + r_{2,t}^2 \quad (B1)$$

when divided by  $r_{2,t}^2$

$$\left(\frac{r_2}{r_{2,t}}\right)^2 = 1 - \left(\frac{r_{1,t}}{r_{2,t}}\right)^2 \int_{r_1}^{r_{1,t}} \frac{G_1(r_1)}{G_2(r_1)} 2 \frac{r_1}{r_{1,t}} \frac{dr_1}{r_{1,t}} \quad (B2)$$

If  $G_1$  and  $G_2$  are not known, and only  $G_1/G_{1,t}$  and  $G_2/G_{2,t}$  are known, a modification is necessary

$$\left(\frac{r_2}{r_{2,t}}\right)^2 = 1 - \left(\frac{r_{1,t}}{r_{2,t}}\right)^2 \frac{G_{1,t}}{G_{2,t}} \int_{r_1}^{r_{1,t}} \frac{\frac{G_1}{G_{1,t}}(r_1)}{\frac{G_2}{G_{2,t}}(r_1)} 2 \frac{r_1}{r_{1,t}} \frac{dr_1}{r_{1,t}} \quad (B3)$$

The value of  $G_{1,t}/G_{2,t}$  is found by the condition that total mass flow at stations 1 and 2 is the same

$$\left(\frac{r_{1,t}}{r_{2,t}}\right)^2 \frac{G_{1,t}}{G_{2,t}} = \frac{1 - \left(\frac{r_{2,h}}{r_{2,t}}\right)^2}{\int_{r_{1,h}}^{r_{1,t}} \frac{\frac{G_1}{G_{1,t}}(r_1)}{\frac{G_2}{G_{2,t}}(r_1)} \frac{r_1}{r_{1,t}} \frac{dr_1}{r_{1,t}}} \quad (B4)$$

Hence

$$\left(\frac{r_2}{r_{2,t}}\right)^2 = 1 - \left[1 - \left(\frac{r_{2,h}}{r_{2,t}}\right)^2\right] \frac{\int_{r_{1,h}}^{r_{1,t}} \frac{\frac{G_1}{G_{1,t}}(r_1)}{\frac{G_2}{G_{2,t}}(r_1)} \frac{r_1}{r_{1,t}} \frac{dr_1}{r_{1,t}}}{\int_{r_{1,h}}^{r_{1,t}} \frac{\frac{G_1}{G_{1,t}}(r_1)}{\frac{G_2}{G_{2,t}}(r_1)} \frac{r_1}{r_{1,t}} \frac{dr_1}{r_{1,t}}} \quad (B5)$$

## APPENDIX C

## SIMPLIFIED-RADIAL-EQUILIBRIUM EQUATIONS

Equations to calculate distributions of gas properties under the simplified-radial-equilibrium approximation for a few types of design are given.

## Free Vortex and Constant Total Enthalpy

For this design

$$\frac{dH_i}{dr_i} = 0, \quad \frac{dt_{i,t}}{dr_i} = 0 \quad (C1)$$

from equation (26a) in the section entitled "Simplified-Radial-Equilibrium Calculation,"

$$\frac{dV_{z,i}}{dr_i} = 0 \quad (C2)$$

The variation in tangential velocity is, by equation (C1),

$$V_{\theta,i} = V_{\theta,i,t} \frac{r_{i,t}}{r_i} \quad (C3)$$

At each station, by using equations (46) and (C3),

$$\gamma \frac{p_t}{\rho_t} \rho^{\gamma-2} \frac{\partial \rho}{\partial r} = \frac{(V_{\theta,t} r_t)^2}{r^3}$$

When the preceding equation is integrated from  $r$  to  $r_t$ , and the relation

$$a = \sqrt{\frac{\gamma p}{\rho}}$$

is used, there is obtained



$$\frac{\rho}{\rho_t} = \left\{ 1 - \frac{\gamma-1}{2} \left( \frac{v_{\theta,t}}{a_t} \right)^2 \left[ \left( \frac{r_t}{r} \right)^2 - 1 \right] \right\}^{\frac{1}{\gamma-1}} \quad (C4)$$

This equation holds for all stations, provided the appropriate values of  $(v_{\theta,t}/a_t)$  are used. It follows from equation (C2) that at each station

$$\frac{G}{G_t} = \frac{\rho}{\rho_t} \quad (C5)$$

The radial position of gas at station 2 or 3 is then obtained by numerically integrating equation (B5) using distributions of specific mass flow given by equation (C5). An alternate method is to expand the right-hand side of equation (C4) into a binomial

series. Because  $\frac{\gamma-1}{2} \left( \frac{v_{\theta,t}}{a_t} \right)^2 \left[ \left( \frac{r_t}{r} \right)^2 - 1 \right]$  is usually less than 0.15, three terms will be sufficient. Let  $\bar{\rho}_r$  represent the average density in the annulus between  $r$  and  $r_t$ , then

$$\begin{aligned} \frac{\bar{\rho}_r}{\rho_t} &= \frac{\int_r^{r_t} 2\pi r \rho \, dr}{\pi(r_t^2 - r^2) \rho_t} \\ &= 1 + \frac{1}{2} \left( \frac{v_{\theta,t}}{a_t} \right)^2 + \frac{2-\gamma}{8} \left( \frac{v_{\theta,t}}{a_t} \right)^4 + \left[ \frac{1}{2} \left( \frac{v_{\theta,t}}{a_t} \right)^2 + \frac{2-\gamma}{4} \left( \frac{v_{\theta,t}}{a_t} \right)^4 \right] \frac{\log_e \left( \frac{r}{r_t} \right)^2}{1 - \left( \frac{r}{r_t} \right)^2} \\ &\quad + \frac{2-\gamma}{8} \left( \frac{v_{\theta,t}}{a_t} \right)^4 \left( \frac{r_t}{r} \right)^2 + \dots \quad (C6) \end{aligned}$$

as

$$\rho_{r,1} v_{z,1} \, dr_1 = \int_{r_2}^{r_{2,t}} 2\pi r \rho_{r,2} v_{z,2} \, dr_2$$

## APPENDIX C

## SIMPLIFIED-RADIAL-EQUILIBRIUM EQUATIONS

Equations to calculate distributions of gas properties under the simplified-radial-equilibrium approximation for a few types of design are given.

## Free Vortex and Constant Total Enthalpy

For this design

$$\frac{dH_i}{dr_i} = 0, \quad \frac{d\zeta_i}{dr_i} = 0 \quad (C1)$$

from equation (26a) in the section entitled "Simplified-Radial-Equilibrium Calculation,"

$$\frac{dv_{z,i}}{dr_i} = 0 \quad (C2)$$

The variation in tangential velocity is, by equation (C1),

$$v_{\theta,i} = v_{\theta,i,t} \frac{r_{i,t}}{r_i} \quad (C3)$$

At each station, by using equations (46) and (C3),

$$\gamma \frac{p_t}{\rho_t} \rho^{\gamma-2} \frac{\partial \rho}{\partial r} = \frac{(v_{\theta,t} r_t)^2}{r^3}$$

When the preceding equation is integrated from  $r$  to  $r_t$ , and the relation

$$a = \sqrt{\frac{\gamma p}{\rho}}$$

is used, there is obtained

$$\frac{\rho}{\rho_t} = \left\{ 1 - \frac{\gamma-1}{2} \left( \frac{v_{\theta,t}}{a_t} \right)^2 \left[ \left( \frac{r_t}{r} \right)^2 - 1 \right] \right\}^{\frac{1}{\gamma-1}} \quad (C4)$$

This equation holds for all stations, provided the appropriate values of  $(v_{\theta,t}/a_t)$  are used. It follows from equation (C2) that at each station

$$\frac{G}{G_t} = \frac{\rho}{\rho_t} \quad (C5)$$

The radial position of gas at station 2 or 3 is then obtained by numerically integrating equation (B5) using distributions of specific mass flow given by equation (C5). An alternate method is to expand the right-hand side of equation (C4) into a binominal series. Because  $\frac{\gamma-1}{2} \left( \frac{v_{\theta,t}}{a_t} \right)^2 \left[ \left( \frac{r_t}{r} \right)^2 - 1 \right]$  is usually less than 0.15, three terms will be sufficient. Let  $\bar{\rho}_r$  represent the average density in the annulus between  $r$  and  $r_t$ , then

$$\begin{aligned} \frac{\bar{\rho}_r}{\rho_t} &= \frac{\int_r^{r_t} 2\pi r \rho \, dr}{\pi(r_t^2 - r^2) \rho_t} \\ &= 1 + \frac{1}{2} \left( \frac{v_{\theta,t}}{a_t} \right)^2 + \frac{2-\gamma}{8} \left( \frac{v_{\theta,t}}{a_t} \right)^4 + \left[ \frac{1}{2} \left( \frac{v_{\theta,t}}{a_t} \right)^2 + \frac{2-\gamma}{4} \left( \frac{v_{\theta,t}}{a_t} \right)^4 \right] \frac{\log_e \left( \frac{r}{r_t} \right)^2}{1 - \left( \frac{r}{r_t} \right)^2} \\ &\quad + \frac{2-\gamma}{8} \left( \frac{v_{\theta,t}}{U_t} \right)^4 \left( \frac{r_t}{r} \right)^2 + \dots \quad (C6) \end{aligned}$$

and inasmuch as

$$\int_{r_1}^{r_{1,t}} 2\pi r_{r,1} v_{z,1} \, dr_1 = \int_{r_2}^{r_{2,t}} 2\pi r_{r,2} v_{z,2} \, dr_2$$

or

$$\bar{\rho}_{r,1} V_{z,1} (r_{1,t}^2 - r_1^2) = \bar{\rho}_{r,2} V_{z,2} (r_{2,t}^2 - r_2^2)$$

$$\frac{\bar{\rho}_{r,1} (r_{1,t}^2 - r_1^2)}{\bar{\rho}_{r,2} (r_{2,t}^2 - r_2^2)} = \frac{V_{z,2}}{V_{z,1}} = \frac{\bar{\rho}_{h,1} (r_{1,t}^2 - r_{1,h}^2)}{\bar{\rho}_{h,2} (r_{2,t}^2 - r_{2,h}^2)}$$

hence

$$\left(\frac{r_2}{r_{2,t}}\right)^2 = 1 - \frac{\left[1 - \left(\frac{r_{2,h}}{r_{2,t}}\right)^2\right]}{\left[1 - \left(\frac{r_{1,h}}{r_{1,t}}\right)^2\right]} \left[1 - \left(\frac{r_1}{r_{1,t}}\right)^2\right] \frac{\frac{\bar{\rho}_{r,1}}{\bar{\rho}_{h,1}}}{\frac{\bar{\rho}_{r,2}}{\bar{\rho}_{h,2}}} \quad (C7)$$

The change of total enthalpy across the rotor is

$$H_2 - H_1 = \omega(\xi_2 - \xi_1)$$

Then

$$\frac{H_2}{H_1} = 1 + \frac{\omega(\xi_2 - \xi_1)}{H_1}$$

For compressor

$$\frac{H_2}{H_1} = 1 + \frac{r_{1,h} V_{z,1,h}}{r_{1,t} U_{1,t}} \frac{\frac{r_{2,h}}{r_{1,h}} V_{\theta,2,h} - V_{\theta,1,h}}{V_{z,1,h}} \frac{U_{1,t}^2}{H_1}$$

where

the quantity  $\frac{\frac{r_{2,h}}{r_{1,h}} V_{\theta,2,h} - V_{\theta,1,h}}{V_{z,1,h}}$  is to be assigned by the

designer. Inasmuch as

$$\begin{aligned} \frac{H_1}{U_{1,t}^2} &= \frac{h_{1,t} + \frac{v_{1,t}^2}{2}}{U_{1,t}^2} \\ &= \frac{a_{1,t}^2}{(\gamma-1) U_{1,t}^2} + \frac{1}{2} \left( \frac{v_{z,1,t}^2}{U_{1,t}^2} + \frac{v_{\theta,1,t}^2}{U_{1,t}^2} \right) \end{aligned}$$

and

$$\begin{aligned} \frac{a_{1,t}^2}{U_{1,t}^2} &= \frac{\left( \frac{W_{1,t}}{M_L} \right)^2}{U_{1,t}^2} \\ &= \frac{1}{M_L^2} \left[ \left( \frac{v_{z,1,t}}{U_{1,t}} \right)^2 + \left( 1 - \frac{v_{\theta,1,t}}{U_{1,t}} \right)^2 \right] \end{aligned}$$

where  $M_L$  is the limiting Mach number to be chosen by the designer;

$$\frac{H_2}{H_1} = 1 + \frac{\frac{r_{1,h}}{r_{1,t}} \frac{v_{z,1,h}}{U_{1,t}} \frac{r_{2,h}}{r_{1,h}} v_{\theta,2,h} - v_{\theta,1,h}}{v_{z,1,h}} \frac{1}{(\gamma-1)M_L^2} \left[ \left( \frac{v_{z,1,t}}{U_{1,t}} \right)^2 + \left( 1 - \frac{v_{\theta,1,t}}{U_{1,t}} \right)^2 \right] + \frac{1}{2} \left[ \left( \frac{v_{z,1,t}}{U_{1,t}} \right)^2 + \left( \frac{v_{\theta,1,t}}{U_{1,t}} \right)^2 \right]}{\quad}$$

(C8)

The pressure distribution at each station is obtained by raising its density distribution (equation (C4)) to the power  $\gamma$ . The pressure changes between the stations at different radii are obtained by combining these pressure distributions with the pressure change across the rotor at the radius where the value of the polytropic exponent is known or assumed. The angle that the gas velocity makes with the axis of the machine at any radius is obtained from the known tangential and axial velocities.

Symmetrical Velocity Diagram and Constant Total Enthalpy

For the case of nontapered passage,  $r_1 = r_2 = r$  and from equations (28) and (32)

$$\frac{d\xi_1}{dr} = \frac{d\xi_2}{dr} = \omega r$$

$$\left. \begin{aligned} \xi_1 &= \frac{\omega r^2}{2} - \frac{r_{1,t} \delta_t U_{1,t}}{2} \\ \xi_2 &= \frac{\omega r^2}{2} + \frac{r_{1,t} \delta_t U_{1,t}}{2} \end{aligned} \right\} \quad (C9)$$

or

$$\left. \begin{aligned} \frac{v_{\theta,1}}{U_{1,t}} &= \frac{1}{2} \frac{r}{r_{1,t}} - \frac{\delta_t r_{1,t}}{2r} \\ \frac{v_{\theta,2}}{U_{1,t}} &= \frac{1}{2} \frac{r}{r_{1,t}} + \frac{\delta_t r_{1,t}}{2r} \end{aligned} \right\} \quad (C10)$$

By substituting equation (C10) into equation (46),

$$\gamma \frac{P_t}{\rho_t^\gamma} \rho^{\gamma-2} \frac{\partial \rho}{\partial r} = \frac{\omega^2 r}{4} \mp \frac{\delta_t U_{1,t}^2}{2r} + \frac{1}{4} (r_{1,t} \delta_t U_{1,t})^2 \frac{1}{r^3}$$

where the minus sign is used for station 1 and the plus sign for station 2. Integration from  $r$  to  $r_t$  yields

$$\frac{\gamma}{\gamma-1} \frac{P_t}{\rho_t^\gamma} (\rho_t^{\gamma-1} - \rho^{\gamma-1}) = \frac{\omega^2}{8} (r_t^2 - r^2) \pm \frac{\delta_t U_{1,t}}{2} \log_e \frac{r_t}{r} - \frac{1}{8} (r_{1,t} \delta_t U_{1,t})^2 \left( \frac{1}{r_t^2} - \frac{1}{r^2} \right)$$

or

$$\frac{\rho}{\rho_t} = \left\{ 1 - \frac{\gamma-1}{8} \frac{U_t^2}{a_t^2} \left[ 1 - \left( \frac{r}{r_t} \right)^2 \pm 4\delta_t \left( \frac{U_{1,t}}{U_t} \right)^2 \log_e \frac{r}{r_t} \right. \right. \\ \left. \left. + \delta_t^2 \left( \frac{U_{1,t}}{U_t} \right)^2 \left( \frac{r_{1,t}}{r_t} \right)^2 \left( \frac{r_t^2}{r^2} - 1 \right) \right] \right\}^{\frac{1}{\gamma-1}} \quad (C11)$$

where the plus sign is used for station 1 and the minus sign for station 2.

The variation of axial velocity is obtained from equation (26a):

$$V_z \frac{dV_z}{dr} = - \frac{1}{r^2} \xi \frac{d\xi}{dr} \\ = - \omega \left( \frac{\omega r}{2} \pm \frac{r_{1,t} \delta_t U_{1,t}}{2r} \right) \\ = - U_{1,t}^2 \left( \frac{r}{2r_{1,t}^2} \pm \frac{\delta_t}{2r} \right) \quad (C12)$$

Integration from  $r_h$  to  $r$  gives

$$\left( \frac{V_z}{U_{1,t}} \right)^2 = \left( \frac{V_{z,h}}{U_{1,t}} \right)^2 - \frac{1}{2} \left( \frac{r^2}{r_{1,t}^2} - \frac{r_h^2}{r_{1,t}^2} \right) \pm \delta_t \log_e \frac{r}{r_h} \quad (C13)$$

where the plus sign in the last term is used for station 1 and the minus sign for station 2. Equation (C12) also gives

$$V_{z,2} \frac{dV_{z,2}}{dr} - V_{z,1} \frac{dV_{z,1}}{dr} = \frac{\delta_t U_{1,t}^2}{r} \quad (C14)$$

In the case of a tapered passage, the gas is assumed to flow in conical surfaces, which gives the value of  $r_2$  as a function of  $r_1$ . Equations (28) and (32) give the distributions of  $\xi$  and  $V_\theta$  as shown by equations (D6) and (D7), respectively, given in appendix D. The distributions of axial velocity and density at

station 2 are the same as those given by equations (D8) and (D5). After these distributions are known, the distribution of specific mass flow  $G$  is known and the radial displacement is found from equation (B5).

In compressors of this design, the maximum value of  $\frac{r_{2,h}}{r_{1,h}} \frac{v_{\theta,2} - v_{\theta,1}}{v_{z,1}}$  is usually at the hub. Its value there is to be set by the designer. Then

$$\delta_h = \frac{\xi_{2,h} - \xi_{1,h}}{r_{1,h} U_{1,t}} = \frac{\frac{r_{2,h}}{r_{1,h}} v_{\theta,2,h} - v_{\theta,1,h} v_{z,1,h}}{v_{z,1,h} U_{1,t}}$$

and

$$\delta_t = \frac{r_{1,h}}{r_{1,t}} \delta_h = \frac{r_{1,h}}{r_{1,t}} \frac{v_{z,1,h}}{U_{1,t}} \frac{\frac{r_{2,h}}{r_{1,h}} v_{\theta,2,h} - v_{\theta,1,h}}{v_{z,1,h}} \quad (C15)$$

In this type of design, the limiting Mach number is usually at the hub. Hence the denominator of the last term of equation (C8) should be replaced by

$$\frac{1}{(\gamma-1)M_L^2} \left[ \left( \frac{v_{z,1,h}}{U_t} \right)^2 + \left( \frac{U_{1,h} - v_{\theta,1,h}}{U_{1,t}} \right)^2 \right] + \frac{1}{2} \left[ \left( \frac{v_{z,1,h}}{U_{1,t}} \right)^2 + \left( \frac{v_{\theta,1,h}}{U_{1,t}} \right)^2 \right]$$

The rest of the calculation is the same as in the previous design.

#### Symmetrical Velocity Diagram and Condition on Axial Velocity

For constant work over the blade height and nontapered passage, equations (C9) to (C11) still hold. If  $dv_{z,2}/dr$  equals 0, equation (27C) under Simplified Radial-Equilibrium Calculation gives

$$v_{z,1} \frac{dv_{z,1}}{dr} = \frac{1}{r^2} r_{1,t} \delta_t U_{1,t} \omega r = \frac{\delta_t U_{1,t}^2}{r}$$



Then

$$\frac{v_{z,1}}{v_{z,1,t}} = \left( 1 + \frac{2\delta_t U_{1,t}^2}{v_{z,1,t}^2} \log_e \frac{r}{r_t} \right)^{1/2} \quad (C16)$$

The enthalpy variation for this case is obtained by using equations (26a), (27a), and (C9)

$$\begin{aligned} \frac{dH_1}{dr} = \frac{dH_2}{dr} &= \frac{1}{r^2} \xi_2 \frac{d\xi_2}{dr} = \frac{1}{r^2} \left( \omega \frac{r^2}{2} + \frac{r_{1,t} \delta_t U_{1,t}}{2} \right) \omega r \\ &= \frac{U_{1,t}^2}{2} \left[ \left( \frac{r}{r_{1,t}} \right)^2 + \frac{\delta_t}{r} \right] \end{aligned}$$

$$\frac{H_t - H}{U_{1,t}^2} = \frac{1}{4} \left[ 1 - \left( \frac{r}{r_{1,t}} \right)^2 \right] + \frac{1}{2} \delta_t \log_e \frac{r_t}{r} \quad (C17)$$

On the other hand if  $\frac{dv_{z,1}}{dr} = 0$

$$v_{z,2} \frac{dv_{z,2}}{dr} = - \frac{U_{1,t}^2 \delta_t}{r}$$

$$\frac{v_{z,2}}{v_{z,2,t}} = \left( 1 - \frac{2\delta_t U_{1,t}^2}{v_{z,2,t}^2} \log_e \frac{r}{r_t} \right)^{1/2} \quad (C18)$$

$$\frac{H_t - H}{U_{1,t}^2} = \frac{1}{4} \left[ 1 - \left( \frac{r}{r_{1,t}} \right)^2 \right] - \frac{1}{2} \delta_t \log_e \frac{r_t}{r} \quad (C19)$$

In order to make the distribution of  $H$  independent of  $\delta_t$ , the compromise condition

$$v_{z,1} \frac{dv_{z,1}}{dr} + v_{z,2} \frac{dv_{z,2}}{dr} = 0$$

may be used. When this relation is combined with equation (27c), there is obtained

$$\frac{V_{z,1}}{V_{z,1,t}} = \left( 1 + \frac{\delta_t U_{1,t}}{V_{z,1,t}^2} \log_e \frac{r}{r_t} \right)^{1/2} \quad (C20)$$

$$\frac{V_{z,2}}{V_{z,2,t}} = \left( 1 - \frac{\delta_t U_{1,t}}{V_{z,2,t}^2} \log_e \frac{r}{r_t} \right)^{1/2} \quad (C21)$$

When equation (26a) is applied to stations 1 and 2, and the two resulting equations are added

$$2 \frac{dH}{dr} = \frac{1}{r^2} \left( \xi_1 \frac{d\xi_1}{dr} + \xi_2 \frac{d\xi_2}{dr} \right)$$

$$\frac{dH}{dr} = \frac{U_t^2}{2} \frac{r}{r_t^2}$$

Then

$$\frac{H_t - H}{U_t^2} = \frac{1}{4} \left[ 1 - \left( \frac{r}{r_t} \right)^2 \right] \quad (C22)$$

If the requirement of constant work over the blade height is abandoned, it is possible to require no change in the axial-velocity distribution across the blade rows, which is the incompressible form of the condition of no radial displacement

$$\frac{dV_{z,1}}{dr_1} = \frac{dV_{z,2}}{dr_2} = \frac{dV_{z,3}}{dr_3} = 0 \quad (C23)$$

When equation (C23) is combined with equation (27b) for the case of nontapered passage

$$\frac{\xi_1}{r^2} \frac{d\xi_1}{dr} = \frac{\xi_2}{r^2} \frac{d\xi_2}{dr} - \omega \left( \frac{d\xi_2}{dr} \frac{d\xi_1}{dr} \right) \quad (C24)$$

By substituting the symmetry conditions (equations (31a) and (31b)) into equation (C24)

$$\frac{1}{r^2} \xi_1 \frac{d\xi_1}{dr} = \frac{1}{r^2} (\omega r^2 - \xi_1) \left( 2\omega r - \frac{d\xi_1}{dr} \right) - \omega \left( 2\omega r - 2 \frac{d\xi_1}{dr} \right)$$

Simplification yields

$$\frac{d\xi_1}{dr} = 2 \frac{\xi_1}{r}$$

$$\frac{\xi_1}{\xi_{1,t}} = \left( \frac{r}{r_{1,t}} \right)^2 \quad (C25)$$

or

$$\frac{v_{\theta,1}}{v_{\theta,1,t}} = \frac{r}{r_{1,t}} \quad (25a)$$

From equations (32) and (C25)

$$\frac{\xi_2}{\xi_{2,t}} = \left( \frac{r}{r_{1,t}} \right)^2 \quad (C26)$$

$$\frac{v_{\theta,2}}{v_{\theta,2,t}} = \frac{r_{2,t}}{r_{1,t}} \left( \frac{r}{r_{1,t}} \right) \quad (C26a)$$

Thus wheel-type rotation exists both in front of and behind the rotor. By equation (27),

$$\begin{aligned} \frac{dH_2}{dr} - \frac{dH_1}{dr} &= \omega \left( \frac{d\xi_2}{dr} - \frac{d\xi_1}{dr} \right) \\ &= \frac{2\omega r}{r_{1,t}^2} (\xi_{2,t} - \xi_{1,t}) \\ &= 2\omega U_{1,t} \delta_t \left( \frac{r}{r_{1,t}} \right) \end{aligned} \quad (C27)$$

which means that the work done is proportional to the square of the radius.

## APPENDIX D

## METHOD OF CALCULATION FOR ZERO AND INFINITE ASPECT RATIOS

The method of calculations is given for the two types of design used in the numerical examples.

## Free Vortex and Constant Total Enthalpy

Zero aspect ratio. - In this type of design, the zero-aspect-ratio case is the same as that of the simplified-radial-equilibrium approximation.

Infinite aspect ratio. - By equations (47) and (A17)

$$\frac{V_{z,2}}{V_{z,1}} = \frac{\rho_1}{\rho_2} = e^{\frac{s_2 - s_1}{R} \left( \frac{H_1 - \frac{V_1^2}{2}}{H_2 - \frac{V_2^2}{2}} \right)^{\frac{1}{\gamma-1}}}$$

$$\left( \frac{V_{z,2}}{V_{z,1}} e^{\frac{s_1 - s_2}{R}} \right)^{\gamma-1} = \frac{2H_1 - (V_{\theta,1}^2 + V_{z,1}^2)}{2H_2 - (V_{\theta,2}^2 + V_{z,2}^2)} \quad (D1)$$

An additional relation between  $V_{z,1}$  and  $V_{z,2}$  is necessary in order to solve the equation. In the section entitled "Infinite-Aspect-Ratio Calculation" two equations are suggested. For this design, equation (48) gives

$$\frac{dV_{z,1}}{dr_1} + \frac{dV_{z,2}}{dr_2} = 0$$

or

$$V_{z,1} + V_{z,2} = \text{constant} \quad (D2)$$

and equation (49) gives

$$V_{z,1} \frac{dV_{z,1}}{dr} + V_{z,2} \frac{dV_{z,2}}{dr} = 0$$

or

$$V_{z,1}^2 + V_{z,2}^2 = \text{constant} \quad (D3)$$

Also from equations (E4) and (E5), neglecting the square term in  $\Delta_e$

$$V_{z,1} V_{z,2} = \text{constant} \quad (D4)$$

The three preceding equations give practically the same results.

A convenient procedure of calculation is as follows:

(1) In order to compare the result with other cases, the same value of  $V_{z,1,m}$  may be used. From equation (D1),  $V_{z,2,m}$  is determined.

(2) Insert these values in either equation (D2), (D3), or (D4) to obtain the constant in the equation.

(3) Assume a number of values of  $V_{z,1}$ ; obtain  $V_{z,2}$  by the same equation. Then use the following equation, which is obtained from equations (D1) and (C3), to solve for  $r/r_t$

$$\left(\frac{r}{r_t}\right)^2 = \frac{(V_{\theta,2,t})^2 - \left(e^{\frac{s_2-s_1}{R} \frac{V_{z,1}}{V_{z,2}}}\right)^{\gamma-1} (V_{\theta,1,t})^2}{2H_1 \left[ \frac{H_2}{H} - \left(e^{\frac{s_2-s_1}{R} \frac{V_{z,1}}{V_{z,2}}}\right)^{\gamma-1} \right] + \left(e^{\frac{s_2-s_1}{R} \frac{V_{z,1}}{V_{z,2}}}\right)^{\gamma-1} (V_{z,1})^2 - (V_{z,2})^2}$$

(4) Plot  $V_{z,1}$  and  $V_{z,2}$  against  $r/r_t$ , and obtain their values at the values of  $r/r_t$  desired.

When the distribution of axial velocity is known, the density variation at any station is obtained by applying equation (A17) at the station

$$\frac{\rho}{\rho_t} = \left[ \frac{H - \left( \frac{v_{\theta}^2}{2} + \frac{v_z^2}{2} \right)}{H - \left( \frac{v_{\theta,t}^2}{2} + \frac{v_{z,t}^2}{2} \right)} \right]^{\frac{1}{\gamma-1}} \quad (D5)$$

The pressure variation at each station is obtained by raising equation (D5) to the  $\gamma$  power. The pressure changes across the stage at different radii and the air angles are obtained in the same manner as in the simplified-radial-equilibrium calculation.

Symmetrical Velocity Diagram Plus Constant Total Enthalpy

Zero aspect ratio. - With radial displacement not equal to zero, the equations for tangential velocities are different from the expressions of equation (C10). From equations (28) and (32)

$$\frac{d\xi_1}{dr_1} = \frac{d\xi_2}{dr_1} = \omega r_1$$

$$\left. \begin{aligned} \xi_1 &= \frac{\omega r_1^2}{2} - \frac{r_{1,t} \delta_t U_{1,t}}{2} \\ \xi_2 &= \frac{\omega r_1^2}{2} + \frac{r_{1,t} \delta_t U_{1,t}}{2} \end{aligned} \right\} \quad (D6)$$

and

$$\left. \begin{aligned} \frac{v_{\theta,1}}{U_{1,t}} &= \frac{\xi_1}{r_1 U_{1,t}} = \frac{r_1}{2r_{1,t}} - \frac{r_{1,t} \delta_t}{2r_1} \\ \frac{v_{\theta,2}}{U_{1,t}} &= \frac{\xi_2}{r_2 U_{1,t}} = \left( \frac{r_1}{2r_{1,t}} + \frac{r_{1,t} \delta_t}{2r_1} \right) \frac{r_1}{r_2} \end{aligned} \right\} \quad (D7)$$

1035

From equation (26) with the last term negligible for this case, inasmuch as  $r_2 - r_1$  is much less than  $L$ ,

$$v_{z,i} \frac{dv_{z,i}}{dr_i} = - \frac{1}{r_i^2} \xi_i \frac{d\xi_i}{dr_i}$$

For station 1, from equation (D6)

$$v_{z,1} \frac{dv_{z,1}}{dr_1} = - \frac{1}{r_1^2} \left( \frac{\omega r_1^2}{2} - \frac{r_{1,t} \delta_t U_{1,t}}{2} \right) \omega r_1 = - U_{1,t}^2 \left( \frac{1}{2} \frac{r_1}{r_{1,t}^2} - \frac{\delta_t}{2r_1} \right)$$

Integration from  $r_h$  to  $r_1$  yields

$$\left( \frac{v_{z,1}}{U_{1,t}} \right)^2 = \left( \frac{v_{z,1,h}}{U_{1,t}} \right)^2 + \delta_t \log_e \frac{r_1}{r_{1,h}} - \frac{1}{2} \left( \frac{r_1^2}{r_{1,t}^2} - \frac{r_{1,h}^2}{r_{1,t}^2} \right)$$

which is the same as equation (C13). For station 2,

$$\begin{aligned} v_{z,2} \frac{dv_{z,2}}{dr_2} &= - \frac{1}{r_2^2} \left( \frac{\omega r_1^2}{2} + \frac{r_{1,t} \delta_t U_{1,t}}{2} \right) \omega r_1 \frac{dr_1}{dr_2} \\ v_{z,2} dv_{z,2} &= - \frac{r_1}{2r_2^2} (\omega^2 r_1^2 + \delta_t U_{1,t}^2) dr_1 \\ &= - \frac{r_1^2}{2 (r_2)^2} U_{1,t}^2 \left( \frac{r_1}{r_{1,t}} + \frac{\delta_t}{r_1} \right) d \left( \frac{r_1}{r_{1,t}} \right) \end{aligned}$$

Integration from  $r_{1,h}$  to  $r_1$  yields

$$\left( \frac{v_{z,2}}{U_t} \right)^2 = \left( \frac{v_{z,2,h}}{U_t} \right)^2 - \int_{\frac{r_{1,h}}{r_{1,t}}}^{\frac{r_1}{r_{1,t}}} \left( \frac{r_1}{r_2} \right)^2 \left( \frac{r_1}{r_{1,t}} + \frac{\delta_t}{r_1} \right) d \left( \frac{r_1}{r_{1,t}} \right) \quad (D8)$$

which differs from equation (C13).

The density distribution at station 1 is the same as the simplified radial approximation, whereas that at station 2 is obtained by using equation (D5). The solution of this case is a process of successive approximations. Values of  $r_2(r_1)$  obtained in the simplified radial approximation can be used here as the starting values. Then the distributions of  $V_{\theta,2}$ ,  $V_{z,2}$ ,  $\rho_2$ , and  $G_2$  are calculated from the preceding equations, and new values of  $r_2(r_1)$  are computed from equation (B5). Usually, only two or three cycles are necessary to obtain the correct value, as the difference between this case and the simplified-radial-equilibrium approximation of this type of design is small.

Infinite aspect ratio. - The first equation for the condition  $G_1 = G_2$  is the same as equation (D1). The second equation necessary to solve this case is a little more complicated than that in the previous type of design because  $\frac{d\xi}{dr} \neq 0$ . If equation (49a) is used

$$\begin{aligned} V_{z,1} \frac{dV_{z,1}}{dr} + V_{z,2} \frac{dV_{z,2}}{dr} &= -\frac{1}{r^2} \left( \xi_1 \frac{d\xi_1}{dr} + \xi_2 \frac{d\xi_2}{dr} \right) \\ &= -\frac{\omega}{r} (\xi_1 + \xi_2) = -\omega^2 r \end{aligned}$$

Then

$$V_{z,1}^2 + V_{z,2}^2 = -\omega^2 r^2 + \text{constant}$$

or

$$\frac{V_{z,1}^2}{U_t^2} + \frac{V_{z,2}^2}{U_t^2} = -\frac{r^2}{r_t^2} + \text{constant} \quad (\text{D10})$$

In order to compare the result of this case with other cases, the same value of  $V_{z,1,m}$  may be used. Then from equation (D1),  $V_{z,2,m}$  is found, and the constant in equation (D10) is evaluated by using this set of  $V_{z,1,m}$  and  $V_{z,2,m}$ . A few values of  $V_{z,1}$  are assumed at any other given radius, with corresponding values of  $V_{z,2}$  obtained from equation (D10). The correct values of  $V_{z,1}$  and  $V_{z,2}$  that will satisfy equation (D1) are obtained by interpolation.



After the distribution of axial velocity is known, the density distributions are obtained from equations (C11) and (D5), and the pressure distributions, total enthalpy change, and air angles are obtained in the same manner as before.

## APPENDIX E

## APPROXIMATE VALUE OF RADIAL DISPLACEMENT ACROSS BLADE ROW

FOR GENERAL CASE IN WHICH  $H_1$ ,  $H_2$ ,  $\xi_1$ , AND  $\xi_2$

ARE DETERMINED BY DESIGN AS FUNCTIONS OF  $r_1$

In the latter part of appendix D, distribution of axial velocity is expressed in terms of known  $H$ ,  $\xi$ ,  $r_1$ , and  $r_2(r_1)$ . Alternatively, this distribution can be expressed in terms of radial displacement and its value determined by the simplified-radial-equilibrium calculation, for which  $\Delta_e = 0$ . For the case of nontapered passage, it is seen from equation (21)

$$V_{z,1} \frac{dV_{z,1}}{dr_1} = V_{z,1,s} \frac{dV_{z,1,s}}{dr_1} + \frac{\Delta_e}{2} \left(\frac{\pi}{L}\right)^2 V_{z,1}^2 \quad (E1)$$

and

$$V_{z,2} \frac{dV_{z,2}}{dr_1} = V_{z,2,s} \frac{dV_{z,2,s}}{dr_1} - \frac{\Delta_e}{2} \left(\frac{\pi}{L}\right)^2 (V_{z,2})^2 \frac{dr_2}{dr_1} + \xi_2 \frac{d\xi_2}{dr_1} \left(\frac{1}{r_1^2} - \frac{1}{r_2^2}\right) \quad (E2)$$

By substituting  $(r_1 + \Delta_e)$  for  $r_2$ , expanding  $\left(1 + \frac{\Delta_e}{r_1}\right)^{-2}$  in a binomial series, and neglecting terms of greater order than  $\left(\frac{\Delta_e}{r_1}\right)^2$ , equation (E2) becomes

$$\begin{aligned} V_{z,2} \frac{dV_{z,2}}{dr_1} = & V_{z,2,s} \frac{dV_{z,2,s}}{dr_1} - \frac{\Delta_e}{2} \left(\frac{\pi}{L}\right)^2 (V_{z,2})^2 \left(1 + \frac{d\Delta_e}{dr_1}\right) \\ & + \xi_2 \frac{d\xi_2}{dr_1} \left(2 \frac{\Delta_e}{r_1^3}\right) - \xi_2 \frac{d\xi_2}{dr_1} \left(\frac{3\Delta_e^2}{r_1^4}\right) \end{aligned} \quad (E3)$$

If  $\Delta_e (r_1)$  is known, equations (E1) and (E3) may be solved as linear first-order differential equations in  $V_{z,1}^2$  and  $V_{z,2}^2$ , respectively, giving (omitting the subscript 1 on r)

$$V_{z,1}^2 = e^{\left(\frac{\pi}{L}\right)^2 \int_{r_m}^r \Delta_e dr} \left[ \int_{r_m}^r \left( \frac{d}{dr} V_{z,1,s}^2 \right) e^{-\left(\frac{\pi}{L}\right)^2 \int_{r_m}^r \Delta_e dr} dr + V_{z,1,m}^2 \right] \quad (E4)$$

and

$$V_{z,2}^2 = e^{-\left(\frac{\pi}{L}\right)^2 \varphi(r)} \left\{ \int_{r_m}^r \left[ \frac{d}{dr} V_{z,2,s}^2 + \frac{2\Delta_e}{r^3} \frac{d}{dr} \xi_2^2 - \frac{3(\Delta_e)^2}{r^4} \frac{d}{dr} \xi_2^2 \right] e^{\left(\frac{\pi}{L}\right)^2 \varphi(r)} dr + V_{z,2,m}^2 \right\} \quad (E5)$$

where

$$\varphi(r) = \int_{r_m}^r \Delta_e dr + \frac{1}{2} \left\{ (\Delta_e)^2 - [\Delta_e (r_m)]^2 \right\}$$

and subscript m may here refer to any radius between hub and tip.

For the limiting case of zero aspect ratio, the last term in equation (E1) approaches zero, so  $V_{z,1} = V_{z,1,s}$ , whereas  $V_{z,2}$  is obtained by integrating equation (E3) with the third term neglected.

$$V_{z,2}^2 = V_{z,2,s}^2 - (V_{z,2,s,m}^2 - V_{z,2,m}^2) + 2 \int_{r_m}^r \frac{\Delta_e}{r^3} \left( \frac{d}{dr} \xi_2^2 \right) dr$$

$$- 3 \int_{r_m}^r \frac{(\Delta_e)^2}{r^4} \left( \frac{d}{dr} \xi_2^2 \right) dr \quad (E6)$$

When equation (E4) is integrated by parts and  $\Delta_e(r_1)$  is replaced by  $y_e g(r)$  as in equation (51), there is obtained

$$V_{z,1}^2 = V_{z,1,s}^2 + e \left( \frac{\pi}{L} \right)^2 y_e \varphi_1(r) \left( V_{z,1,m}^2 - V_{z,1,m,s}^2 \right)$$

$$- e \left( \frac{\pi}{L} \right)^2 y_e \varphi_1(r) \int_{r_m}^r V_{z,1,s}^2 \frac{d}{dr} e^{-\left( \frac{\pi}{L} \right)^2 y_e \varphi_1(r)} dr$$

in which

$$\varphi_1(r) = \int_{r_m}^r g(r) dr$$

If it is desired to compare the general case with other cases on the basis of the same  $V_{z,1,m}$ , then  $V_{z,1,m} = V_{z,1,m,s}$ . By the use of the mean value theorem of integral calculus, the preceding equation can be written as

$$\begin{aligned} V_{z,1}^2 - V_{z,1,s}^2 &= - e^{\left(\frac{\pi}{L}\right)^2} y_e \varphi_1(r) \frac{1}{V_{z,1,s}^2} \left[ e^{-\left(\frac{\pi}{L}\right)^2} y_e \varphi_1(r) - 1 \right] \\ &= \frac{1}{V_{z,1,s}^2} \left[ e^{\left(\frac{\pi}{L}\right)^2} y_e \varphi_1(r) - 1 \right] \end{aligned} \quad (E7)$$

where  $\overline{V_{z,1,s}^2}$  is a mean value of  $V_{z,1,s}^2$  between  $r$  and  $r_m$ , the mean depending on the choice of the function  $g(r)$ . If the approximation is made in letting  $V_{z,2,m} = V_{z,2,m,s}$ , equation (E5) may be written as

$$\begin{aligned} V_{z,2}^2 - V_{z,2,s}^2 &= \frac{1}{V_{z,2,s}^2} \left[ e^{-\left(\frac{\pi}{L}\right)^2} y_e \varphi_2(r) - 1 \right] + y_e \varphi_3(r) \\ &\quad - y_e^2 \varphi_4(r) \end{aligned} \quad (E8)$$

where

$$\varphi_2(r) = \frac{\varphi(r)}{y_e} = \varphi_1(r) + \frac{1}{2} y_e \left\{ [g(r)]^2 - [g(r_m)]^2 \right\}$$

$$\varphi_3(r) = e^{-\left(\frac{\pi}{L}\right)^2} \varphi(r) \int_{r_m}^r e^{\left(\frac{\pi}{L}\right)^2} \varphi(r) \frac{2g(r)}{r^3} \frac{d}{dr} \xi_2^2 dr$$

and

$$\varphi_4(r) = e^{-\left(\frac{\pi}{L}\right)^2} \varphi(r) \int_{r_m}^r e^{\left(\frac{\pi}{L}\right)^2} \varphi(r) \frac{3[g(r)]^2}{r^4} \frac{d}{dr} \xi_2^2 dr$$

The change in the distributions of  $V_{z,1}$  and  $V_{z,2}$  with the maximum displacement  $y_e$  for a given  $g(r)$  is now determined by differentiating equations (E7) and (E8), assuming that  $r_m$ ,  $\overline{V_{z,1,s}^2}$ , and  $\overline{V_{z,2,s}^2}$  are independent of  $y_e$

$$2 \frac{d}{dy_e} \log_e V_{z,1} = \frac{\overline{V_{z,1,s}^2}}{V_{z,1}^2} \left(\frac{\pi}{L}\right)^2 \varphi_1(r) e^{\left(\frac{\pi}{L}\right)^2 y_e} \varphi_1(r) \quad (\text{E9})$$

$$2 \frac{d}{dy_e} \log_e V_{z,2} = - \frac{\overline{V_{z,2,s}^2}}{V_{z,2}^2} \left(\frac{\pi}{L}\right)^2 e^{-\left(\frac{\pi}{L}\right)^2 y_e} \varphi_2(r) \left( \varphi_1(r) + y_e \left\{ [g(r)]^2 - [g(r_m)]^2 \right\} \right) \\ + \frac{\varphi_3(r)}{V_{z,2}^2} + \frac{y_e}{V_{z,2}^2} \frac{d\varphi_3(r)}{dy_e} - 2y_e \frac{\varphi_4(r)}{V_{z,2}^2} - \frac{y_e^2}{V_{z,2}^2} \frac{d\varphi_4(r)}{dy_e} \quad (\text{E10})$$

By subtracting equation (E10) from (E9) and neglecting three small terms containing  $y_e/V_{z,2}^2$

$$\frac{d}{dy_e} \log_e \frac{V_{z,1}}{V_{z,2}} = \frac{1}{2} \left(\frac{\pi}{L}\right)^2 \varphi_1(r) \left( \frac{\overline{V_{z,1,s}^2}}{V_{z,1}^2} e^{\left(\frac{\pi}{L}\right)^2 y_e} \varphi_1(r) \right. \\ \left. + \frac{\overline{V_{z,2,s}^2}}{V_{z,2}^2} e^{-\left(\frac{\pi}{L}\right)^2 y_e} \varphi_2(r) \left[ 1 + y_e \frac{[g(r)]^2 - [g(r_m)]^2}{\varphi_1(r)} \right] \right) - \frac{1}{2} \frac{\varphi_3(r)}{V_{z,2}^2} \quad (\text{E11})$$

The equation of continuity, equation (14), may be written as

$$\frac{\rho_1 V_{z,1}}{\rho_2 V_{z,2}} = \left[ 1 + \frac{y_c g(r)}{r} \right] \left[ 1 + y_c \frac{d}{dr} g(r) \right] \quad (E12)$$

by replacing  $r_2$  with  $r_1 + y_c g(r)$ . It is here being assumed that the displacement  $\Delta_c$  for the continuity equation has the same form as, but may differ in magnitude from,  $\Delta_e$ . If the variation of  $\rho_1/\rho_2(r)$  with  $y_c$  is neglected, that is, the density distribution is assumed to be determined primarily by the tangential velocity distribution, differentiation with respect to  $y_c$  for a given  $g(r)$  gives

$$\frac{d}{dy_c} \log_e \frac{V_{z,1}}{V_{z,2}} = \frac{\frac{g(r)}{r}}{1+y_c \frac{g(r)}{r}} + \frac{\frac{d}{dr} g(r)}{1+y_c \frac{d}{dr} g(r)} \quad (E13)$$

If the same distribution of  $V_{z,1}$  and  $V_{z,2}$  satisfies both the continuity and equilibrium equations,  $y_c$  is a function of  $y_e$  determined by the differential equation, which is obtained by dividing equation (E11) by equation (E13):

$$\frac{dy_c}{dy_e} = \frac{1}{2} \frac{\left(\frac{\pi}{L}\right)^2 \varphi_1(r)}{\frac{\frac{g(r)}{r}}{1+y_c \frac{g(r)}{r}} + \frac{\frac{d}{dr} [g(r)]}{1+y_c \frac{d}{dr} [g(r)]}}$$

$$\left( \frac{\overline{V_{z,1,s}^2}}{V_{z,1}^2} e^{\left(\frac{\pi}{L}\right)^2 y_e} \varphi_1(r) + \frac{\overline{V_{z,2,s}^2}}{V_{z,2}^2} e^{-\left(\frac{\pi}{L}\right)^2 y_e} \varphi_2(r) \right)$$

$$\left\{ 1 + y_e \frac{[g(r)]^2 - [g(r_m)]^2}{\varphi_1(r)} \right\} - \frac{\varphi_3(r)}{V_{z,2}^2 \left(\frac{\pi}{L}\right)^2 \varphi_1(r)} \quad (E14)$$

In order to evaluate equation (E14), the form of  $g(r)$ , which is implicit in the equations used, must be found. An order-of-magnitude result may be obtained, however, by equating the right-hand side of equation (E14) to a constant  $-K^2$  and determining the value of the constant from the boundary conditions on  $g(r)$ . Because this assumption involves setting  $dy_c/dy_e$  equal to a constant, it is equivalent to the assumption already stated that for the selected  $\Delta_e = y_e g(r)$ , the corresponding  $\Delta_c$  differs only in amplitude. In order to obtain the order-of-magnitude result, the right-hand side of equation (E14) is simplified by

- (a) Setting the first two terms in the bracket equal to 2
- (b) Considering the terms involving  $y_c$  and  $y_e$  negligible when they are compared with unity
- (c) Ignoring the last term in the bracket because it contains  $v_{z,2}^2 \left(\frac{\pi}{L}\right)^2$  in the denominator. (If equation (E14) is written in terms of  $r/r_t$  instead of  $r$ , the term  $\left(\frac{\pi}{L}\right)^2$  becomes  $\left(\frac{\pi r_t}{L}\right)^2$ , which is about 250 for  $A = 2$  and  $\frac{r}{r_t} = 0.6$ .)

As a result of this simplification, equation (E14) becomes

$$\frac{dy_c}{dy_e} = \frac{\left(\frac{\pi}{L}\right)^2 \varphi_1(r)}{\frac{g(r)}{r} + \frac{d}{dr} g(r)} = -K^2 \quad (\text{E15})$$

Rewriting equation (E15) gives

$$-\left(\frac{\pi}{L}\right)^2 \frac{1}{K^2} \varphi_1(r) = \frac{g(r)}{r} + \frac{d}{dr} g(r) \quad (\text{E16})$$

When equation (E16) is differentiated with respect to  $r$  and the relation  $\frac{d}{dr} \varphi_1(r) = g(r)$  is used,

$$\frac{d^2}{dr^2} g(r) + \frac{1}{r} \frac{d}{dr} g(r) + \left[ \left(\frac{\pi}{LK}\right)^2 - \frac{1}{r^2} \right] g(r) = 0$$



This equation gives  $g(r)$  as a Bessel function of the first order and argument  $(\pi/LK)$ . The value of  $(\pi/LK)$ , and thus of  $K$ , is determined by the boundary conditions  $g(r_h) = g(r_t) = 0$ . In order that  $g(r)$  have a single maximum, the first eigenvalue of this boundary-value problem must be taken. A satisfactory approximation to this solution may be obtained without involving Bessel functions by replacing  $g(r)/r$  in equation (E16) by  $g(r)/r_m$ , differentiating, and solving:

$$g(r) = e^{-\frac{r}{2r_m}} (K_1 \cos \lambda r + K_2 \sin \lambda r)$$

where

$$\lambda = \sqrt{\left(\frac{\pi}{L}\right)^2 \frac{1}{K^2} - \frac{1}{(2r_m)^2}}$$

The boundary conditions determine, using the first eigenvalue for  $K$ ,

$$K = \frac{\pi}{r_t - r_h}$$

$$g(r) = K_3 e^{-\frac{r}{2r_m}} \sin \frac{r - r_h}{r_t - r_h} \pi \quad (\text{E17})$$

and therefore,

$$\left(\frac{\pi}{L}\right)^2 \frac{1}{K^2} = \frac{\pi^2}{(r_t - r_h)^2} + \frac{1}{4r_m^2} \approx \frac{\pi^2}{(r_t - r_h)^2}$$

(This approximate equality is correct within 1 percent for  $(r_h/r_t) > 0.5$ .) Substituting this result in equation (E15) gives

$$\frac{dy_c}{dy_e} = -K^2 = -\left(\frac{r_t - r_h}{L}\right)^2 = -A^2 \quad (\text{E18})$$

In this very rough approximation  $dy_c/dy_e$  is therefore equal to minus the square of the aspect ratio. By integrating equation (E18)

and by letting  $y_{c,s}$  equal the value of  $y_c$  corresponding to  $y_e = 0$  (simplified-radial-equilibrium approximation):

$$y_c = y_{c,s} - A^2 y_e \quad (E19)$$

A solution corresponds to  $y_c = y_e = y$ , which when substituted into equation (E18) gives

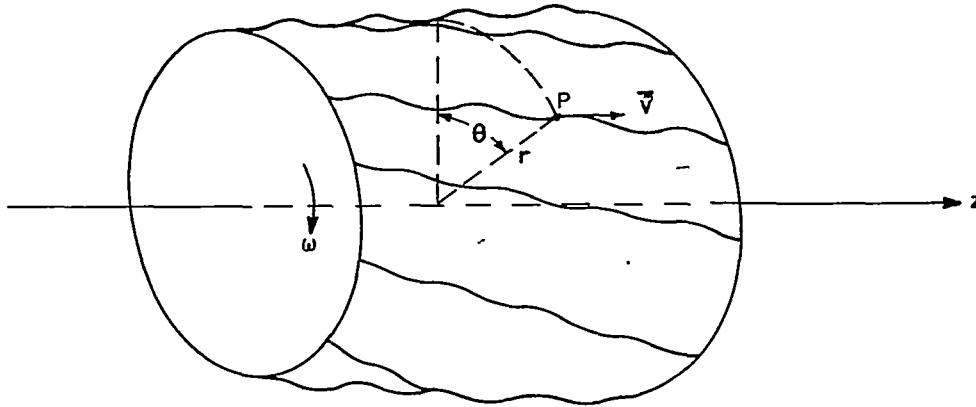
$$y = \frac{y_{c,s}}{1 + A^2}$$

or

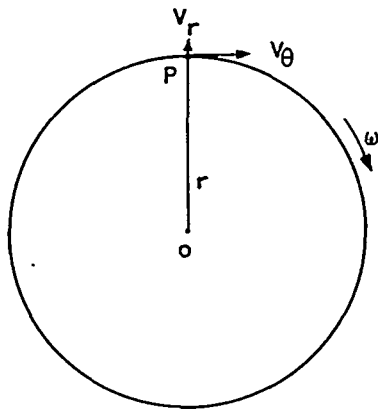
$$\Delta = \frac{\Delta_{c,s}}{1 + A^2} \quad (50)$$

#### REFERENCES

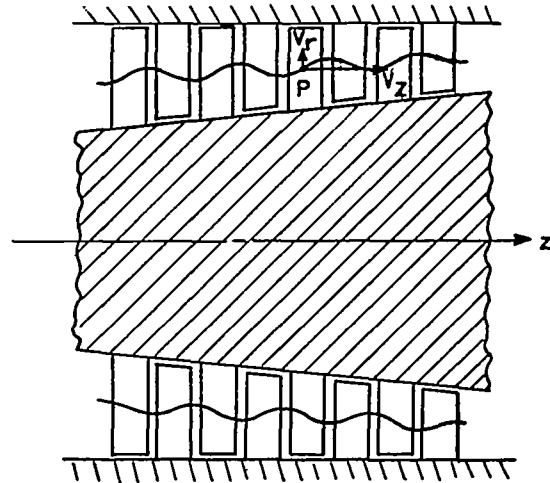
1. Ruden, P.: Investigation of Single Stage Axial Fans. NACA TM No. 1062, 1944.
2. Howell, A. R.: Fluid Dynamics of Axial Compressors. War Emergency Issue No. 12 pub. by Inst. Mech. Eng. (London), 1945. (Reprinted in U.S. by A.S.M.E., Jan. 1947, pp. 441-452.)
3. Eckert, and Korbacher: The Flow through Axial Turbine Stages of Large Radial Blade Length. NACA TM No. 1118, 1947.
4. Lamb, Horace: Hydrodynamics. Cambridge Univ. Press, 6th ed., 1932, articles 10, 329, 358.
5. Vazsonyi, Andrew: On Rotational Gas Flows. Quarterly Appl. Math., vol. 3, no. 1, April 1945, pp. 29-37.
6. Sinnette, John T., Jr., Schey, Oscar W., and King, J. Austin: Performance of NACA Eight-Stage Axial-Flow Compressor Designed on the Basis of Airfoil Theory. NACA Rep. No. 758, 1944.
7. Pochobradsky, B.: Effect of Centrifugal Force in Axial-Flow Turbines. Engineering, vol. 163, no. 4234, March 21, 1947, pp. 205-207.



(a) Stream surface over four stages of multistage turbomachine.



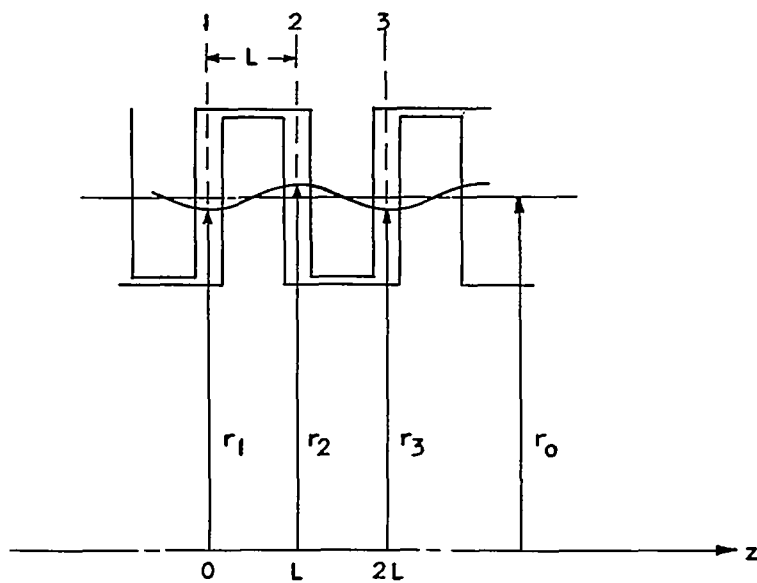
(b) Intersection of stream surface with plane normal to axis.



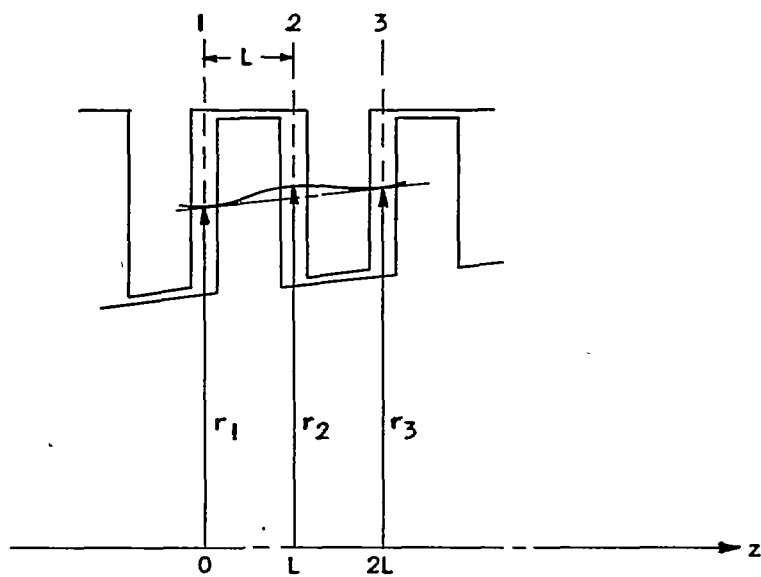
(c) Intersection of stream surface with axial plane.



Figure 1. - Stream surface over four stages of multistage turbomachine and its intersection with planes normal to and containing axis of machine.



(a) Nontapered passage.



(b) Tapered passage.



Figure 2. - Stations between blade rows.

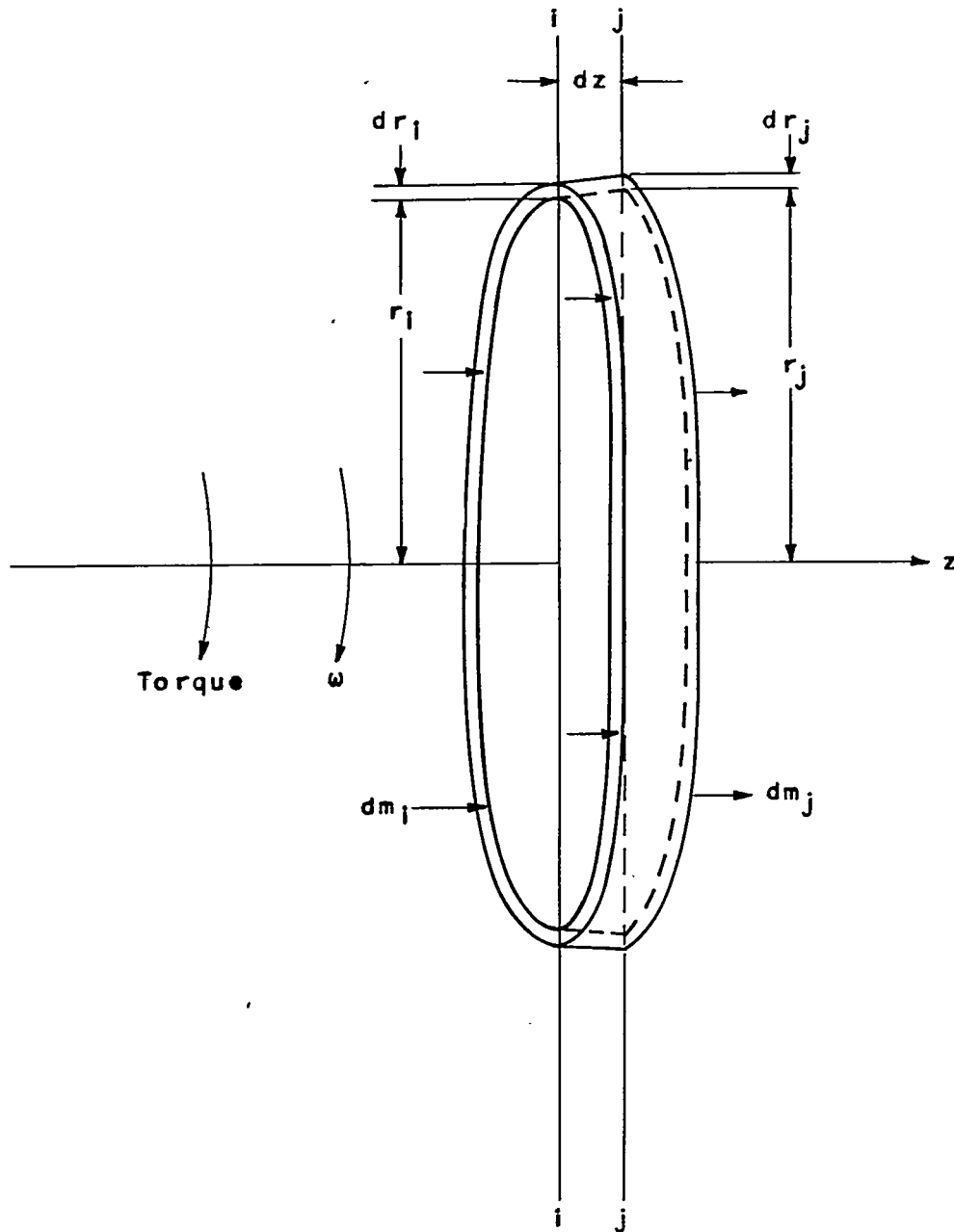
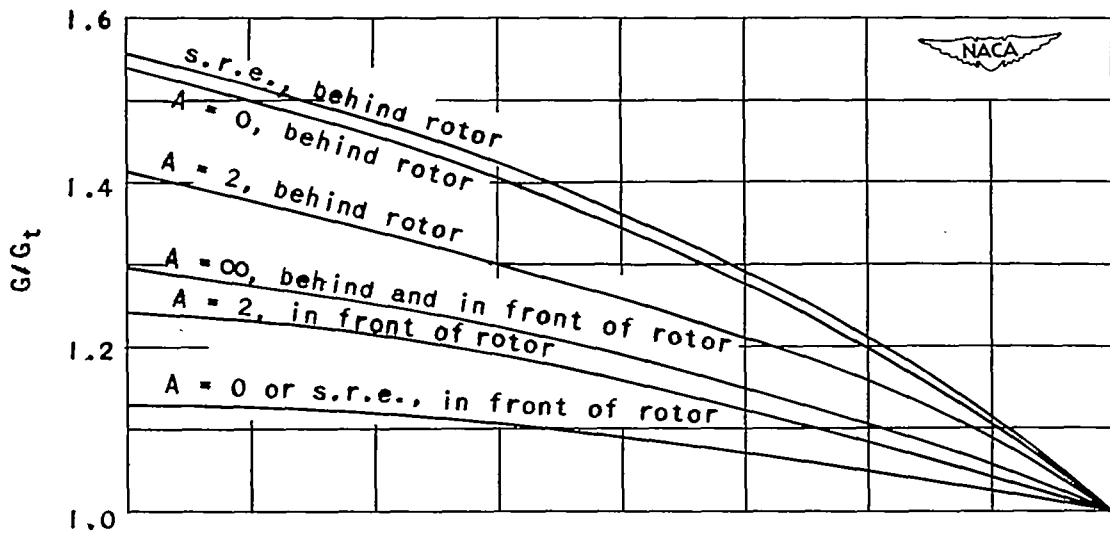
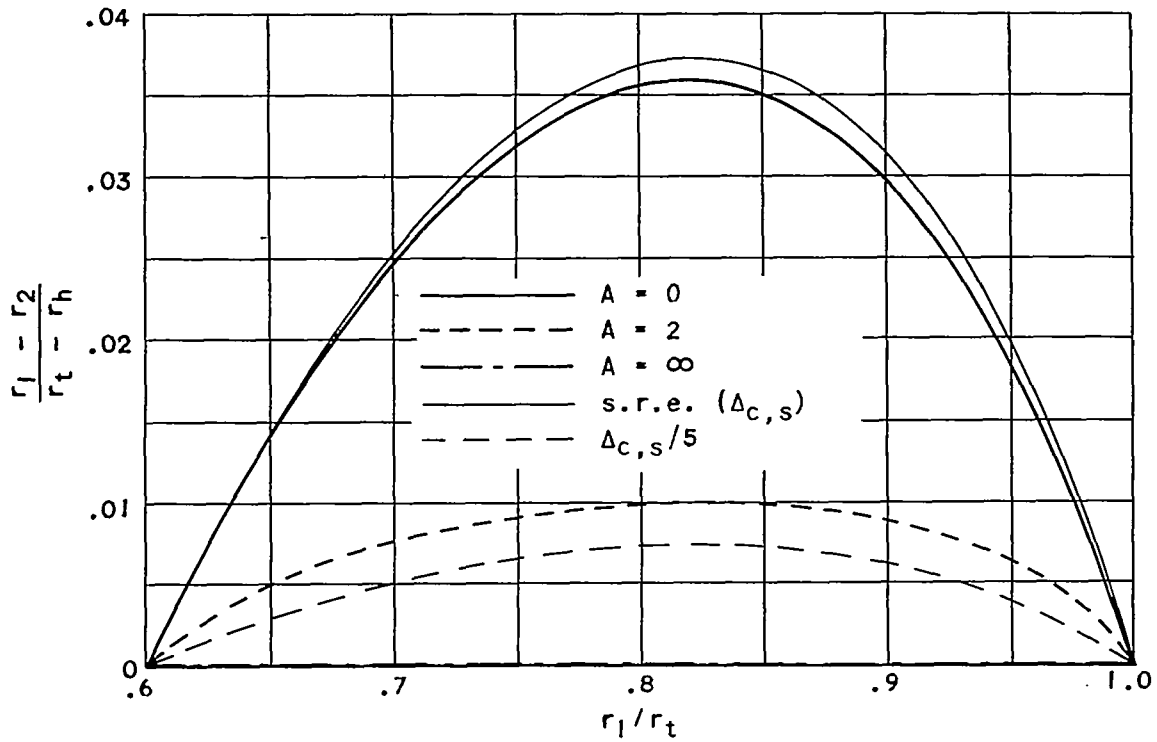


Figure 3. - Stations  $i$  and  $j$  short distance apart.

1035

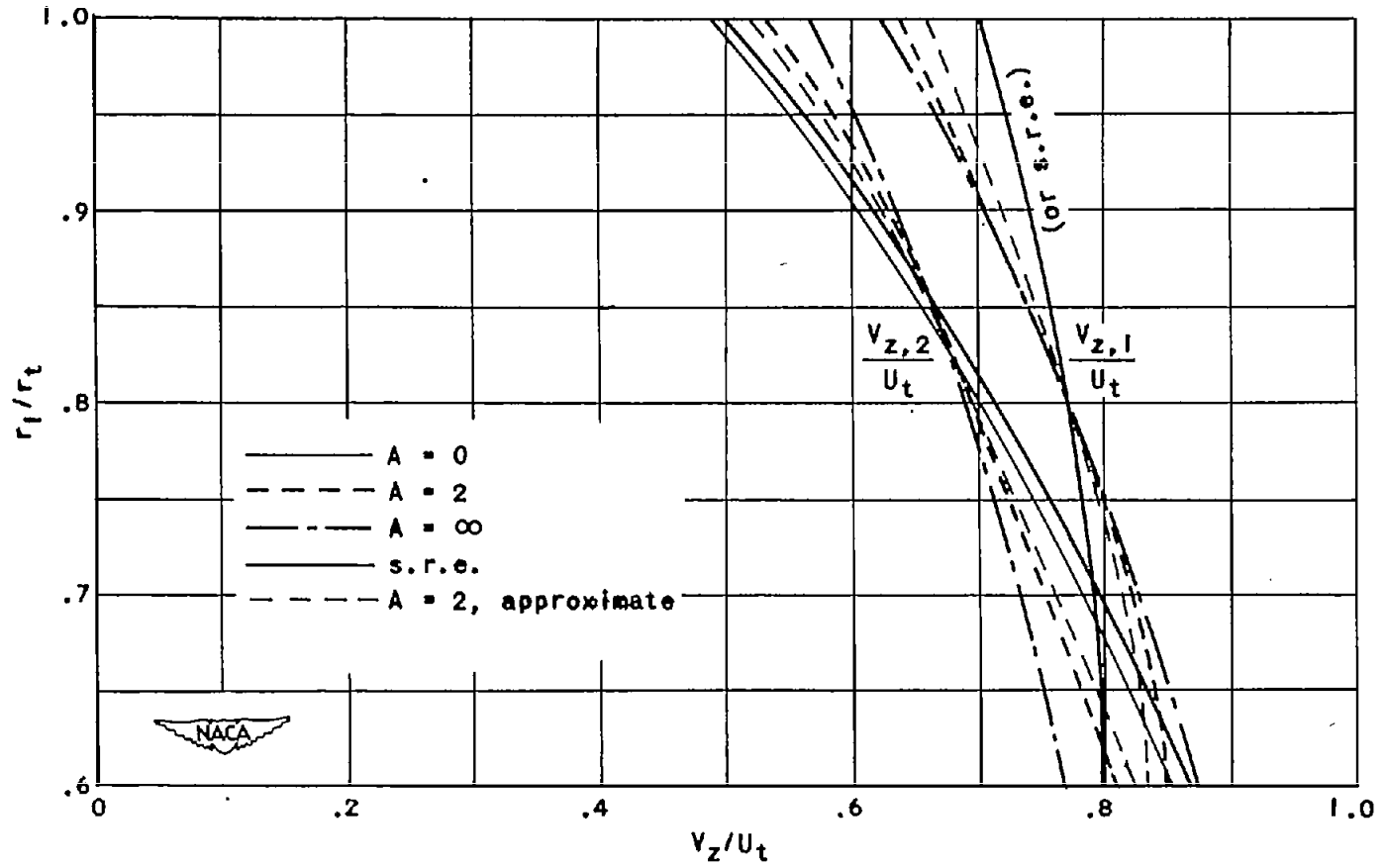


(a) Distribution of specific mass flow.



(b) Radial displacement across rotor.

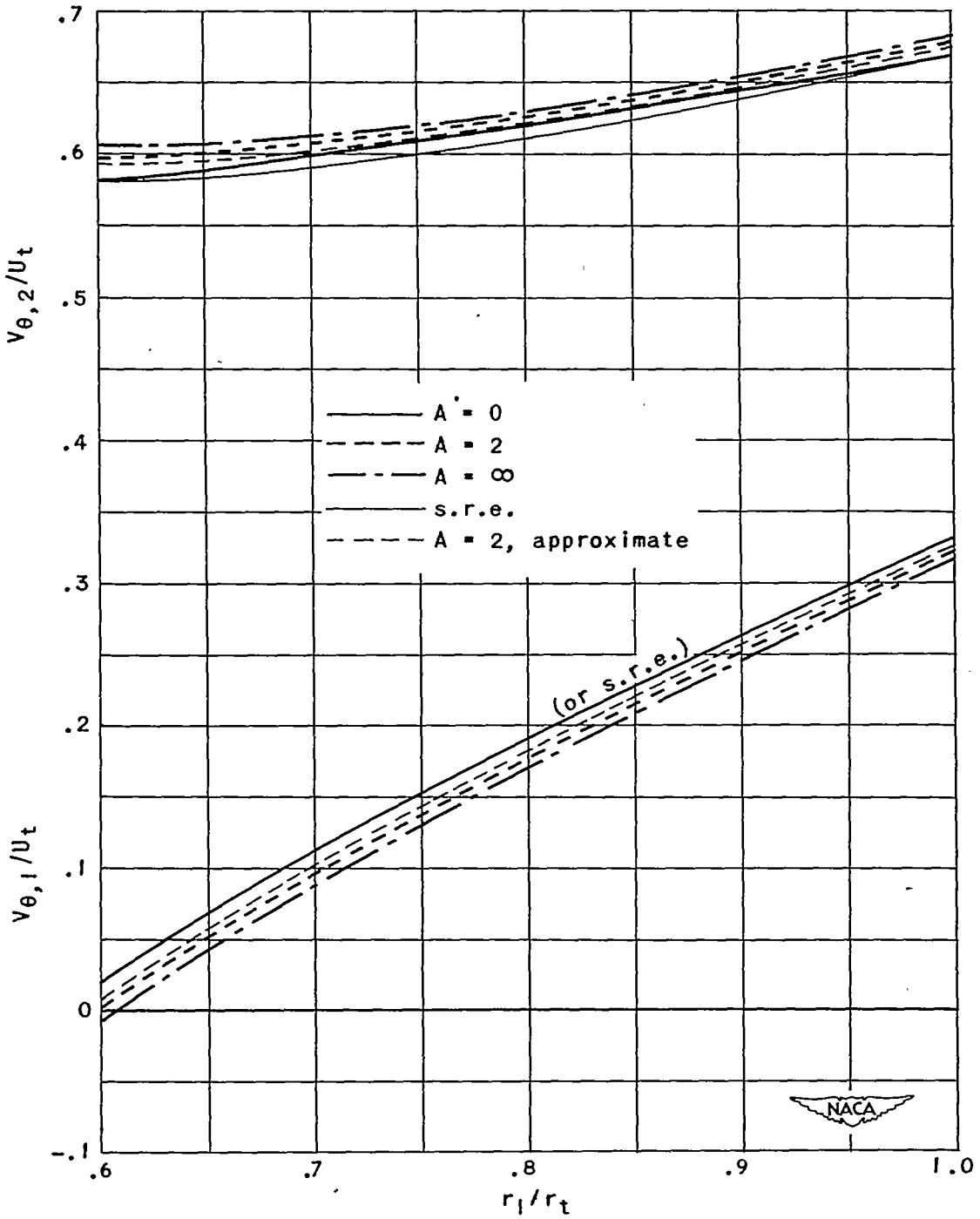
Figure 4. - Symmetrical-velocity-diagram and constant-total-enthalpy compressor.



(c) Variation of axial velocities.

Figure 4. - Continued. Symmetrical-velocity-diagram and constant-total-enthalpy compressor.

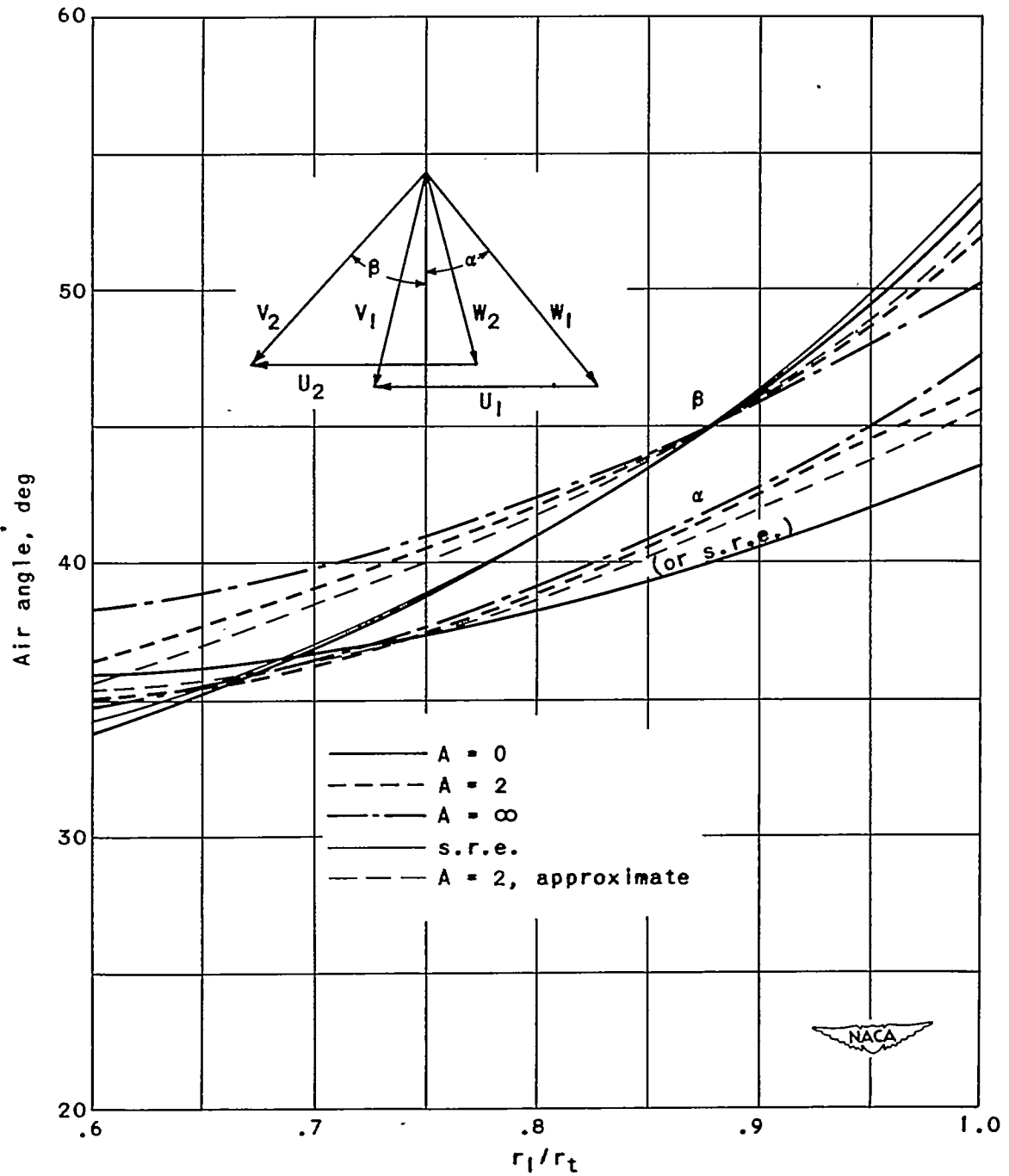
1035



(d) Variation of tangential velocities.

Figure 4. - Continued. Symmetrical-velocity-diagram and constant-total-enthalpy compressor.

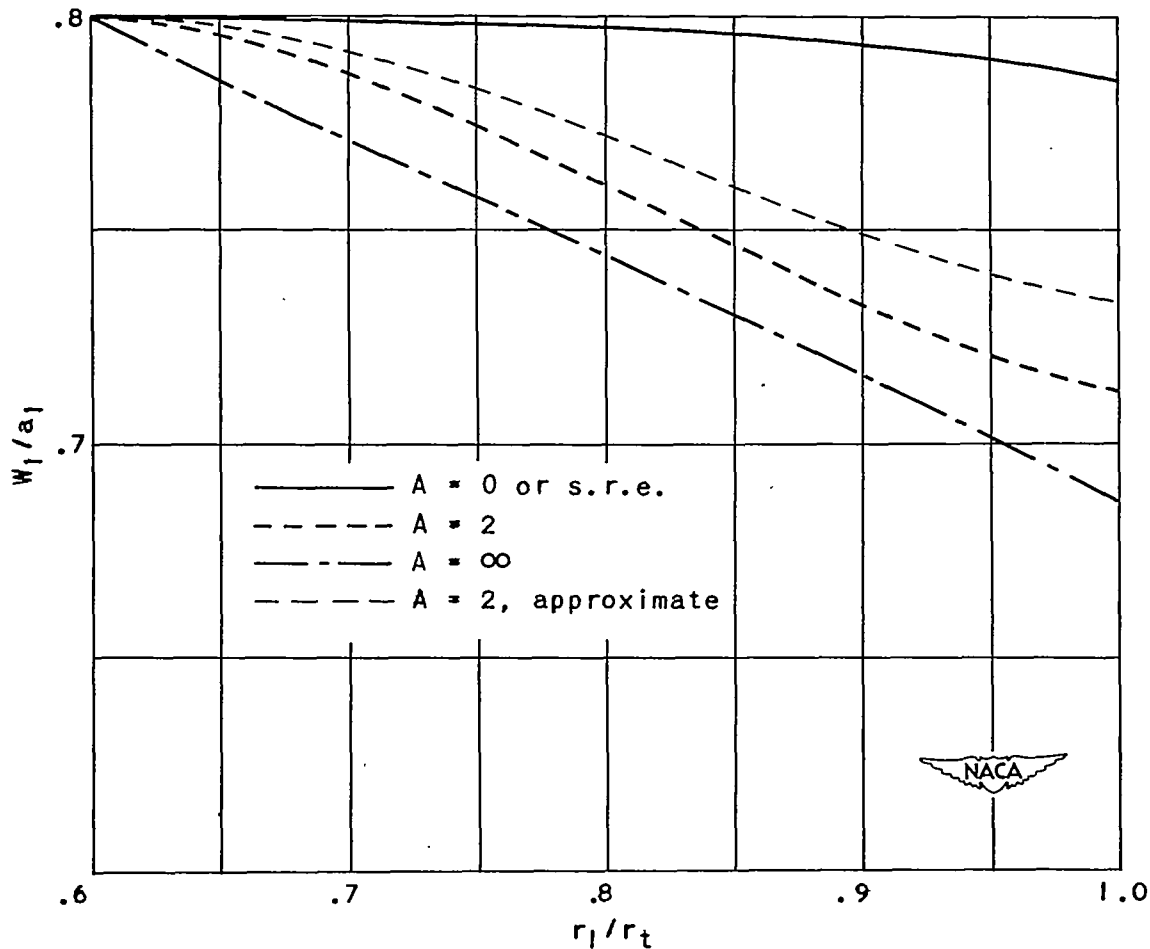




1035

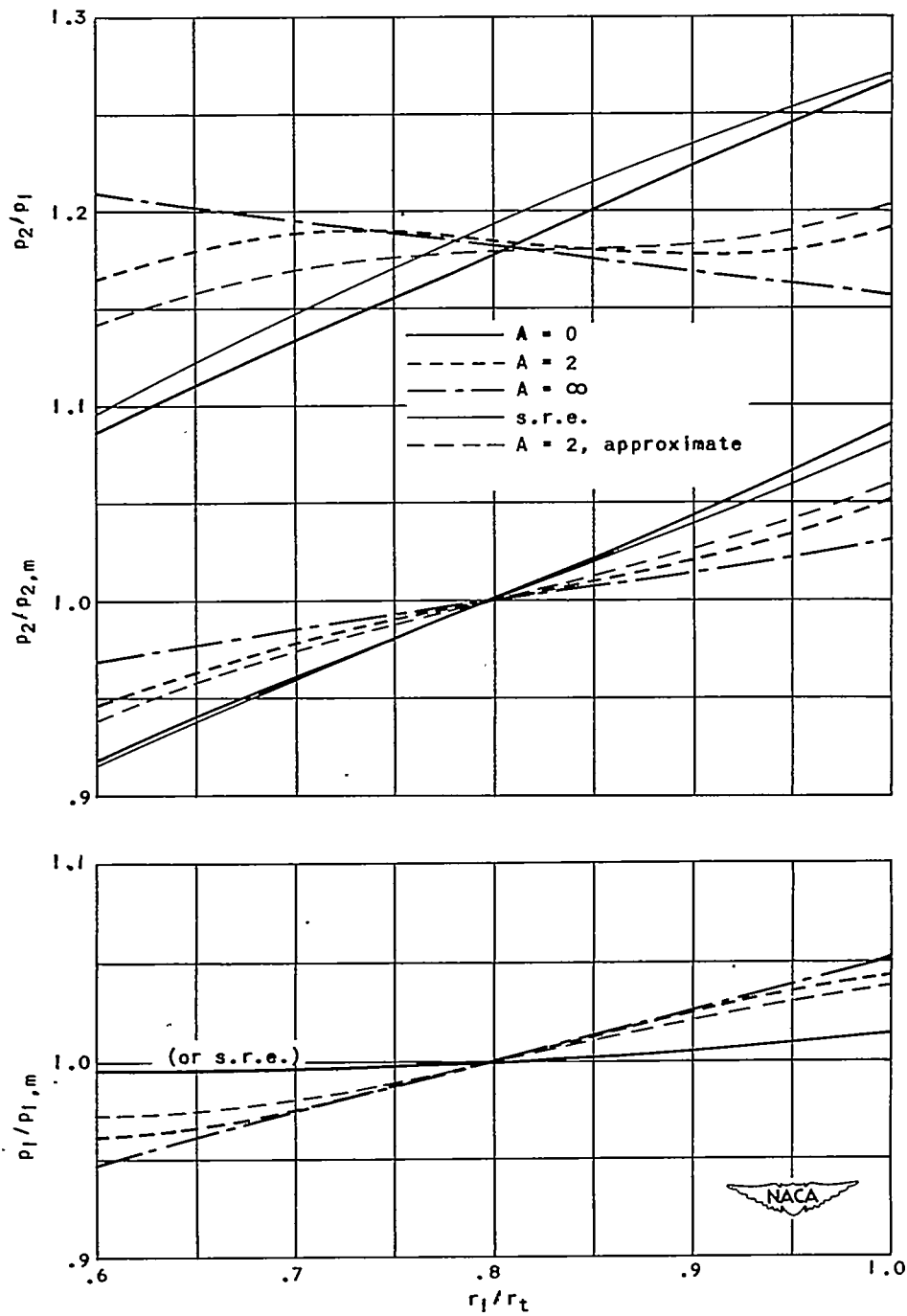
(e) Variation of air angles.

Figure 4. - Continued. Symmetrical-velocity-diagram and constant-total-enthalpy compressor.



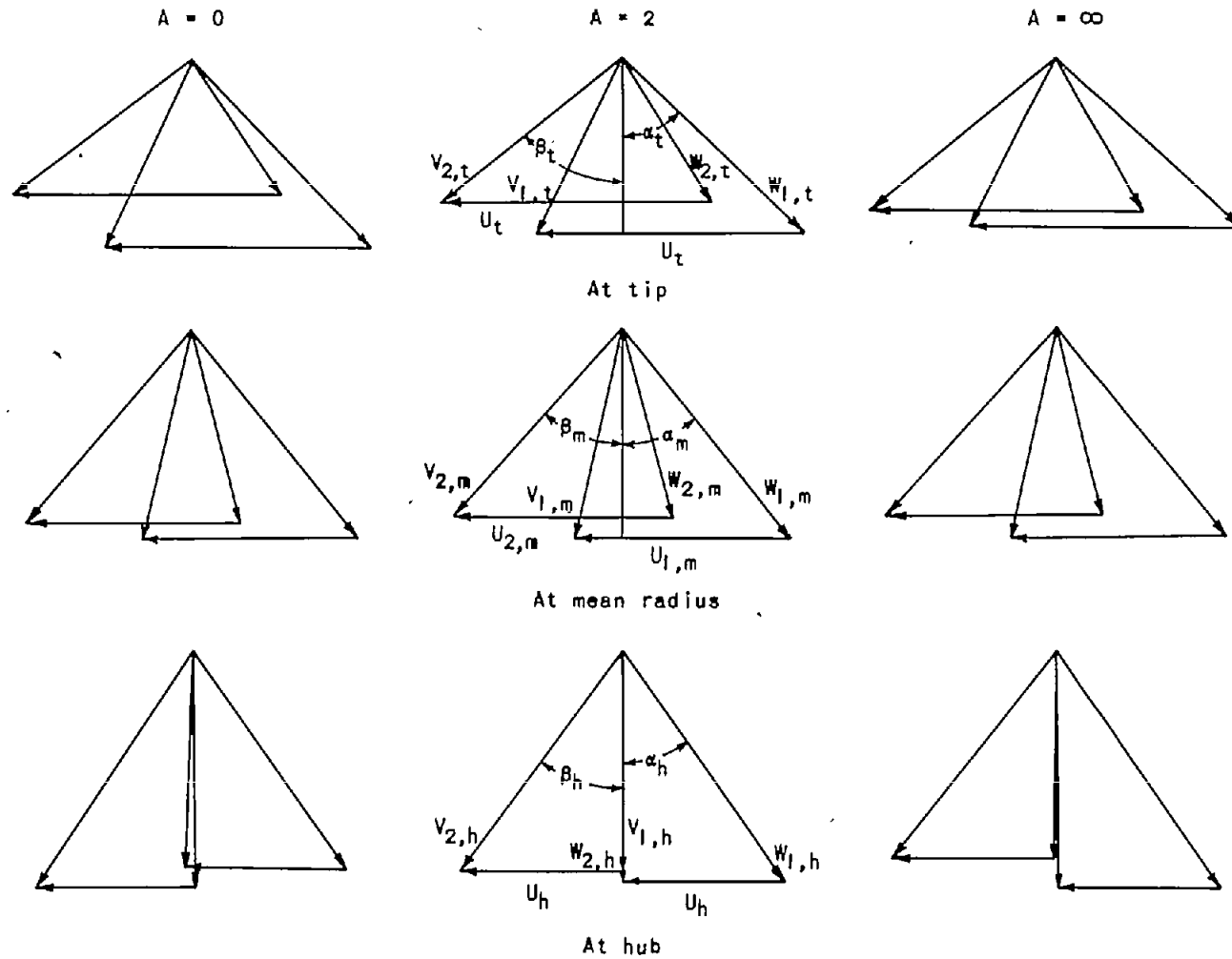
(f) Variation of Mach number relative to rotor blades.

Figure 4. - Continued. Symmetrical-velocity-diagram and constant-total-enthalpy compressor.



(g) Pressure distributions and pressure rise across rotor.

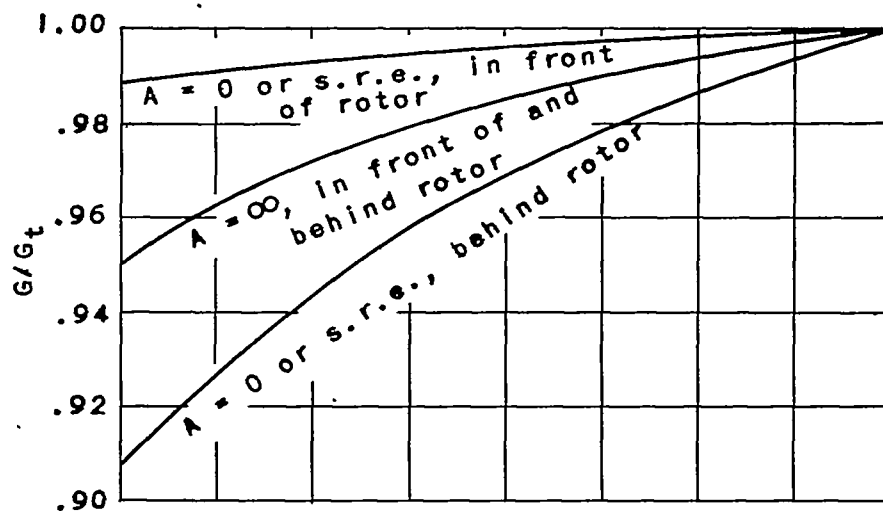
Figure 4. - Continued. Symmetrical-velocity-diagram and constant-total-enthalpy compressor.



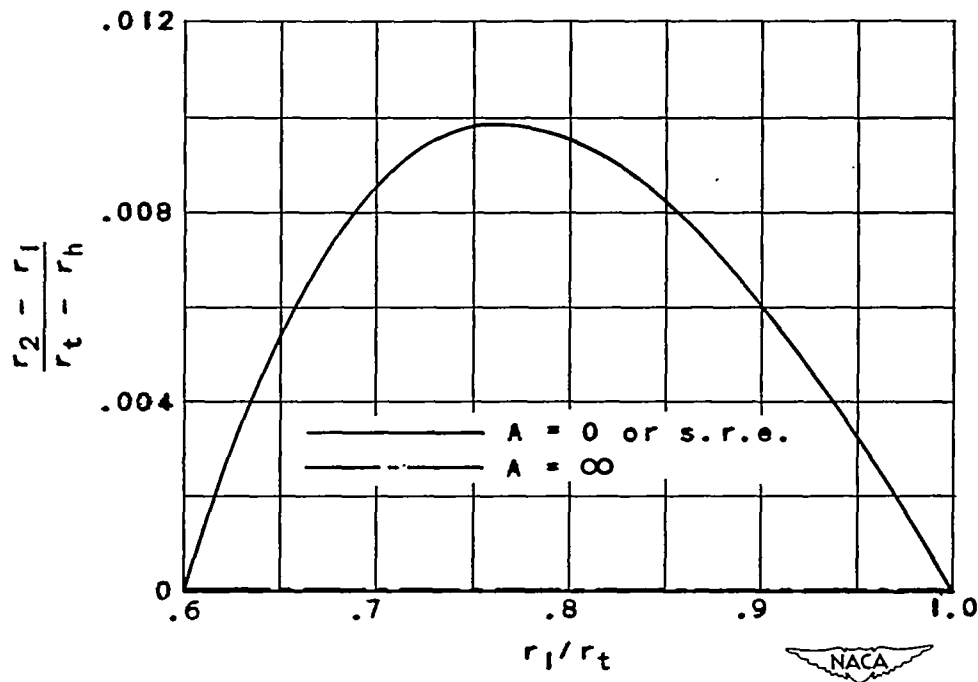
(h) Velocity diagrams at different radii.



Figure 4. - Concluded. Symmetrical-velocity-diagram and constant-total-enthalpy compressor.

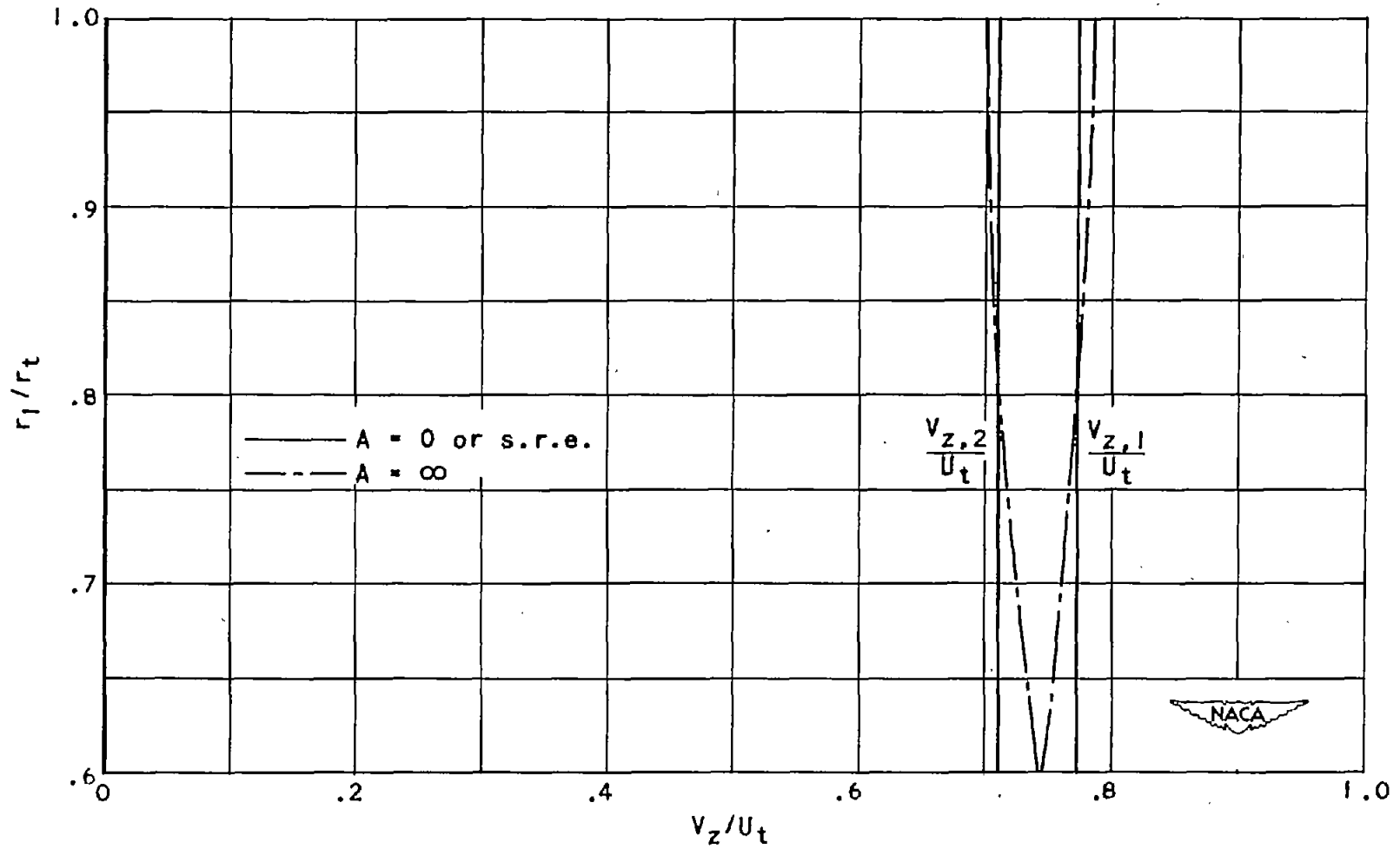


(a) Distribution of specific mass flow.



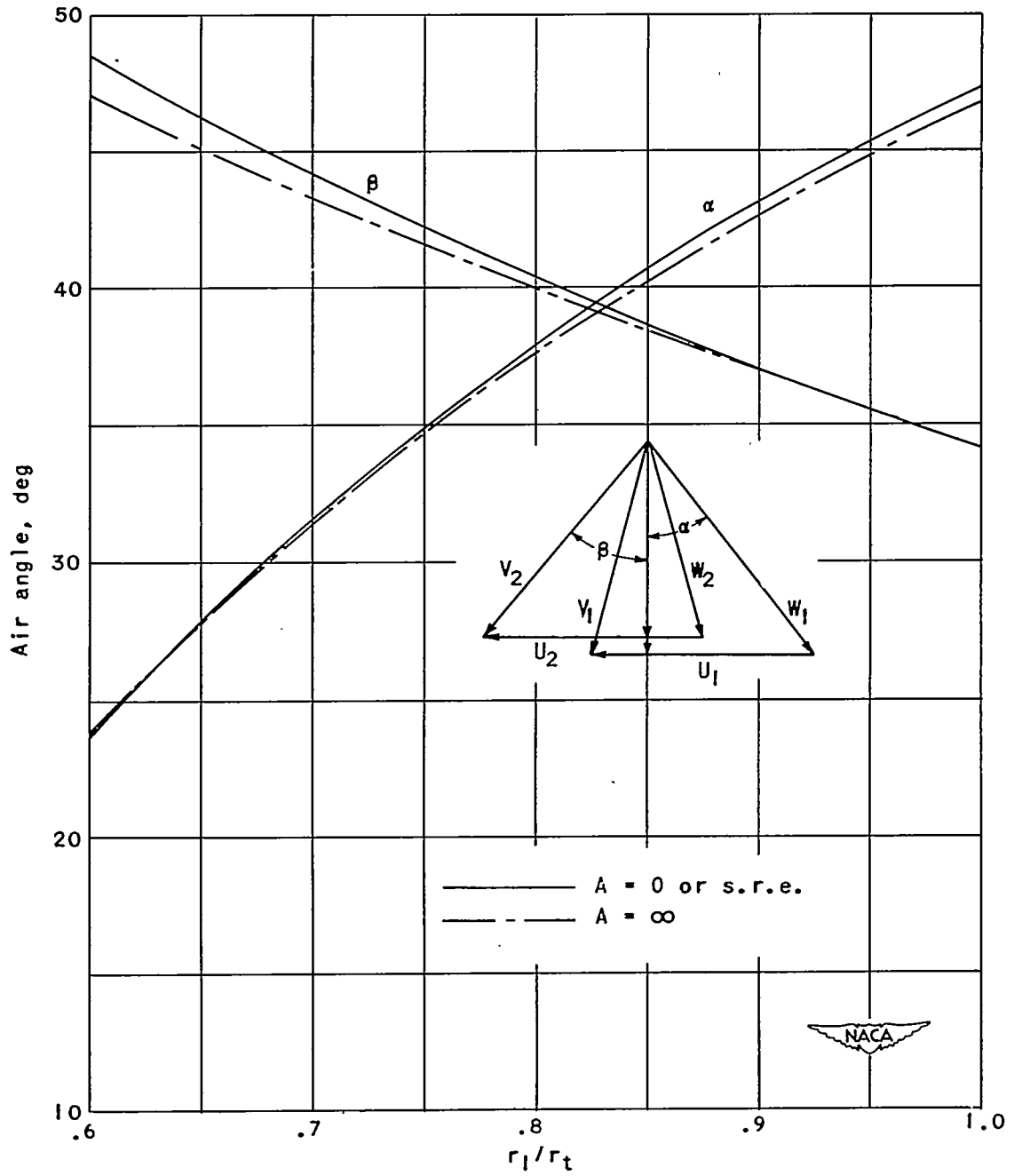
(b) Radial displacement across rotor.

Figure 5. - Free-vortex and constant-total-enthalpy compressor.



(c) Variation of axial velocities.

Figure 5. - Continued. Free-vortex and constant-total-enthalpy compressor.

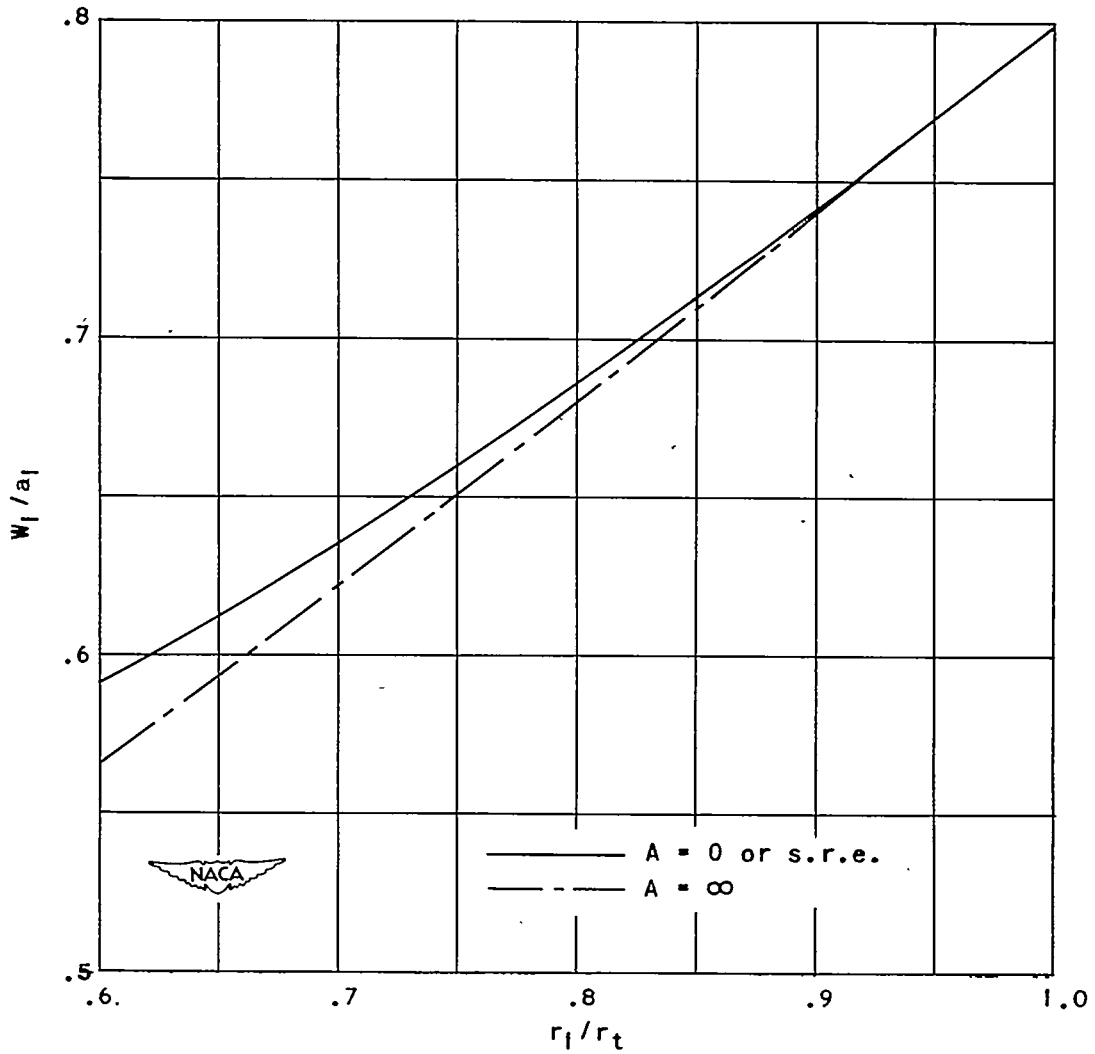


1035

(d) Variation of air angles.

Figure 5. - Continued. Free-vortex and constant-total-enthalpy compressor.

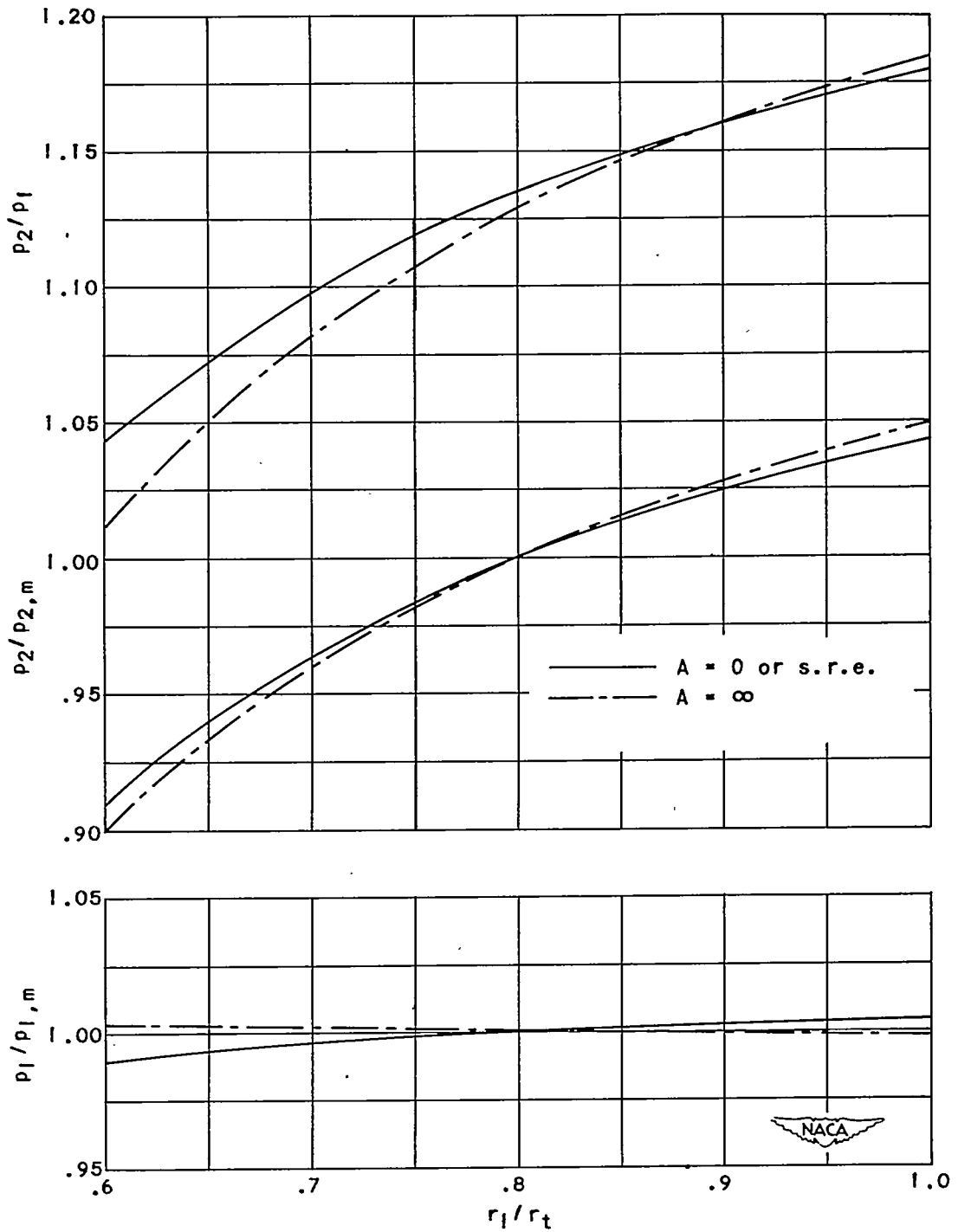
1035



(e) Variation of Mach number relative to rotor blades.

Figure 5. - Continued. Free-vortex and constant-total-enthalpy compressor.



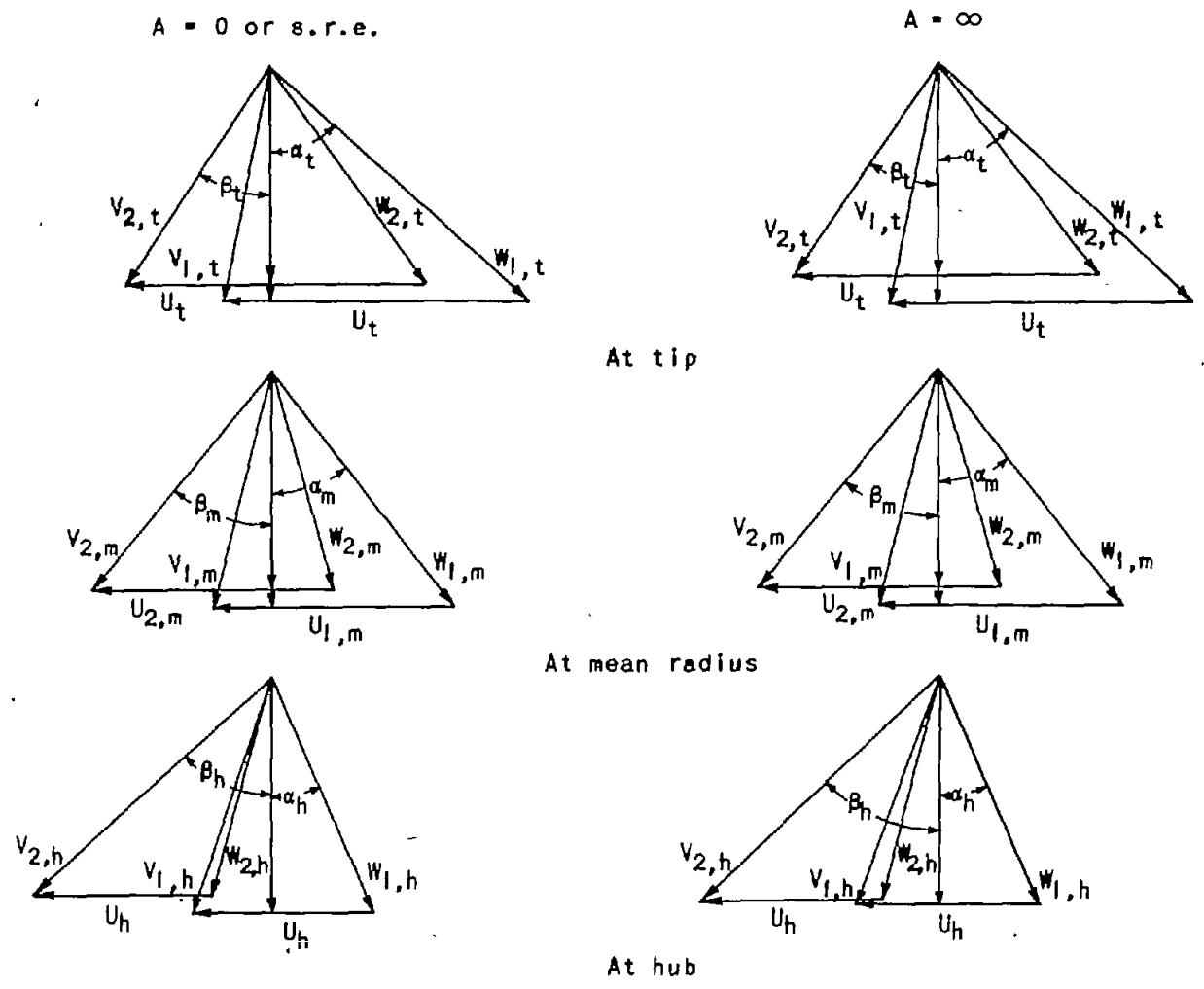


1035

(f) Pressure distributions and pressure rise across rotor.

Figure 5. - Continued. Free-vortex and constant-total-enthalpy compressor.

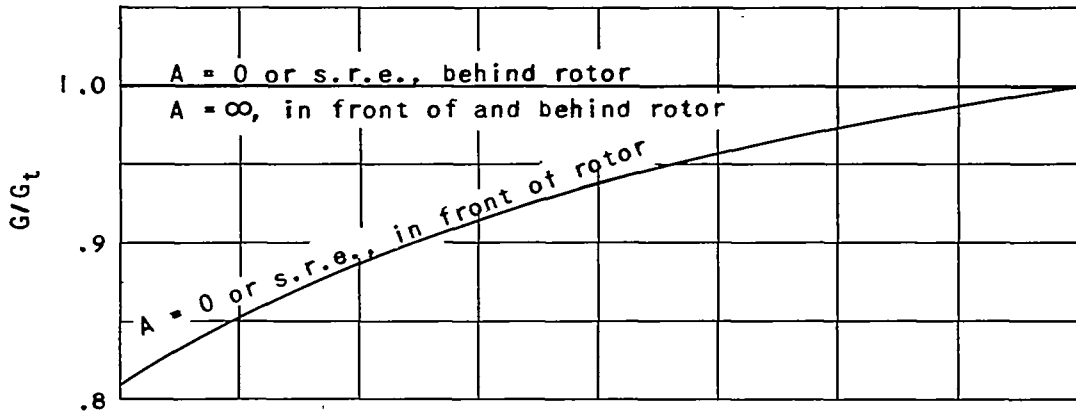




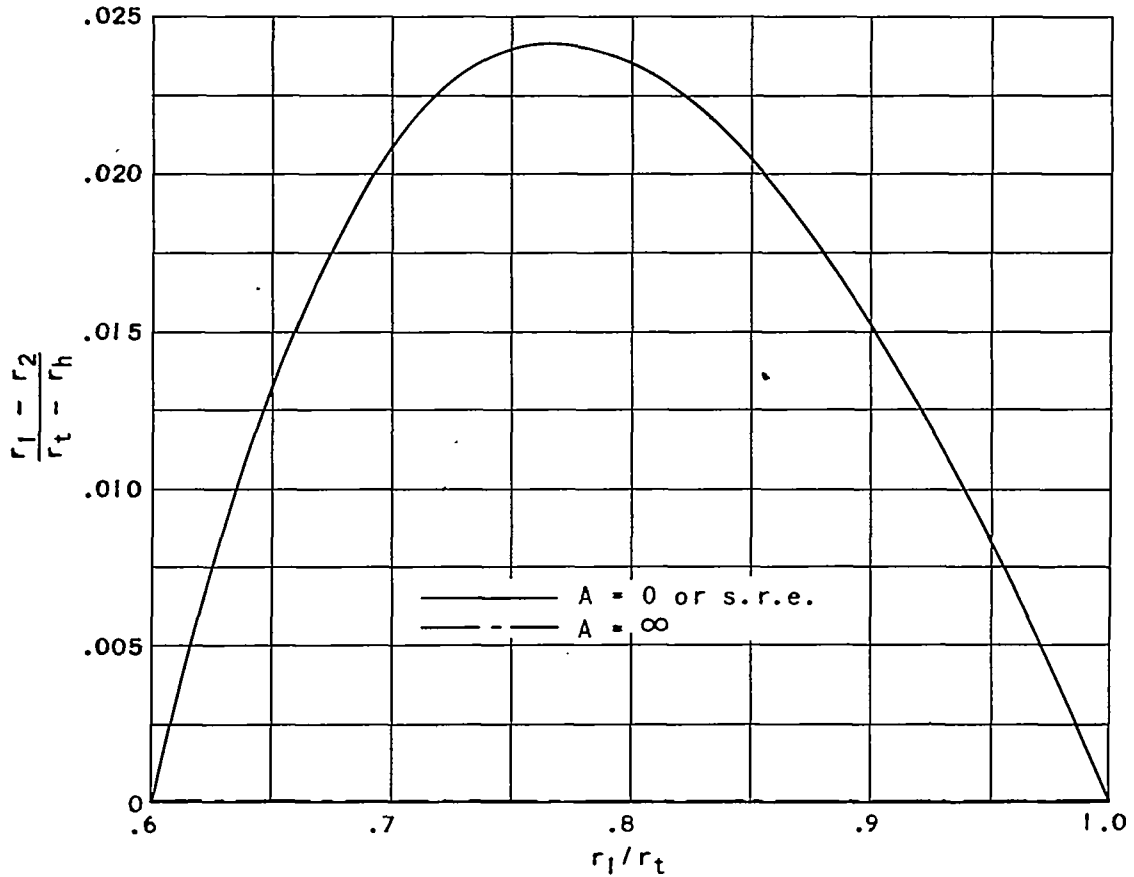
(g) Velocity diagrams at different radii.



Figure 5. - Concluded. Free-vortex and constant-total-enthalpy compressor.



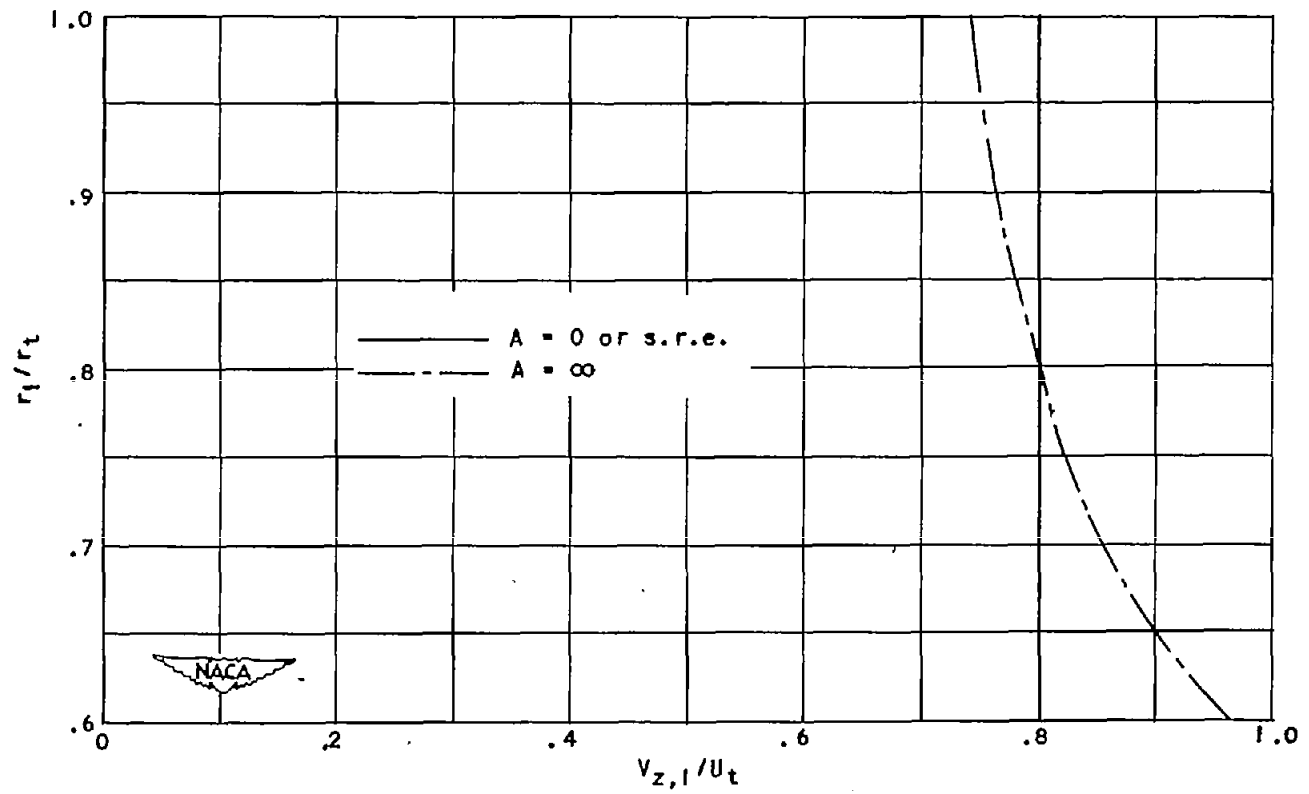
(a) Distribution of specific mass flow.



(b) Radial displacement across rotor.

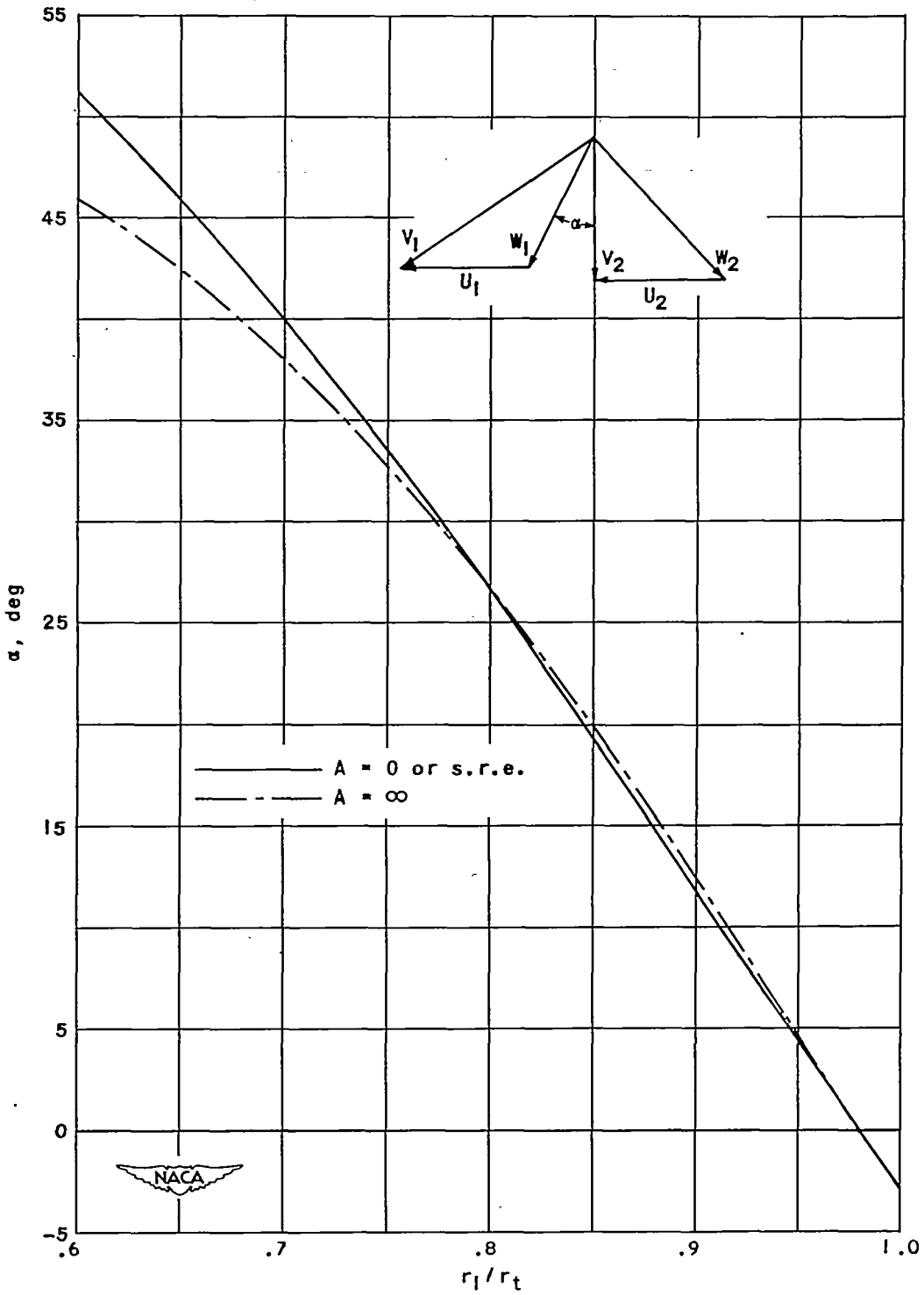


Figure 6. - Free-vortex and constant-total-enthalpy turbine.



(c) Variation of axial velocity in front of rotor.

Figure 6. - Continued. Free-vortex and constant-total-enthalpy turbine.

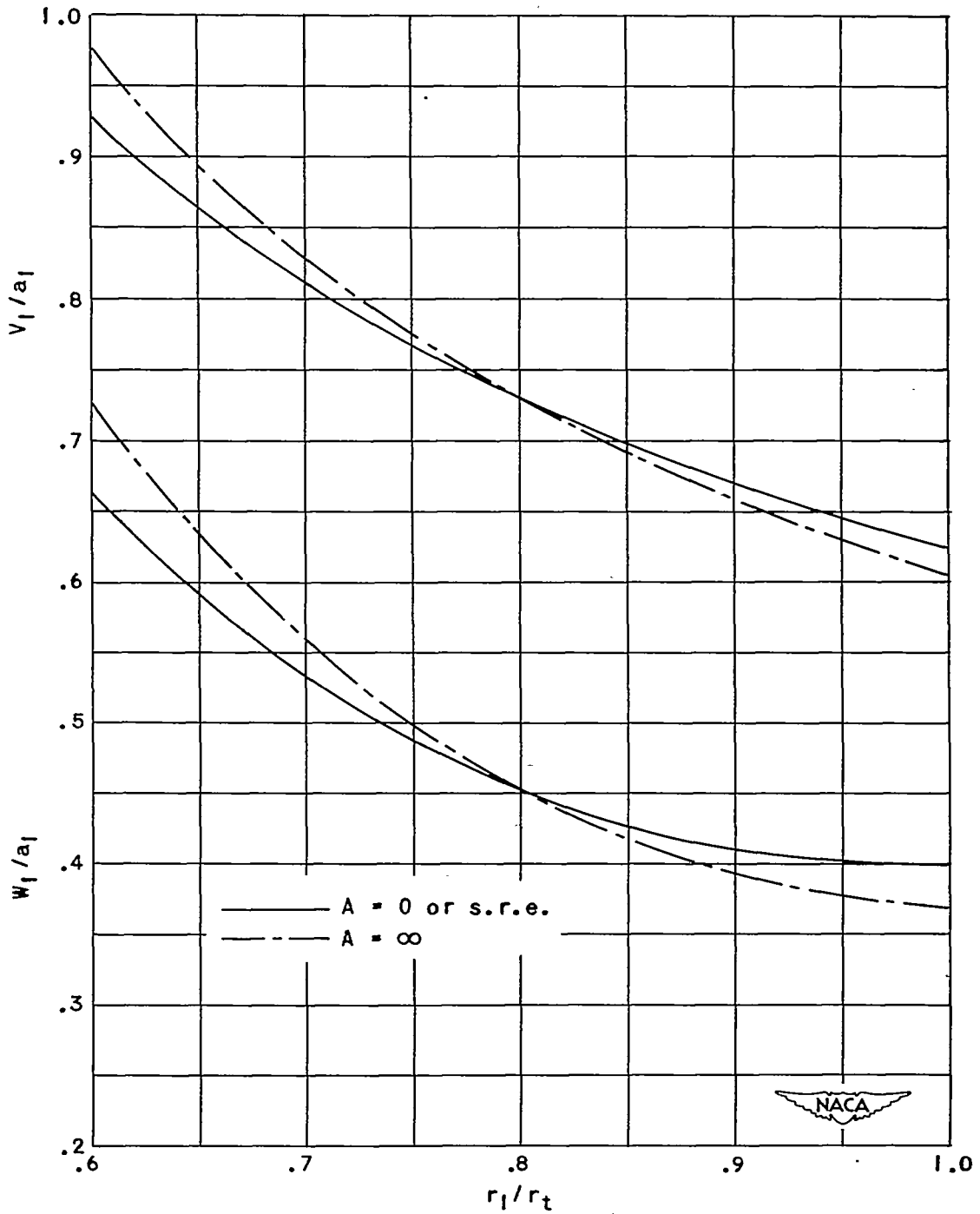


1035

(d) Variation of gas angle entering rotor blade.

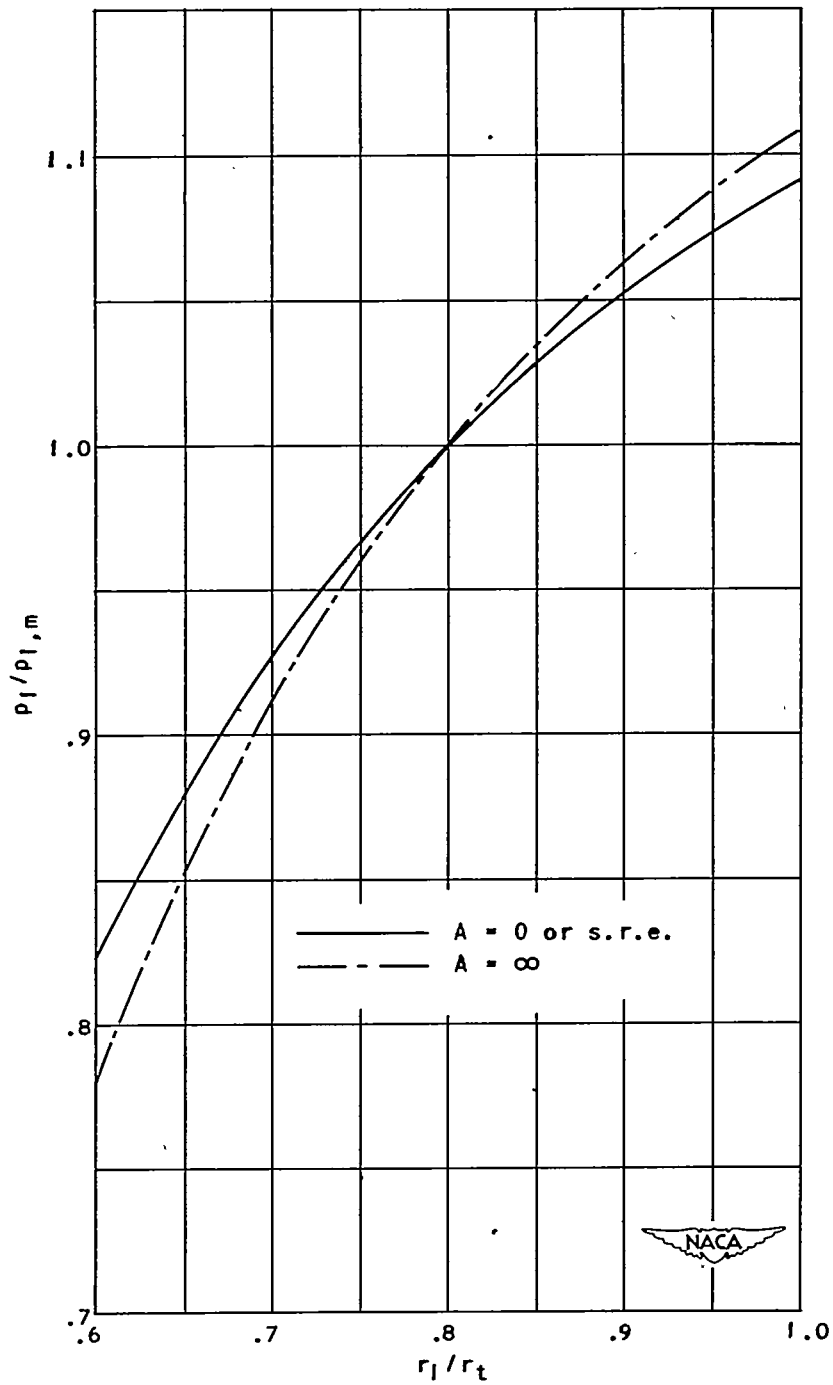
Figure 6. - Continued. Free-vortex and constant-total-enthalpy turbine.

1035



(e) Variation of Mach number in front of rotor.

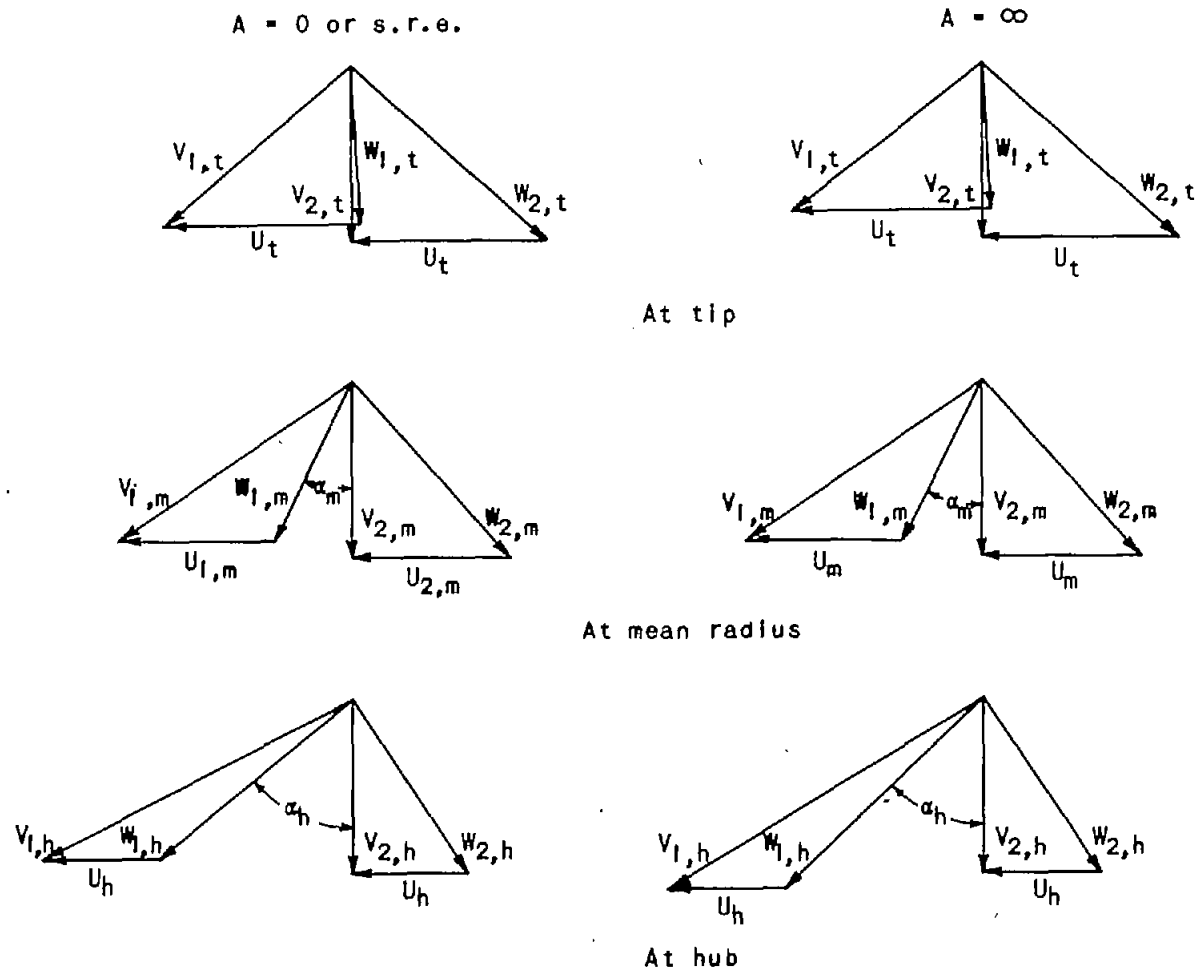
Figure 6. - Continued. Free-vortex and constant-total-enthalpy turbine.



(f) Pressure distribution.

Figure 6. - Continued. Free-vortex and constant-total-enthalpy turbine.

1035



(g) Velocity diagrams at different radii.



Figure 6. - Concluded. Free-vortex and constant-total-enthalpy turbine.



**TITLE:** Application of Radial-Equilibrium Condition to Axial-Flow Compressor and Turbine Design

**AUTHOR(S):** Wu, Chung-Hua; Wolfenstein, L.

**ORIGINATING AGENCY:** Lewis Flight Propulsion Lab., Cleveland, O.

**PUBLISHED BY:** National Advisory Committee for Aeronautics, Washington, D. C.

ATI- 45538

REVISION

(None)

ORIG. AGENCY NO.

(None)

PUBLISHING AGENCY NO.

TN-1795

DATE	DOC. CLASS.	COUNTRY	LANGUAGE	PAGES	ILLUSTRATIONS
Jan '49	Unclass.	U.S.	English	101	tables, diagrs, graphs

**ABSTRACT:**

Basic general equations governing the three-dimensional motion of gas through a compressor or turbine are given in terms of velocity components, total enthalpy and entropy. These equations are used to determine the radial motion of gas through an axial-flow turbomachine and the corresponding effect on the radial variations of the gas state between successive blade rows in the case of steady axially symmetrical flow. The maximum compatible number of the radial variations of the gas properties between successive blade rows that a designer is free to specify and the possible types obtained by different ways of using up these degrees of freedom are discussed. A general procedure is given to calculate the characteristics of a compressor or turbine of any given type of design, taking into account the effect of radial motion of gas.

**DISTRIBUTION:** Request copies of this report only from Publishing Agency

**DIVISION:** Power Plants, Jet and Turbine (5)

**SECTION:** Compressors (3)

**SUBJECT HEADINGS:** Compressors, Axial - Performance (24310); Compressors, Radial (24510); Turbines, Axial - Design (95520.77)

**ATI SHEET NO.:** R-5-3-12

Air Documents Division, Intelligence Department  
Air Materiel Command

**AIR TECHNICAL INDEX**

Wright-Patterson Air Force Base  
Dayton, Ohio